AD A015 268

AMRL-TR-75-8

12 B.S.

STABILITY AND LIMB DISLODGEMENT FORCE MEASUREMENTS WITH THE F-105 AND ACES-II EJECTION SEATS

PAYNE, INC.
1910 FOREST DRIVE
ANNAPOLIS, MARYLAND 21401

DDC
RECEIVED
OCT 14 1975
C

JULY 1975

Approved for public release; distribution unlimited

AEROSPACE MEDICAL RESEARCH LABORATORY
AEROSPACE MEDICAL DIVISION
Air Force Systems Command
Wright-Patterson Air Force Base, Ohio 45433

NOTICES

When US Government drawings, specifications, or other data are used for any purpose other than a definitely related Government procurement operation, the Government thereby incurs no responsibility nor any obligation whatsoever, and the fact that the Government may have formulated, furnished, or in any way supplied the said drawings, specifications, or other data, is not to be regarded by implication or otherwise, as in any manner licensing the holder or any other person or corporation, or conveying any rights or permission to manufacture, use, or sell any patented invention that may in any way be related thereto.

Organizations and individuals receiving announcements or reports via the Aerospace Medical Research Laboratory automatic mailing lists should submit the addressograph plate stamp on the report envelope or refer to the code number when corresponding about change of address or cancellation.

Do not return this copy. Retain or destroy.

Please do not request copies of this report from Aerospace Medical Research Laboratory. Additional copies may be purchased from:

National Technical Information Service
5285 Port Royal Road
Springfield, Virginia 22151

This report has been reviewed and cleared for open publication and/or public release by the appropriate Office of Information (OI) in accordance with AFR 190-17 and DODD 5230.0. There is no objection to unlimited distribution of this report to the public at large, or by DDC to the National Technical Information Service (NTIS).

This technical report has been reviewed and is approved for publication.

FOR THE COMMANDER

HENNING E. VON GIERKE
Director
Biodynamics and Bionics Division
Aerospace Medical Research Laboratory

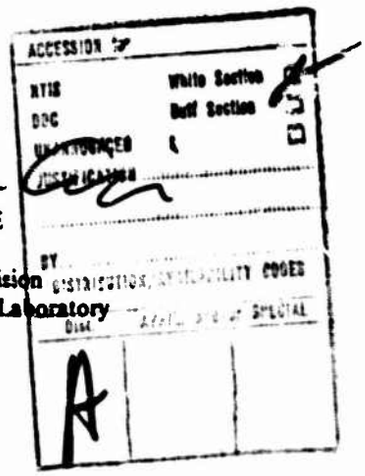

SECURITY CLASSIFICATION OF THIS PAGE (When Data Entered)

REPORT DOCUMENTATION PAGE

READ INSTRUCTIONS BEFORE COMPLETING FORM

1. REPORT NUMBER: AMRL-TR-75-8	2. GOVT ACCESSION NO.
3. RECIPIENT'S CATALOG NUMBER	
4. TITLE (and Subtitle): STABILITY AND LIMB DISLODGEMENT FORCE MEASUREMENTS WITH THE F-105 AND ACES-II EJECTION SEATS.	5. TYPE OF REPORT & PERIOD COVERED: Final Report, 1 Nov 73 - 31 Jan 75
	6. PERFORMING ORG. REPORT NUMBER: Working Paper 119-7
7. AUTHOR(s): Peter R. Payne, Fred W. Hawker, Anthony J. Euler	8. CONTRACT OR GRANT NUMBER(s): F33615-74-C-4015
9. PERFORMING ORGANIZATION NAME AND ADDRESS: PAYNE, INC. 1910 Forest Drive Annapolis, Maryland 21401	10. PROGRAM ELEMENT, PROJECT, TASK AREA & WORK UNIT NUMBERS: 7231 AF 723106
11. CONTROLLING OFFICE NAME AND ADDRESS: Aerospace Medical Research Laboratory, Aerospace Medical Division, Air Force Systems Command Wright-Patterson Air Force Base, Ohio	12. REPORT DATE: July 1975; NUMBER OF PAGES: 158 (162)
14. MONITORING AGENCY NAME & ADDRESS (if different from Controlling Office)	15. SECURITY CLASS. (of this report): UNCLASSIFIED
	15a. DECLASSIFICATION/DOWNGRADING SCHEDULE

16. DISTRIBUTION STATEMENT (of this Report)

Approved for public release; distribution unlimited

17. DISTRIBUTION STATEMENT (of the abstract entered in Block 20, if different from Report)

DDC RECEIVED OCT 14 1975 C

18. SUPPLEMENTARY NOTES

19. KEY WORDS (Continue on reverse side if necessary and identify by block number)

Ejection Seats
Human Body Aerodynamics
Aerodynamic Force Measurements

20. ABSTRACT (Continue on reverse side if necessary and identify by block number)

Forces on the arms and legs of test subjects seated in the F-105 and ACES-II ejection seats were measured over a range of speeds in a wind tunnel. It was found that the forces varied considerably between individuals. The variation was not identified with any outwardly visible physical features of the individuals. Averaged values for the group were compared over a range of pitch and yaw angles and between two different seats. Outward force at the

DD FORM 1 JAN 73 1473 EDITION OF 1 NOV 65 IS OBSOLETE

AIR FORCE - [illegible]

259 770

20. Abstract

knee was found to vary systematically with yaw angle up to 30 deg, and to be little affected by pitch, and to be practically the same on both seats. Forces at the feet and hands showed less systematic variation and were different between the two seats. Attempts to modify the forces by appurtenances attached to the limbs succeeded only in reducing them for some conditions at the expense of others. Both seats were shown to be statically unstable, with and without occupant, in free flight. Static stability was exhibited when equipped with an array of in-plane stabilizer plates on both the F-105 and ACES-II ejection seats. Pressures inside the helmet, and overall forces tending to remove it, were also measured. ~~as a parallel investigation~~ Powerful lift forces were derived from low pressures over the outside, quite sufficient to ensure helmet loss at high speed, unless the retention strap is designed to react large loads; in which case, some form of neck injury can be anticipated. Pressures measured inside the helmet were low and are therefore relatively unimportant as a cause of the helmet lift.

PREFACE

This report was prepared in partial fulfillment of Contract No. F33615-74-C-4015. The research was accomplished by Payne, Inc., 1910 Forest Drive, Annapolis, Maryland 21401. Peter R. Payne was the Principal Investigator.

The Air Force Technical Monitor was James W. Brinkley of the Impact Branch, Biodynamics and Bionics Division of the Aerospace Medical Research Laboratory. The work was performed in support of Project 7231, "Biodynamics of Aerospace Operations," Task 723106, "Impact Exposure Limits and Personnel Protection Criteria."

TABLE OF CONTENTS

PRECEDING PAGE BLANK-NOT FILMED

TABLE OF CONTENTS (continued)

LIST OF FIGURES

LIST OF FIGURES (Continued)

LIST OF FIGURES (Continued)

LIST OF FIGURES (Continued)

LIST OF FIGURES (Continued)

LIST OF TABLES

SUMMARY

Forces on the arms and legs of test subjects seated in the F-105 and ACES-II ejection seats were measured over a range of speeds up to 183 ft/sec in a wind tunnel. These were expressed as "force areas," these being the measured force divided by dynamic pressure. It was found that the force areas varied considerably between the individuals in a manner that could not be established with the small number of test results. The variation was not identified with any outwardly visible physical feature of the individuals.

Averaged values for the group were compared over a range of pitch and yaw angles and between two different seats. Outward force at the knee was found to vary systematically with yaw angle up to 30°, and to be little affected by pitch, and to be practically the same on both seats. Forces at the feet and hands showed less systematic variation and were different between the two seats. Attempts to modify the forces by appurtenances attached to the limbs succeeded only in reducing them for some conditions at the expense of others. Blinker boards attached to the seat beside the legs had little effect on the leg forces and actually increased the arm forces.

Both seats were shown to be statically unstable, with and without occupant, in free flight. Static stability was exhibited when equipped with an array of in-plane stabilizer plates on both the F-105 and ACES-II ejection seats.

The data obtained are compared with that available for other seats in the literature. In general, all data are consistant, except for pitching moment, which is extremely variable for the various configurations.

Pressures inside the helmet, and overall forces tending to remove it, were measured as a parallel investigation, and are reported in Appendix I. Powerful lift forces were derived from low pressures over the outside, quite sufficient to ensure helmet loss at high speed, unless the retention strap is designed to react large loads; in which case, some form of neck injury can be anticipated. Pressures measured inside the helmet were low and are therefore relatively unimportant as a cause of the helmet lift.

In Appendix II, a closed form solution is obtained (for the first time, it is believed) for the problem of the angular motion (in one plane) of a decelerating body.

TEST OBJECTIVES AND SET UP

Scope of the Experiment

The motion of an ejection seat with its occupant installed in it has received attention from many investigators. Wind tunnel measurements on models occupied by anthropometric dummies have yielded static lift, drag and moment data for all directions of the relative wind. Seats have been designed with provision for the occupant's limbs to be lodged in preferred positions during ejection, with the intention of minimizing the chances of injury. Yet despite these efforts the records of actual escapes show instances where the escapee has suffered injury after a limb has been dislodged from its position and flung outwards and backwards, to be arrested by some part of the seat structure or by the limb joint beyond its normal limit of travel. These "flail injuries", so called, do not occur significantly at low airspeeds but at the higher speeds severe dislocations and fractures have been experienced.

The probability of serious flail injury, as a function of airspeed at ejection, is given in Figure 1, based on USAF non-combat experience in the period 1964-1970 (Reference 1); together with earlier RAF experience (Reference 2) with flail injury, and quite recent U.S. Navy experience. Some theoretical background to flail injury is given in Reference 3.

Static forces are generally not sufficient to dislocate the shoulder or hip joint. For such injury it is necessary for the limb to have acquired a considerable angular velocity relative to the body in order that there may be sufficient kinetic energy to cause the damage. This energy, it is supposed, is accumulated over the length of stroke from the initial lodgement to the position of arrest. The question therefore arises as to what causes the dislodgement. Is it inertial force due to the seat motion or aerodynamic force due to pressure on the limb; are these forces of irresistably large magnitude or is the occupant caught unawares and compelled to let go at force levels which he normally could resist? Are there physical differences in people and seats which cause this, or do circumstances alter cases and cause variations of unexpected magnitude?

In the present series of tests, minor variations in the seat and occupant were examined for their effect upon the static forces on the limbs and upon the configuration as a whole. With two types of seat and four* individuals as test subjects, and with an assortment of devices intended to modify these forces, we looked for variability in force levels in relation to changes in configuration.

The tests were made in the wind tunnel at the Glenn L. Martin Institute of Technology at the University of Maryland, under its Director, Donald S. Gross. The tests using the F-105 seat were run during April 1973, and those on the ACES-II seat in September 1973. The cooperation of the director and the tunnel staff was greatly appreciated during these experiments.

---

* Three, four and occasionally five.

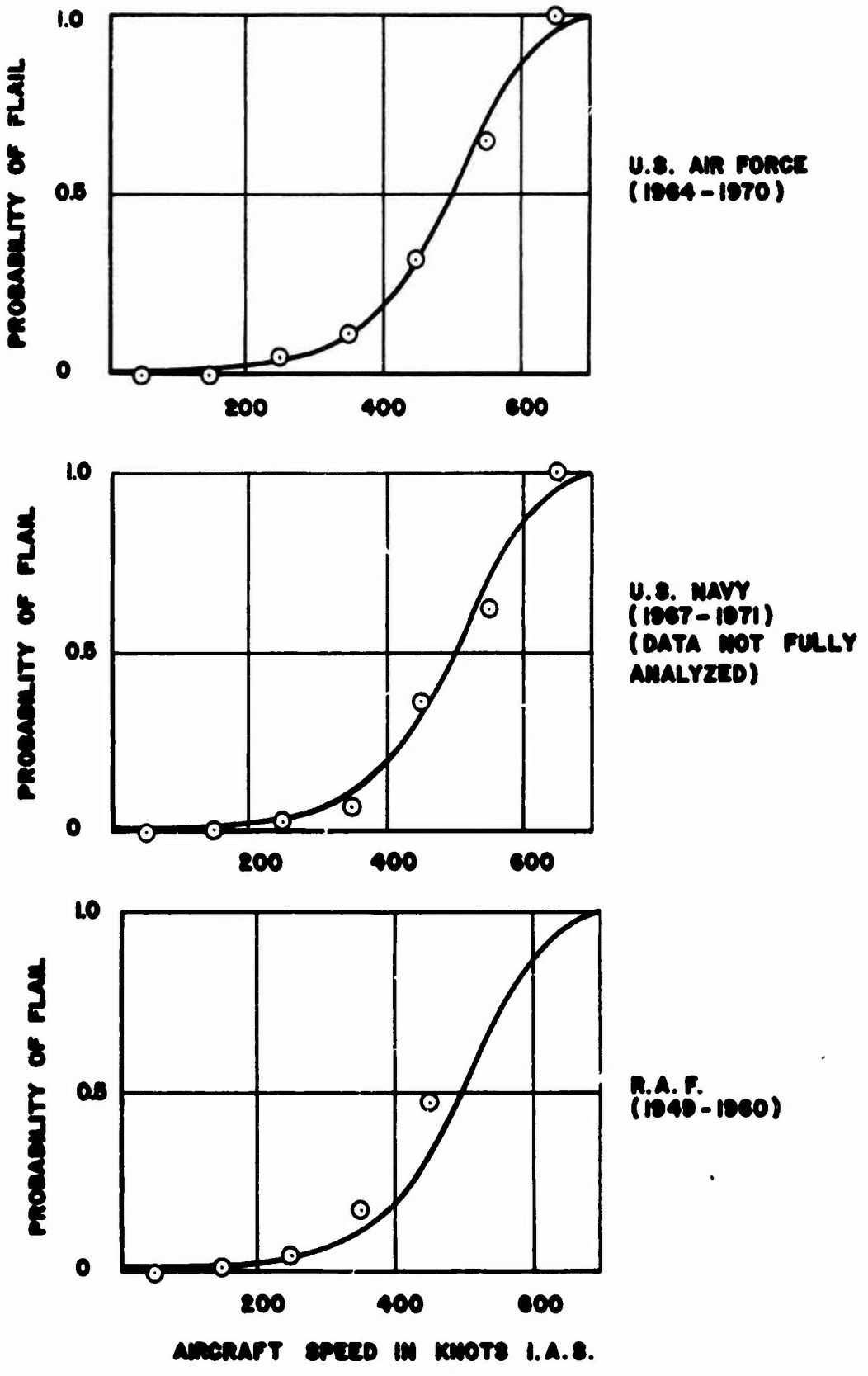

Figure 1. Comparative Flail Injury Probability for Three Services, As a Function of Aircraft Speed at Ejection. The Solid line is the Best Fit to the USAF Data, Taken from Reference 1.

Test Facilities and Equipment

The wind tunnel is of the single return type with a rectangular working section 7.75 feet high by 11.04 feet wide. The tunnel is vented to the test house ambient pressure at the working section, establishing the pressure reference datum. Dynamic pressure ($q = \frac{1}{2} \rho V^2$) at maximum tunnel operating speed is 135 lb/ft^2, corresponding to a speed of 337 ft/sec.

The tunnel is particularly suitable for tests with live subjects, since the test section accommodates a human figure, plus ejection seat, for less than 10 percent blockage and with adequate clearance above and below. The section is well lighted and has glass viewing panels on either side and above, so that the subject is under observation from the control room and additional vantage posts. Voice communication is available but is hardly practicable during the test because of the high noise levels within the subject's helmet. Voice communication up to start, and immediately after shut-down, with a code of digital signs and head movements during the running, were found to be sufficient for all necessary purposes. As a safety measure, the test subject was provided with a press-button switch which, if released, would activate shut-down in an emergency.

Forces and Moments Acting on the Seat Assembly

The seats were mounted on a pedestal attached to the force and moment balance platform in the tunnel floor. Forces and moments on the seat are transmitted by mechanical linkages to the six component balance system located beneath the test section. The balancing is automatic, electrically driven, displaying six-component data at the tunnel operator's position at the central console and on a lighted number panel for plotting. All the indicated data are automatically recorded in a printout and on IBM punched cards.

Force and Moment Measurements

1. Direction of Force Measurement

   a. Lift. . . . . Vertical with respect to tunnel center line

   b. Drag. . . . . Horizontal (fore and aft) with respect to tunnel center line

   c. Side Force. . . . . Horizontal and perpendicular to fore and aft tunnel center line

2. Axes of Moment Measurement

   a. Pitching Moment . . Horizontal and through the front model support trunnion axis, at 0° yaw angle

b. Rolling Moment. . . Horizontal with respect to tunnel center line - intersecting pitching moment axes on tunnel center line

c. Yawing Moment . . . Vertical through center line of tunnel - intersecting pitching moment axis at front model support trunnions

Balance and Support System Limitations

Force and Moment Measurement of Basic Unit

Measurement	Range	Accuracy
Lift (lb)	0 to ±5000	±0.50 lb
Drag (lb)	0 to ±500	±0.10 lb
Side Force (lb)	0 to ±1000	±0.10 lb
Pitching Moment (ft-lb)	0 to ±1000	±0.20 lb
Rolling Moment (ft-lb)	0 to ±1000	±0.20 lb
Yawing Moment (ft-lb)	0 to ±1000	±0.20 lb

Accuracies apply to loadings of less than 10% of forces and 20% of moments. Loadings in excess of these percentages can be measured with an accuracy of one tenth of one percent (.1%). The accuracy of the tunnel velocity is +0.5%.

The tunnel services include programs for transfer of force and moment data from tunnel axes to body axes (or indeed any other workable system of coordinates). Figure 2 is a sketch showing the seat displaced through an angle of yaw (azimuth) and pitch (elevation). In most aerodynamic studies these angles are small and it is customary to refer to wind axes through the body center of mass or some other geometrically convenient point as origin. In the present study, body axes are employed for gross forces and moments with the CG approximated as shown in Figure 3.

Local Force and Pressure Measurements

The tunnel instrumentation provided 58 automated data channels, including 10 galvanometer systems linear to 600 Hz. Fifteen of these channels were used to record limb segment and helmet forces and moments from pressure or strain transducers mounted on the seat assembly. As with the force and moment balance data, the local measurements on these channels were automatically punched on IBM cards. Any six channels on this system could be switched to dynamic recording, linear to 150 Hz, if examination of transients in real time should be required.

Figure 2 shows the locations of the limb dislodgement force measurements. The major dislodgement forces are identified as the rearward force on the lower leg and the outward force at the foot; and the sideways (especially outwards) force at the knee, since these three are opposed somewhat ineffectually by the available muscles. Therefore, the (leg) measured quantities are:

Rearward Force at the Foot.

Outward Force at the Foot.

Sideways Force at the Knee.

Figures 4, 5, 6 and 7 illustrate arrangements on the F-105 seat and Figures 8, 9, 10, 11, 12 and 13 illustrate arrangements on the ACES-II seat.

The arm is not so favorably disposed for restraint by the muscles. So long as the grip upon the handhold can be maintained the hand is virtually fixed to the seat structure and the only freedom of movement of the arm is outwards at the elbow. But the grip may be relaxed for various reasons, or simply overcome by the forces acting on the man. The up-down forces at the hand are presumed to be adequately resisted by the arm muscles, leaving the sideways and rearwards forces for investigation. The rearwards force was taken at the elbow for the F-105 seat and since there was no elbow support in the ACES-II seat the side and back loads were measured at the handle grip (Figure 12). Therefore, the measured forces in the arm are:

Side Force at the Hand (F-105 seat)

Rearwards Force at the Elbow (F-105 seat)

Outward Force at the Elbow (F-105 seat)

Side Force at the Hand (ACES-II seat)

Back Force at the Hand (ACES-II seat)

Seat Modifications for Wind Tunnel Testing

a) F-105 Ejection Seat Alterations

The following modifications were made to the F-105 ejection seat:

1) The headrest was slotted to provide room for a cantilever mechanism to hold the helmet and provide for adjustment to accommodate different size test subjects (Figure 4).

2) The side arm handles (single-motion ejection control) were represented by instrumented handles (Figure 4) so that arm out and arm back loads could be measured.

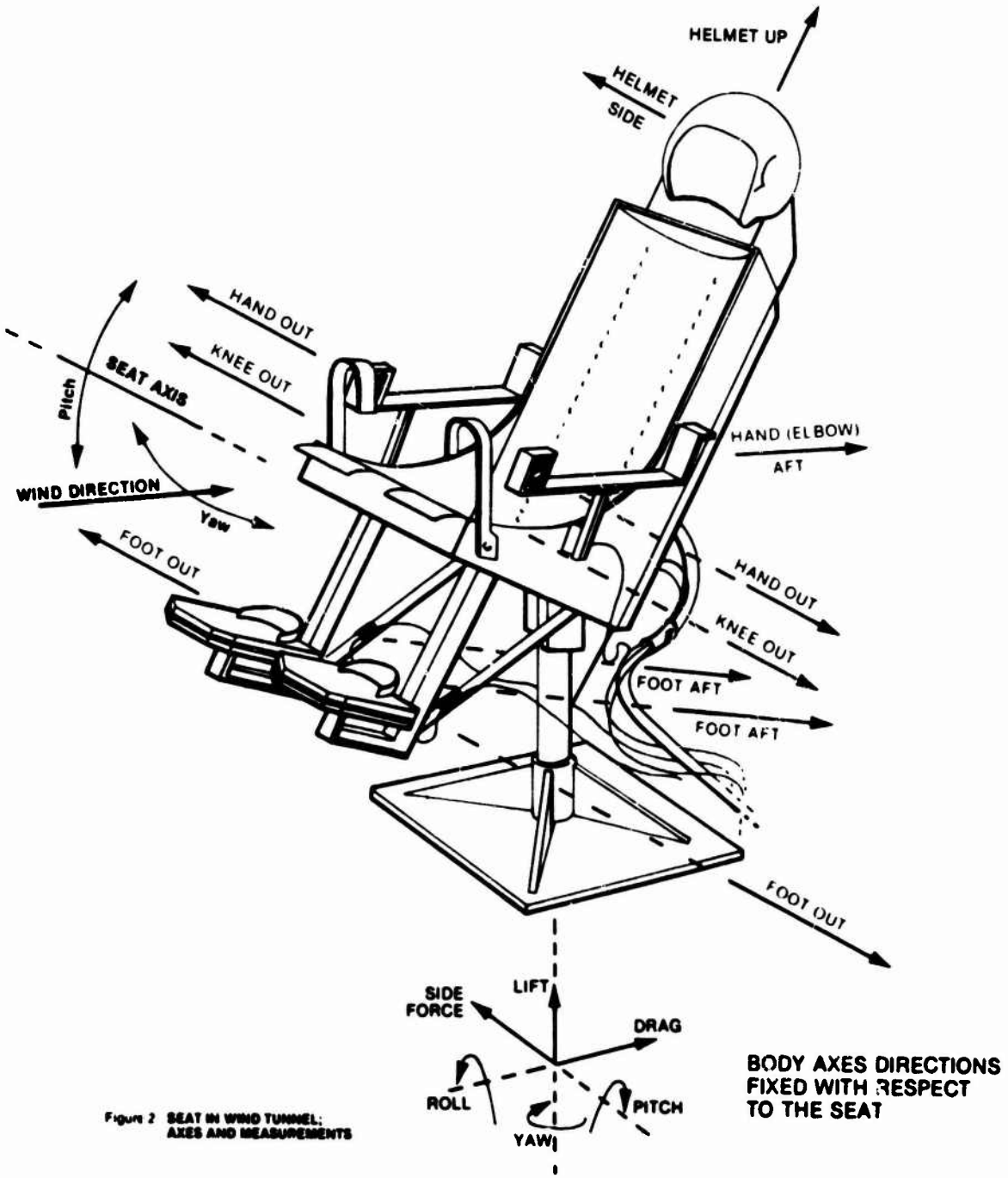

Figure 2 SEAT IN WIND TUNNEL: AXES AND MEASUREMENTS

NOTES:

1) SEAT BACK ANGLE IS 13°.

2) ANGLE θ IS MEASURED FROM THE HORIZONTAL.

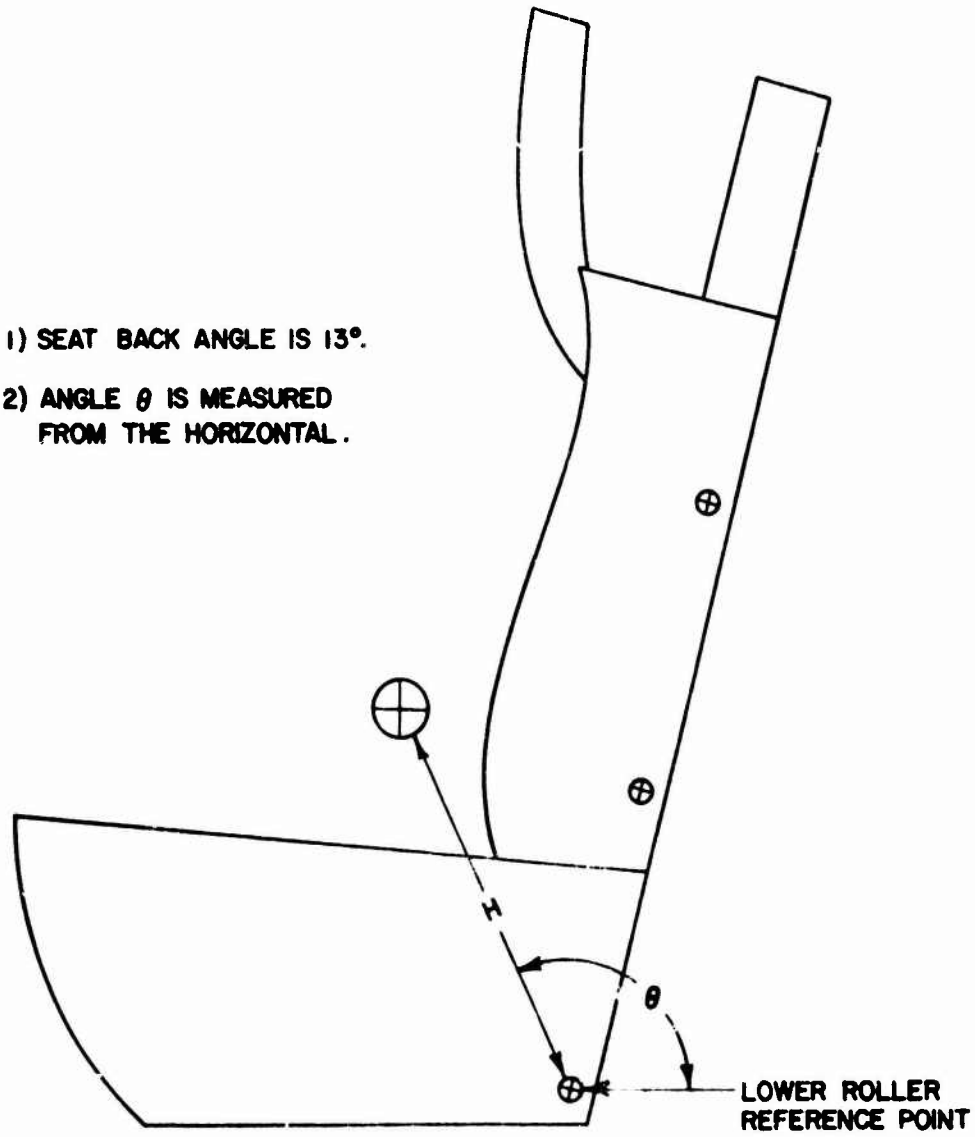

C.G. LOCATIONS IN POLAR COORDINATE FORM FOR SEAT-MAN COMBINATION

SEAT	OCCUPANT	H	θ
ACES II	5%	1.692	110.9
ACES II	50%	1.669	113.1
ACES II	95%	1.649	115.4
F-105	ALL	2.10	109.7

Figure 3. ACES-II and F-105 Center of Gravity Locations Used in Data Reduction.

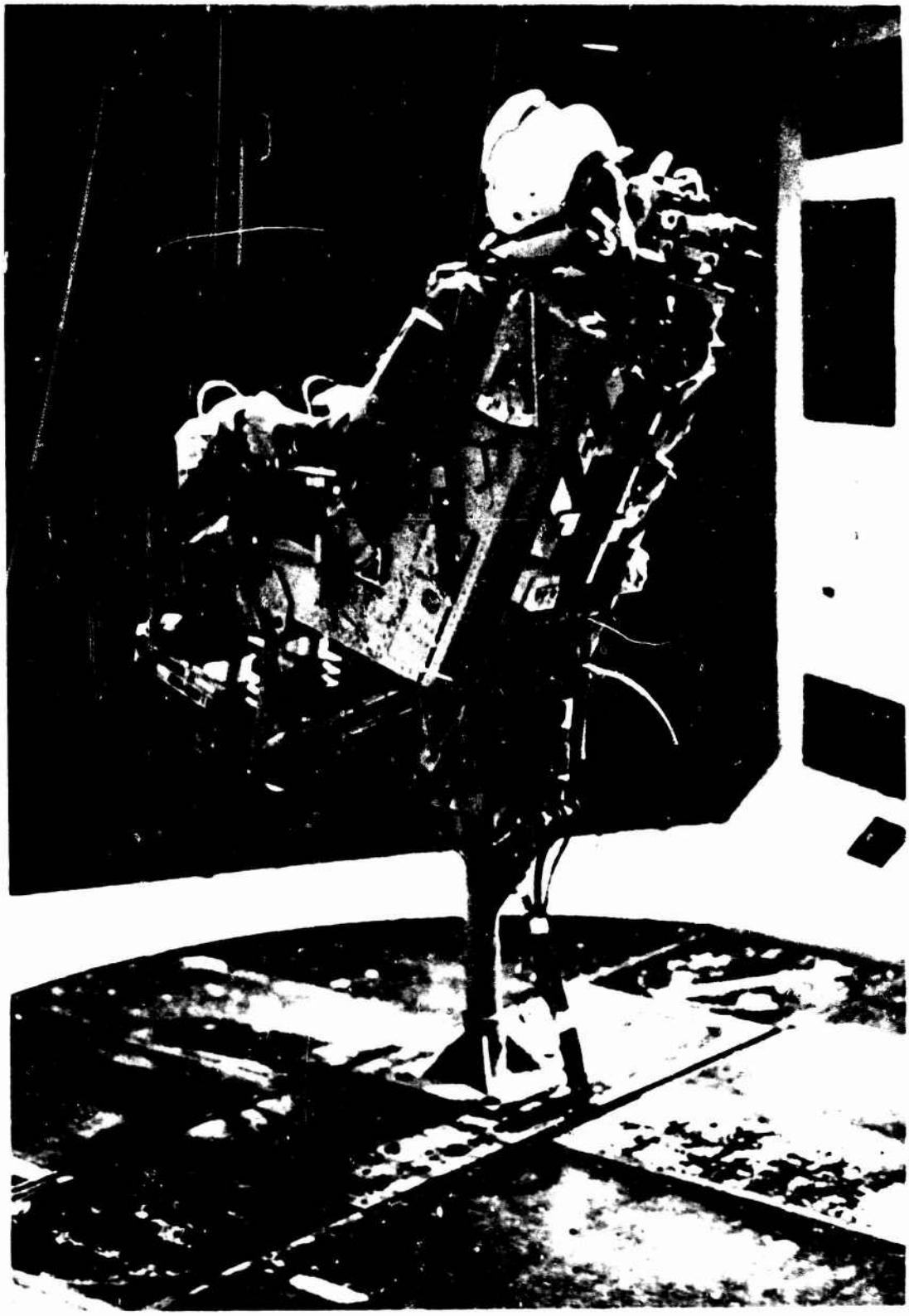

Figure 4. A Subject in the F-105 Seat, at +15° Incidence and 50° Yaw.

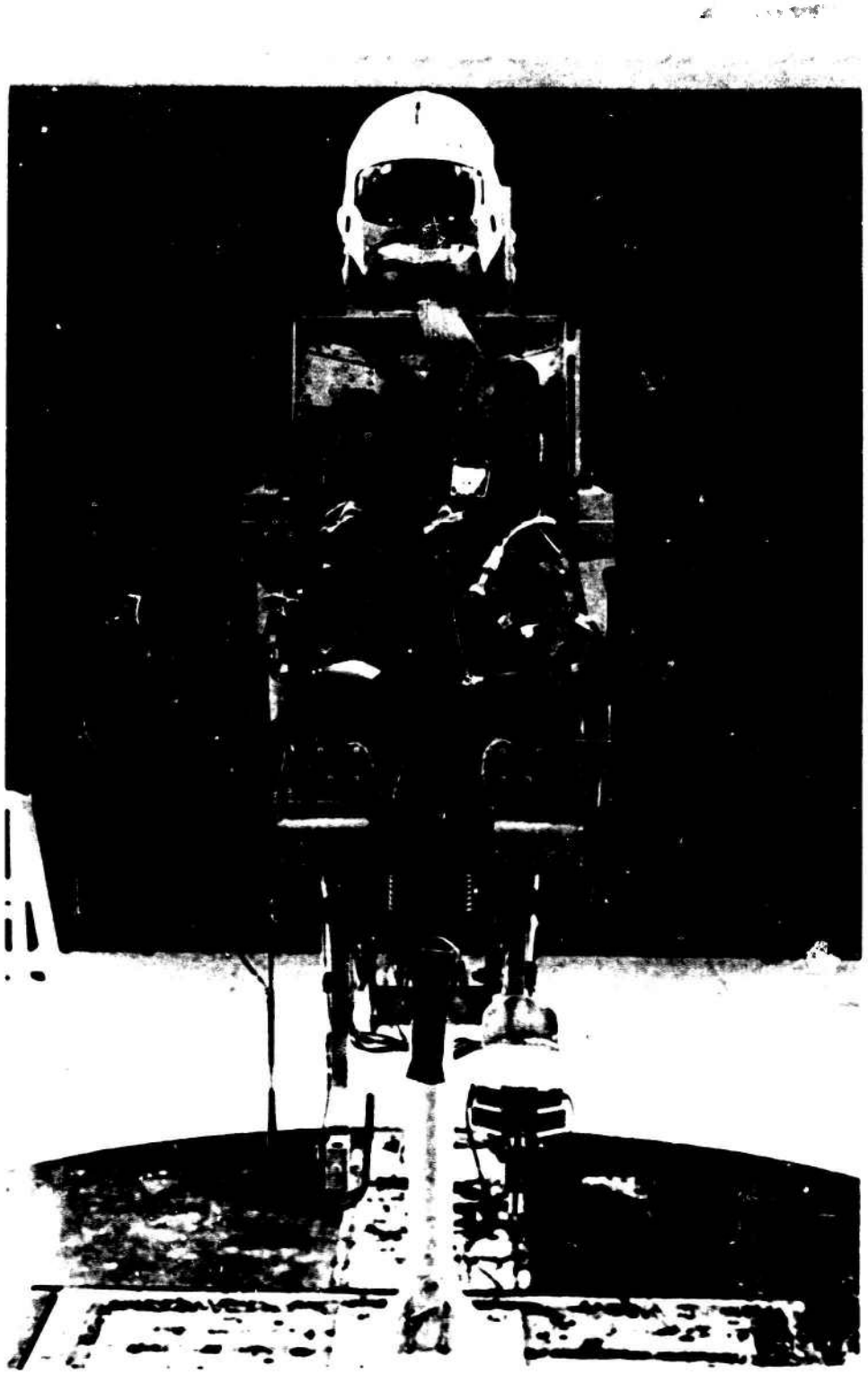

Figure 5. Front View of the Unoccupied F-105 Test Seat. One foot plate has been removed and the starboard knee restraint has been lowered to ease subject egress.

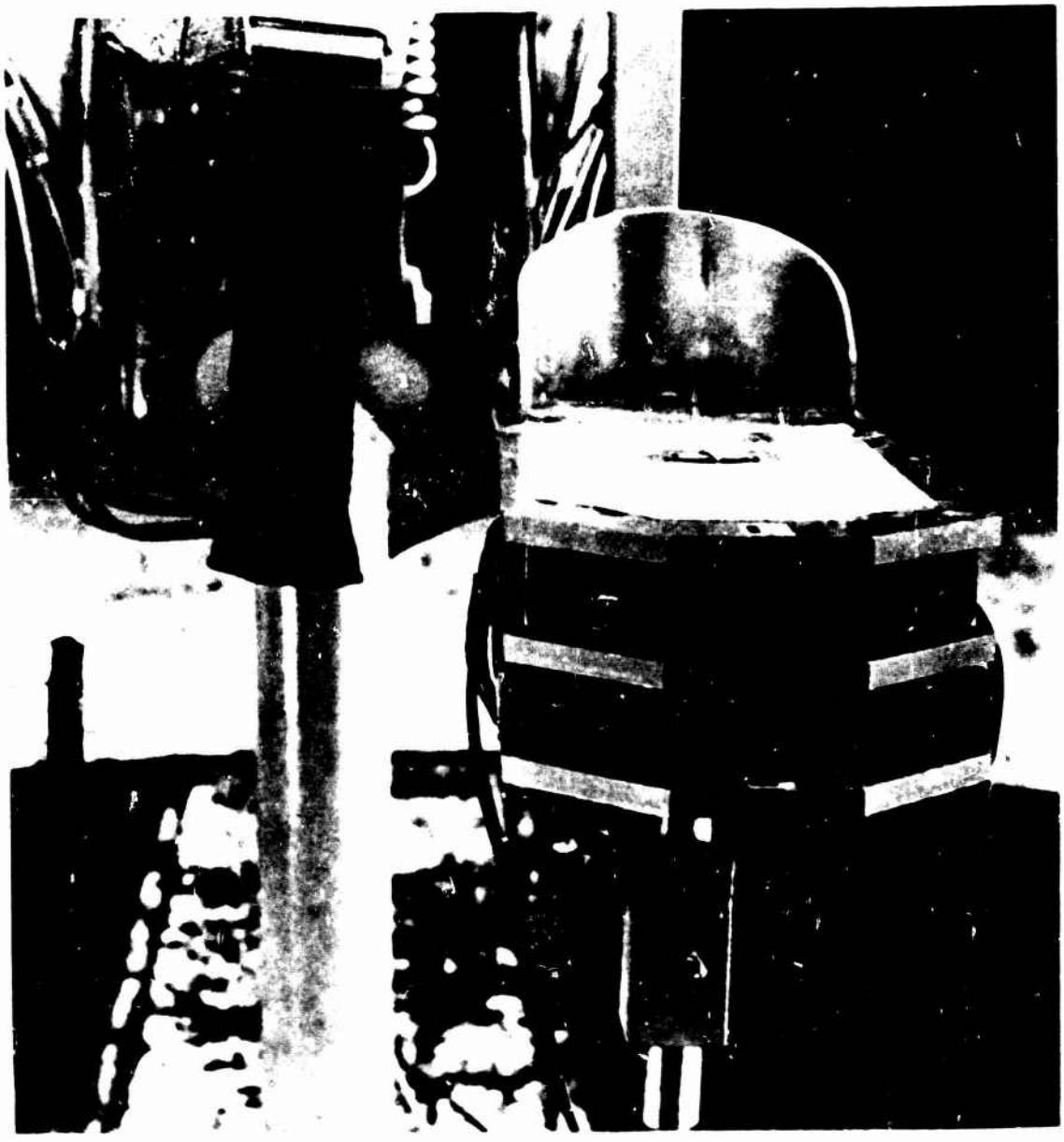

Figure 6. Front View of Foot-Plate on the F-105 Seat.

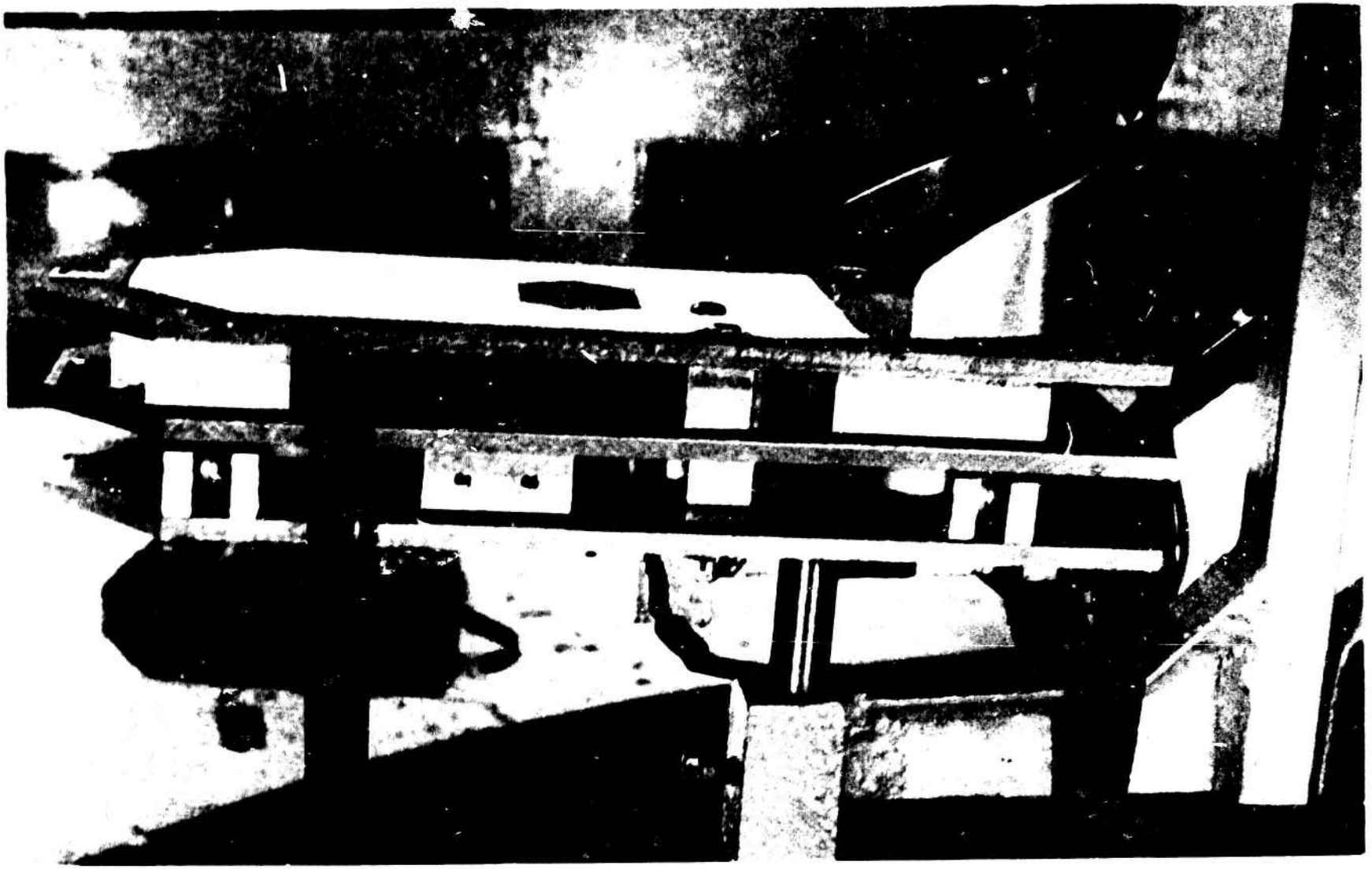

Figure 7. Side View of the F-105 Seat Foot-Plate.

Figure 8. A Subject in the ACES-II Seat at -15° Yaw, -15° Pitch.

Figure 9. Rear View of the ACES-II Seat and the Mounting Stand Built to Support it in the Tunnel. Pitch Angle is Controlled by the Inclined Strut at the Rear.

Figure 10. The ACES-II Side Arm Control Handles were Mounted on Strain-Gauged Cantilever Beams Which Permit "in-out" and "Forward-Back" Forces to be Measured.

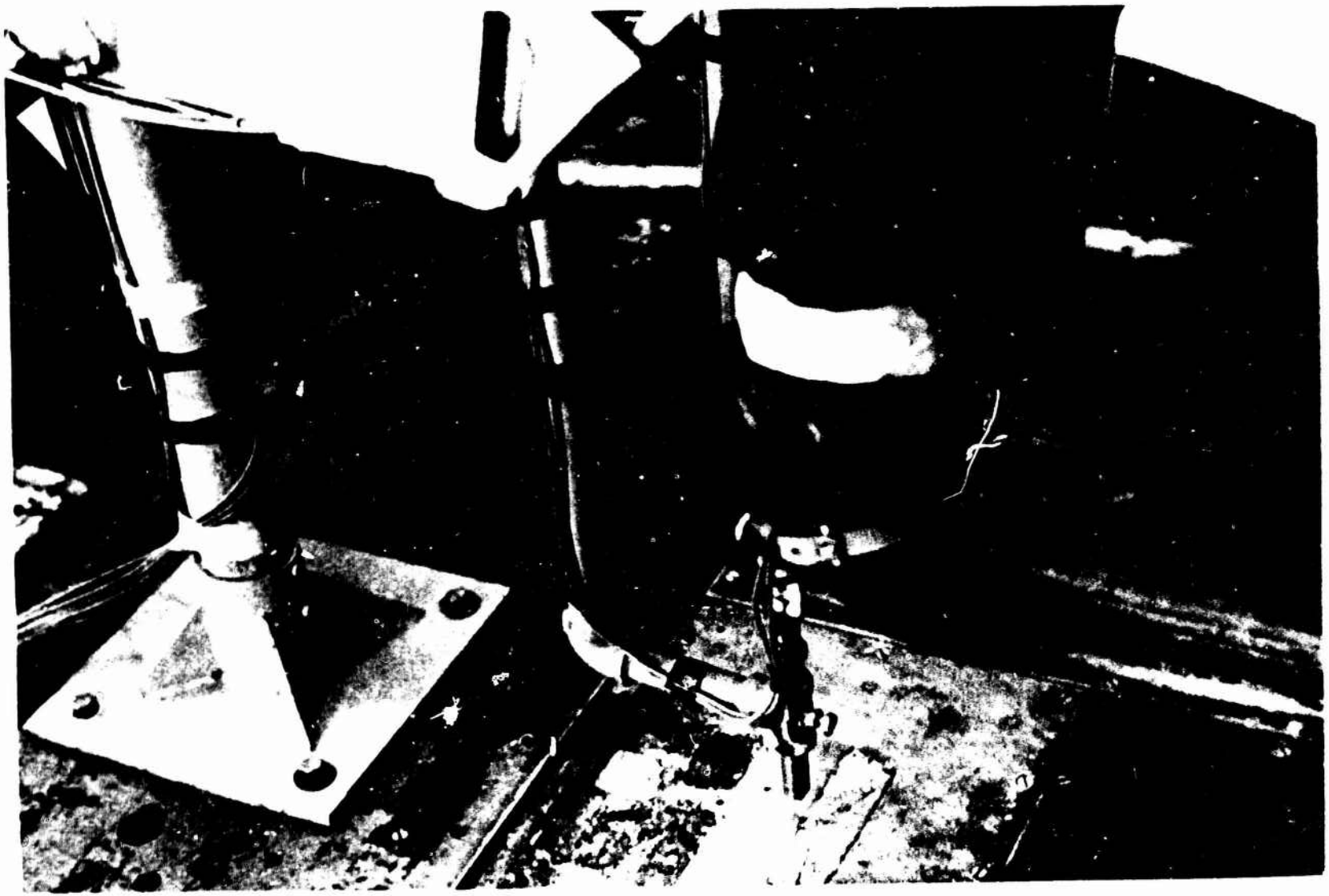

Figure 11. ACES-II Foot Force ("Forward-Back" and "in-out") was Measured on the Vertical Beams Supporting the Stirrups to Which the Subject's Feet are Strapped.

Figure 12. Detail of the ACES-II Side Control Force Measuring Beam.

Figure 15. The Right Knee "In-out" Force Measuring Beam of the MFS II Seat.

3) The drop plate leg support was removed in order that special feet support plates could be installed to measure foot loads.

4) The seat/catapult attachment yoke was not supplied and not simulated.

The foot plate modification was the most radical design change to the operational seat (Figure 7). The additional drag of the support affects both the forces and moments. In later tests of the ACES-II seat, a design change was initiated in the foot force measuring device that made the foot support structure more streamlined (Figure 11).

b) ACES-II Ejection Seat Alterations

A design review of the F-105 ejection seat modifications for wind tunnel testing concluded that changes to the ACES-II seat should be held to a minimum of additional support structures. The following modifications were made to the ACES-II ejection seat:

1) The ejection handles were positioned to accept strain-gauged beams (Figure 12).

2) The feet were also supported on strain-gauged beams with low frontal area support structures (Figure 11).

The seats were mounted in the tunnel in such a manner that the angle made by the seat rails with the vertical was 13° for the datum or zero pitch attitude. This is the normal wind entry angle for most USAF ejection seats.

Helmet Forces and Pressures

Arrangements were made to measure these during some of the runs. This topic is reported in Appendix I.

Standard Test Procedure

We assumed that all aerodynamic forces are proportional to the tunnel dynamic pressure. Typically,

$$\text{Force} = (\text{coefficient}) \times (\text{area}) \times \left(\frac{1}{2}\rho V^2\right)$$

Since the significant area for a forearm or knee is hard to determine, the product (coefficient) x (area) is amalgamated into a single term (K) having the dimensions of area.

Then

$$\text{Force} = Kq$$

Similarly a moment, being the product of a force and a distance, may be represented by a volume

$$\text{Moment} = K_{vol}\, q$$

One object of the experiment is to determine values for K for the various parts of the body.

In the standard procedure the particular test configuration is set up and remains fixed during the run. The tunnel is started and brought up to $q = 10$ lb/ft^2. The experimental quantities (tunnel balance data, strain gauges) are read and recorded by the automatic system; the tunnel q is then advanced to 20, 30, 40 lb/ft^2 and dropped back to 30, 20, 10 lb/ft^2, with the readings taken at each pressure level; then, shut-down and preparation for the next test.

The data on IMB cards goes to the University's IBM 1620 computer. The tunnel balance data is entered in a program provided by the University to apply the conventional tunnel corrections and prints out force areas and moment volumes for each value of q. Printout comes in two versions; one with respect to tunnel axes of reference and another with the data transferred to body axes.

The dislodgement force data was treated similarly by a program prepared by Payne, Inc. which inserted the calibration for each gauge, solved the sting moment equations, and printed out the forces and moments for each value of the tunnel dynamic pressure q, then plotted the values against q, and by a least mean squares fit, found the best value for K for each case.

Standard procedure was abridged occasionally in special tests, usually by ignoring unwanted strain gauge signals when flail avoidance devices (FADs) were under test and/or when the seat carried special equipment. These tests are described in the discussion of results.

RESULTS AND DISCUSSION

The Test Data

The output from the IBM data processing is given in Tables 1 and 2 (limb dislodgement) and Tables 3, 4, 5, 6 and 7 (seat forces and moments). Data for the helmet pressure taps have been segregated and appear in Appendix I.

Limb Dislodgement Forces

Looking at the results for the limb dislodgement forces we observe quite large differences between the same measurement, made on the four test subjects. The experimental error has been largely suppressed by the extraction of the K factor as an area characteristic of the individual, therefore the variation between individuals is attributable to differences in size, posture, fit of clothing and other factors unknown (Table 8).

The number of individuals in the present test is too small to constitute a representative sample of all potential occupants of the seat. Therefore no serious attempt is made to establish the distribution pattern from the present data. As an illustration we note values for the two seats at zero yaw and zero pitch, taking the average (arithmetic mean) and standard deviation (root mean square) despite the smallness of the samples.

For the purposes of this comparison, the two separate outward forces at the hand and elbow have been added together as a single arm-out force. This is because the ACES-II seat, unlike the F-105, does not have support for the elbows. All the forces on the arm are reacted at the hand and shoulder. On this showing, the limb forces on the ACES-II seat are greater than on the F-105 seat, with the exception of the knee-out forces, which are of comparable magnitude.

Figures 14 and 15 show the variation in knee force with yaw angle. The yaw angles are negative (turning to the left) and, as might be expected, the outward force on the left increases with the yaw, the right outward force decreasing. The agreement between the two seats is remarkable. Each is only slightly affected by the pitch. The rates of increase between the two seats are almost identical.

There is some measure of agreement between the outward forces at the feet, for the two seats. The ACES-II results in a pattern similar to that for the knee forces (Figure 16). The side force on the left foot increases, that on the right decreases, with increasing yaw angle. For the F-105 seat (Figure 17) the foot force increases in much the same manner as on the ACES-II. The effect of the combined knee plus foot forces of the F-105 seat shows the force areas for the right and left legs (Figure 18).

Table 1. Basic Tests - Limb Dislodgement Force Areas for the F-105 Seat

Yaw Angle	Pitch Angle	Subject	Run No.	1 Right Foot Back	4 Left Foot Back	2 Right Foot Out	3 Left Foot Out	9 Right Knee Out	5 Left Knee Out	8 Right Arm Out	6 Left Arm Out	10 Right Arm Back	7 Left Arm Back
0	-15	RM	23	0.18	N.D.*	0.05	0.0	0.27	0.30	0.24	0.22	0.11	B.D.**
0	-15	JP	25	0.24	N.D.	0.14	0.12	0.31	0.31	0.16	0.14	0.08	B.D.
0	-15	JS	32		N.D.	0.16	-0.10	0.10	0.14	0.14	0.08	0.15	0.07
0	0	BC	7	0.23	0.25	0.05	0.04	0.23	0.19	0.10	0.09	0.08	B.D.
0	0	RM	8	0.09	0.10	0.04	0.11	0.20	0.22	0.04	B.D.	B.D.	B.D.
0	0	JP	11	0.22	0.24	0.09	0.11	0.25	0.23	0.07	0.06	0.06	B.D.
0	0	JS	14	0.13	0.15	-0.09	0.05	0.20	0.23	0.08	0.10	B.D.	0.08
0	0	JB	17	0.17	N.D.	0.0	0.1	0.24	B.D.	0.13	0.12	0.17	B.D.
0	+15	RM	20	0.10	N.D.	0.03	0.01	0.08	B.D.	0.08	0.07	0.11	B.D.
0	+15	JP	28	0.17	N.D.	0.04	-0.02	0.24	0.33	0.03	0.03	0.13	0.0
0	+15	JS	29	0.14	N.D.	0.09	B.D.	0.06	0.17	0.02	0.02	0.19	0.03
-15	-15	RM	24	0.18	N.D.	-0.16	0.07	0.06	0.35	0.14	0.25	0.15	0.0
-15	0	RM	9	B.D.	B.D.	B.D.	0.25	0.01	0.51	0.07	0.06	B.D.	B.D.
-15	0	JP	12	0.12	0.26	0.0	0.21	0.05	0.40	0.02	0.10	0.08	0.0
-15	0	JS	15	B.D.	B.D.	-0.13	0.25	0.0	0.52	-0.02	0.18	0.27	0.0
-15	0	JB	18	0.18	N.D.	-0.07	0.28	0.0	0.52	0.04	0.15	0.30	0.06
-30	-15	RM	22	0.11	N.D.	-0.34	0.21	-0.06	0.52	0.03	0.23	0.1	0.0
-30	-15	JP	26	0.16	N.D.	-0.30	0.23	-0.21	0.49	0.0	0.15	0.11	0.05
-30	-15	JS	31	0.19	N.D.	-0.40	0.25	-0.11	0.83	-0.05	0.19	0.22	0.0

* N.D. - No Data from channel.

** B.D. - Data too scattered to use.

Table 1. Basic Tests - Limb Dislodgement Force Areas for the F-105 Seat (Continued)

Yaw Angle	Pitch Angle	Subject	Run No.	1 Right Foot Back	4 Left Foot Back	2 Right Foot Out	3 Left Foot Out	9 Right Knee Out	5 Left Knee Out	8 Right Arm Out	6 Left Arm Out	10 Right Arm Back	7 Left Arm Back
-30	0	RM	10	0.12	0.09	-0.22	0.41	-0.31	0.51	0.01	0.10	B.D.	B.D.
-30	0	JP	13	0.14	0.21	-0.09	0.32	-0.07	0.56	0.01	0.05	0.10	0.0
-30	0	JS	16	B.D.	0.09	-0.25	0.47	-0.08	0.56	-0.10	0.17	0.35	0.10
-30	0	JB	19	0.20	N.D.	-0.23	0.45	-0.11	0.70	0.0	0.17	0.33	0.0
-30	+15	RM	21	B.D.	N.D.	-0.38	0.18	-0.32	0.34	-0.08	0.06	0.27	0.0
-30	+15	JP	27	0.15	N.D.	-0.33	0.11	-0.10	0.61	-0.03	0.06	0.31	0.03
-30	+15	JS	30	0.13	N.D.	-0.39	0.22	-0.09	0.65	-0.10	0.085	0.33	0.02
		WITH WEDGES											
0	0	RM	35	0.19	N.D.	-0.01	-0.10	0.31	0.19	0.20	0.19	0.17	0.0
0	-15	RM	36	0.22	N.D.	-0.07	-0.05	0.35	0.29	0.21	0.21	0.11	0.05
0	+15	RM	37	0.18	N.D.	-0.02	0.0	0.22	0.31	0.09	0.08	0.18	0.05
-30	+15	RM	38	0.12	N.D.	-0.37	0.24	-0.10	0.79	-0.02	0.02	0.35	0.0
-30	-15	RM	39	0.15	N.D.	-0.35	0.25	0.0	0.79	0.08	0.21	0.36	0.0
		WITH FIRST MOD LEG BOARDS											
0	-15	JP	40	0.16	N.D.	0.13	-0.09	0.36	0.32	0.16	0.19	0.07	0.01

Table 2. Limb Dislodgement Force Areas (Force/q) for the ACES II Seat

Yaw Angle	Pitch Angle	Subject	Run No.	8 Right Foot Back	5 Left Foot Back	7 Right Foot Out	6 Left Foot Out	9 Right Knee Out	10 Left Knee Out	3 Right Arm Out	2 Left Arm Out	4 Right Arm Back	1 Left Arm Back
0	-15	RM	8	0.34	0.32	0.15	0.17	0.17	0.18	0.19	0.16	0.36	0.28
0	-15	JS	15	0.38	0.33	0.04	0.20	0.26	0.25	0.11	0.14	0.28	0.53
0	-15	JP	27	0.36	0.29	0.03	0.07	0.21	0.15	0.16	0.12	0.29	0.30
0	0	RM	3	0.30	0.35	0.23	0.11	0.29	0.28	0.13	0.17	0.34	0.35
0	0	JS	14	0.42	0.41	0.02	0.11	0.15	0.12	0.19	0.11	0.21	0.44
0	0	JP	26	0.35	0.37	0.05	0.02	0.17	B.D.	0.17	0.15	0.37	0.42
0	+15	RM	9	0.19	0.25	0.10	0.08	0.14	N.D.	0.12	0.08	0.33	0.26
0	+15	JS	20	0.33	0.35	B.D.	0.05	0.08	0.11	0.07	0.14	0.30	0.57
0	+15	JP	21	0.29	0.29	0.0	0.0	0.10	0.0	0.12	0.09	0.25	0.24
-15	-15	RM	7	0.20	0.28	-0.01	0.31	-0.06	0.57	0.06	0.20	0.23	0.21
-15	-15	JS	16	0.31	0.31	-0.04	0.33	0.0	0.48	0.04	0.20	0.40	0.24
-15	-15	JP	28	0.28	0.33	0.05	0.18	0.02	0.35	0.14	0.19	0.36	0.21
-15	0	RM	4	0.30	0.28	0.0	0.25	0.0	0.63	0.03	0.25	0.27	0.33
-15	0	JS	13	0.35	0.34	-0.24	0.22	-0.06	0.49	0.05	0.25	0.40	0.34
-15	0	JP	25	0.31	0.30	-0.05	0.21	-0.02	0.25	0.04	0.24	0.49	0.36
-15	+15	RM	10	0.23	0.25	B.D.	B.D.	-0.06	N.D.	0.0	0.18	0.29	0.30
-15	+15	JS	19	0.31	0.30	-0.13	0.16	-0.07	0.48	0.0	0.25	0.49	0.35
-15	+15	JP	22	0.24	0.24	-0.10	0.17	0.06	0.16	0.03	0.17	0.23	0.28
-30	-15	RM	6	0.16	0.29	B.D.	0.28	-0.30	0.50	0.0	0.30	0.15	0.23
-30	-15	JS	17	0.31	0.31	-0.11	0.66	-0.33	0.85	-0.02	0.32	0.24	0.10
-30	-15	JP	29	0.33	0.19	-0.06	0.35	-0.26	0.31	-0.02	0.25	0.14	0.20

Table 2. Limb Dislodgement Force Areas (Force/q) for the ACES II Seat (continued)

Yaw Angle	Pitch Angle	Subject	Run No.	8 Right Foot Back	5 Left Foot Back	7 Right Foot Out	6 Left Foot Out	9 Right Knee Out	10 Left Knee Out	3 Right Arm Out	2 Left Arm Out	4 Right Arm Back	1 Left Arm Back
-30	0	RM	5	0.27	0.39	-0.15	0.21	B.D.	0.55	B.D.	0.35	B.D.	B.D.
-30	0	JS	12	0.39	0.30	-0.14	0.54	-0.15	0.93	-0.13	0.30	B.D.	0.10
-30	0	JP	24	0.29	0.26	-0.19	0.46	-0.15	0.42	-0.04	0.31	0.04	0.17
-30	+15	RM	11	0.18	0.22	-0.20	0.49	-0.15	N.D.	-0.05	0.22	B.D.	0.16
-30	+15	JS	18	0.16	0.35	-0.20	0.42	-0.06	0.74	-0.11	0.15	0.38	0.11
-30	+15	JP	23	0.26	0.22	-0.04	0.27	-0.10	0.37	-0.06	0.29	0.20	0.23

Table 3. Forces and Moments for the Empty F-105 Seat

Yaw Angle	Pitch Angle	Run No.	Lift Area	Drag Area	Side Force Area	Pitch Moment Volume	Yaw Moment Volume	Roll Moment Volume
0°	0°	2	-2.2	6.28	-0.2	-3.2	0.2	-0.2
0°	0°	3	-2.4	6.48	-0.2	-3.7	0.2	0.0
-15°	0°	3	-2.5	6.44	-2.1	-4.2	0.1	2.8
-30°	0°	3	-2.5	6.28	-4.0	-4.5	-0.[illegible]	5.8
0°	+15°	4	-2.2	5.52	-0.1	-1.2	0.4	-0.1
-15°	+15°	4	-1.9	5.34	-2.4	-1.3	0.	2.7
-30°	+15°	4	-1.7	5.22	-4.0	-1.0	1.[illegible]	5.4
0°	-15°	5	-4.1	6.52	-0.4	-4.1	0.0	0.0

Table 4. Forces and Moments for the Basic (Unstabilized) F-105 Seat Plus Subject

Yaw Angle	Pitch Angle	Run No.	Subject	Lift Area	Drag Area	Side Force Area	Pitch Moment Volume	Yaw Moment Volume	Roll Moment Volume
0°	-15°	23	RM	-3.3	6.51	0.1	-3.9	-0.2	0.1
0°	-15°	25	JP	-2.8	6.25	0.2	-4.0	-0.2	0.0
0°	-15°	32	JS	-2.7	6.4	0.2	-3.0	-0.2	-0.1
0°	0°	7	BC	-1.6	6.36	0.0	-3.4	0.1	-0.2
0°	0°	8	RM	-1.5	6.20	-0.2	-3.5	0.2	-0.3
0°	0°	11	JP	-1.6	6.18	0.0	-3.6	0.1	-0.4
0°	0°	14	JS	-1.7	6.59	-0.1	-3.2	0.2	-0.3
0°	0°	17	JB	-1.9	6.92	0.0	-3.5	-0.1	-0.1
0°	+15°	20	RM	-0.1	5.86	-0.4	-3.6	0.1	-0.1
0°	+15°	28	JP	0.0	5.77	-0.1	-3.8	-0.1	-0.2
0°	+15°	29	JS	-0.3	6.32	-0.1	-3.1	-0.1	-0.3
-15°	-15°	24	RM	-3.1	6.65	-2.0	-4 1	-1.2	1.7
-1[illegible]	0°	9	RM	-1.3	6.09	-2.9	-3.7	-1.0	2.1
-15°	0°	12	JP	-1.5	6.08	-2.5	-3.7	-1.0	2.0
-15°	0°	15	JS	-1.6	6.57	-2.9	-3.5	-1.2	2.0
-15°	0°	18	JB	-1.8	6.83	-2.8	-3.6	-1.3	1.9
-30°	-15°	22	RM	-3.0	6.31	-5.1	-4.0	-1.9	4.0
-30°	-15°	26	JP	-2.8	6.29	-5.0	-4.1	-1.9	3.7
-30°	-15°	31	JS	-2.6	6.26	-5.3	-3.4	-1.9	3.6
-30°	0°	10	RM	-1.2	5.54	-5.4	-3.8	-1.8	3.3
-30°	0°	13	JP	-1.3	5.82	-5.1	-3.9	-1.6	3.4

Table 5. Forces and Moments for the Basic (Unstabilized) F-105 Seat Plus Occupant

Yaw Angle	Pitch Angle	Run No.	Subject	Lift Area	Drag Area	Side Force Area	Pitch Moment Volume	Yaw Moment Volume	Roll Moment Volume
-30°	0°	16	JS	-1.4	6.25	-5.7	-3.5	-1.6	3.3
-30°	0°	19	JB	-1.5	6.34	-5.7	-3.8	-1.9	3.2
-30°	+15°	21	RM	0.2	5.30	-5.6	-3.2	-1.9	5.2
-30°	+15°	27	JP	0.2	5.38	-5.6	-3.4	-1.9	5.3
-30°	+15°	30	JS	0.3	5.55	-5.5	-2.9	-1.9	5.4
WEDGE SPOILERS ON LIMBS AND HELMET FAD									
0°	0°	35	RM	-2.1	7.32	-0.3	-4.1	0.0	-0.2
0°	-15°	36	RM	-3.2	6.95	0.1	-3.8	0.0	-0.4
0°	+15°	37	RM	-0.1	6.29	-0.1	-3.8	0.0	-0.4
-30°	+15°	38	RM	0.1	5.51	-5.3	-3.1	-1.8	3.0
-30°	-15°	39	RM	-3.3	6.48	-4.8	-3.4	-1.5	3.2
FIRST MOD LEGBOARDS									
0°	-15°	40	JP	-3.1	6.88	-0.1	-3.9	-0.5	-0.1
-30°	-15°	41	JP	-2.8	6.30	-6.8	-4.0	-5.1	5.6
NET RESTRAINTS AND VIKING WINGS ON HELMETS									
0°	0°	42	JS	-2.1	7.15	-0.1	-4.0	0.1	-0.6
NET RESTRAINTS PLUS STRAPS; STANDARD HELMET									
0°	+15°	47	RM	-0.2	6.26	0.2	-4.3	0.3	-0.5
0°	0°	47	RM	-1.9	6.80	0.0	-3.5	0.2	-0.3
0°	-15°	47	RM	-2.6	7.15	0.5	-4.1	0.1	0.1

Table 6. Gross Force Areas (Force/q) and Moment Volumes (Moment/q) for the ACES-II Seat

Yaw Angle	Pitch Angle	Subject	Run No.	Lift Area	Drag Area	Side Force Area	Pitch Moment Volume	Yaw Moment Volume	Roll Moment Volume
0	0	RM	3	-1.08	6.52	- .04	-2.46	.32	.38
0	0	JS	14	- .8	6.92	- .14	-1.9	.1	.68
0	0	JP	26	-1.0	6.44	0.0	-2.74	.04	.60
AVERAGE				- .96	6.63	- .09	-2.37	.15	.55
0	-15	RM	8	-1.92	6.58	0.0	-2.16	.16	.32
0	-15	JS	15	-1.58	6.71	- .2	-1.88	.03	.75
0	-15	JP	27	-1.68	6.26	- .74	7.5	.14	.52
AVERAGE				-1.73	6.52	- .31	-1.85	.11	.53
0	15	RM	9	.38	5.95	.1	-1.92	.26	.7
0	15	JS	20	.44	6.44	- .2	-2.32	0.0	.94
0	15	JP	21	.46	5.98	- .1	-2.24	.18	.92
AVERAGE				.43	6.05	- .06	-2.16	.15	.85
-15	0	RM	4	-1.04	6.63	-2.46	-2.12	-1.76	2.06
-15	0	JS	13	- .6	6.78	-2.08	-1.40	-1.86	2.40
-15	0	JP	25	- .88	6.40	-2.06	-2.26	-1.72	2.08
AVERAGE				- .84	6.60	-2.20	-1.93	-1.78	2.18

Table 6. Gross Force Areas (Force/q) and Moment Volumes (Moment/q) for the ACES-II Seat (Continued)

Yaw Angle	Pitch Angle	Subject	Run No.	Lift Area	Drag Area	Side Force Area	Pitch Moment Volume	Yaw Moment Volume	Roll Moment Volume
-15	-15	RM	7	-1.9	6.57	-2.40	-2.12	-1.96	1.76
-15	-15	JS	16	-1.48	6.53	-1.88	-1.14	-1.6	1.74
-15	-15	JP	28	-1.80	6.33	-1.76	-2.10	-1.44	1.86
AVERAGE				-1.73	6.48	-2.01	-1.79	-1.68	1.79
-15	15	RM	10	.34	6.11	-2.84	-1.66	-1.84	2.06
-15	15	JS	19	.52	6.08	-2.44	-1.56	-1.98	3.22
-15	15	JP	22	.4	5.81	-2.48	-2.12	-1.62	2.89
AVERAGE				.42	6.00	-2.59	-1.79	-1.81	2.71
-30	0	RM	5	-1.08	6.17	-5.76	-2.28	-3.16	3.54
-30	0	JS	12	- .74	6.25	-5.76	-2.06	-2.84	3.58
-30	0	JP	24	-1.16	6.29	-5.72	-1.70	-2.58	2.76
AVERAGE				- .99	6.24	-5.75	-2.01	-2.86	3.29
-30	-15	RM	6	-1.82	6.05	-5.62	-2.52	-2.78	3.26
-30	-15	JS	17	-1.58	6.04	-5.72	-1.88	-2.76	3.16
-30	-15	JP	29	-1.64	5.84	-5.82	-2.19	-2.60	2.34
AVERAGE				-1.68	5.98	-5.72	-2.20	-2.71	2.92

Table 6. Gross Force Areas (Force/q) and Moment Volumes (Moment/q) for the ACES-II Seat (Continued)

Yaw Angle	Pitch Angle	Subject	Run No.	Lift Area	Drag Area	Side Force Area	Pitch Moment Volume	Yaw Moment Volume	Roll Moment Volume
-30	15	RM	11	.16	5.8	-5.70	-1.42	-2.86	3.74
-30	15	JS	18	.44	5.48	-5.56	-2.08	-2.30	3.76
-30	15	JP	23	- .02	5.7	-5.7	-1.86	-2.46	3.48
AVERAGE				.19	5.66	-5.65	-1.79	-2.54	3.66

Table 7. Variation Among Seat Occupants

Variation Among Seat Occupants (F-105 Seat) [Pitch 0°, Yaw 0°]

Limb Force	No. Tested	Arith. Mean	Std. Dev.
Right Foot Back	5	0.17	.05
Left Foot Back	4	0.19	.06
Right Foot Out	5	0.02	.06
Left Foot Out	5	0.08	.035
Right Knee Out	5	0.22	.008
Left Knee Out	4	0.22	.015
Right Arm Out	5	0.08	.03
Left Arm Out	4	0.09	.02
Right Arm Back	3	0.10	.048
Left Arm Back	1	0.08	--

Variation Among Seat Occupants (ACES-II Seat) [Pitch 0°, Yaw 0°]

Limb Force	No. Tested	Arith. Mean	Std. Dev.
Right Foot Back	3	.36	.035
Left Foot Back	3	.38	.025
Right Foot Out	3	.10	.09
Left Foot Out	3	.08	.04
Right Knee Out	3	.20	.062
Left Knee Out	3	.20	.08
Right Arm Out	3	.16	.025
Left Arm Out	3	.14	.025
Right Arm Back	3	.31	.068
Left Arm Back	3	.40	.038

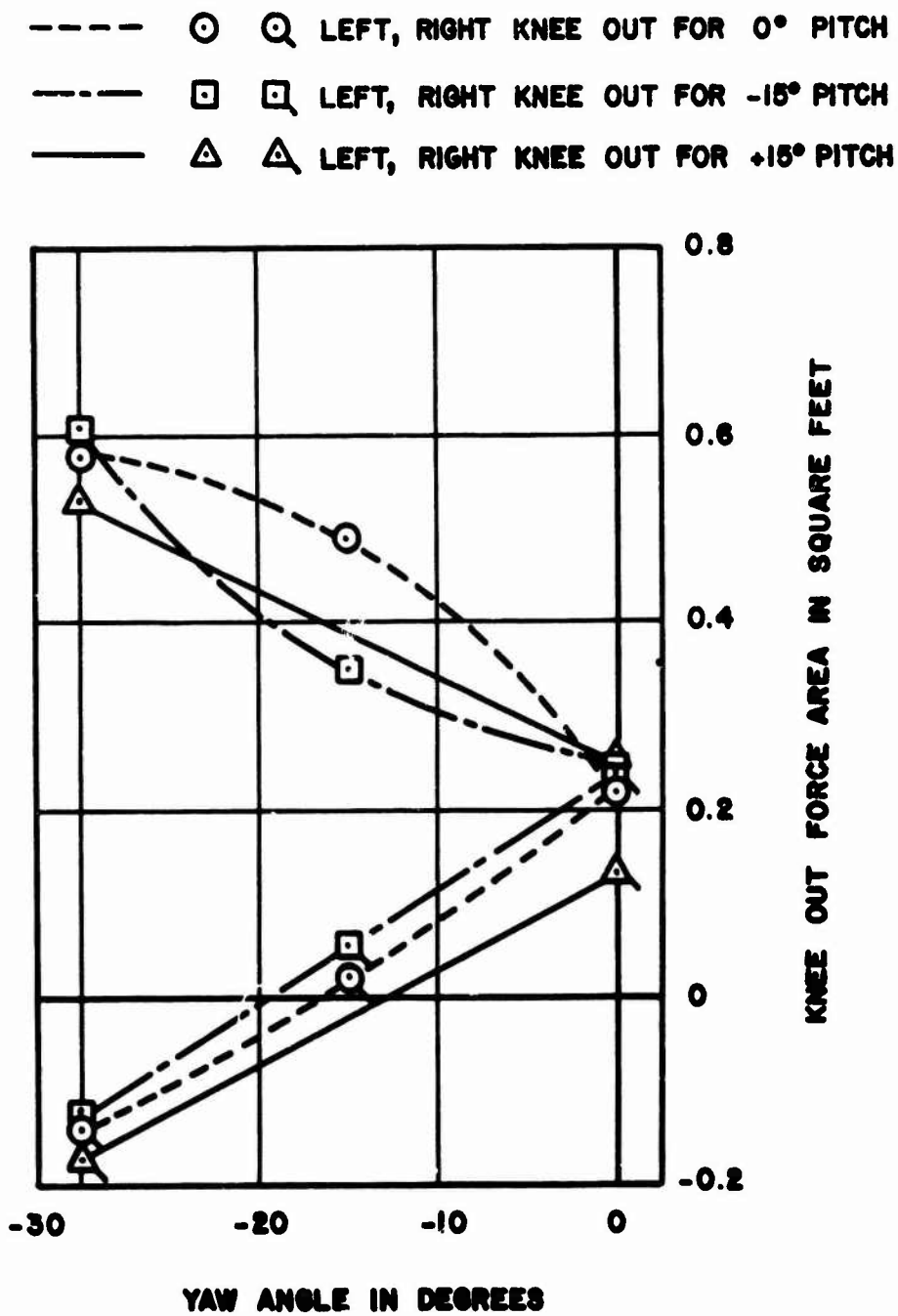

Figure 14. Effect of Pitch and Yaw Angle on the Average Outward Force on the Knees in an F-105 Ejection Seat.

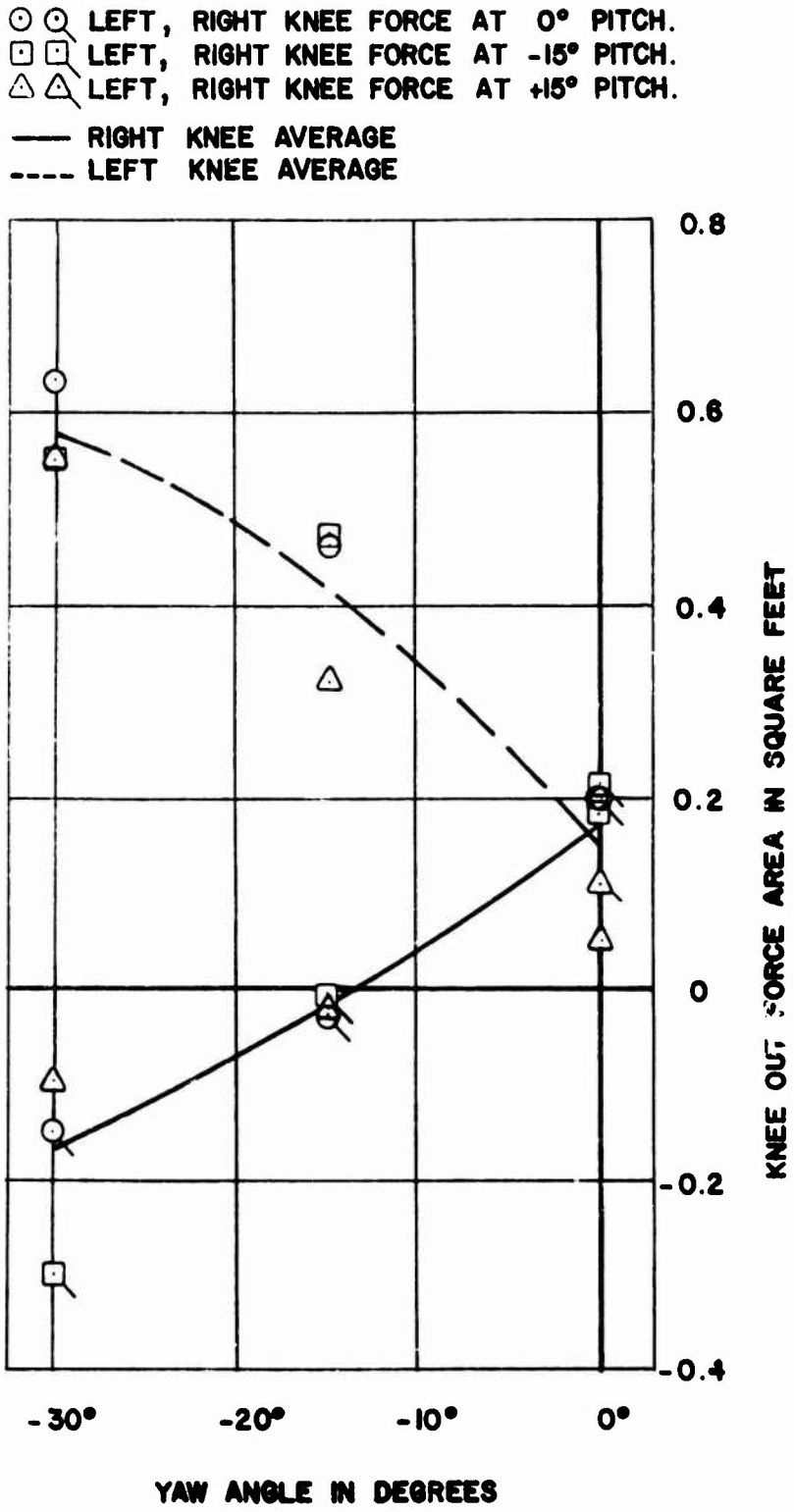

Figure 15. Variation of Knee Out Force with Yaw Angle for the ACES-II Ejection Seat.

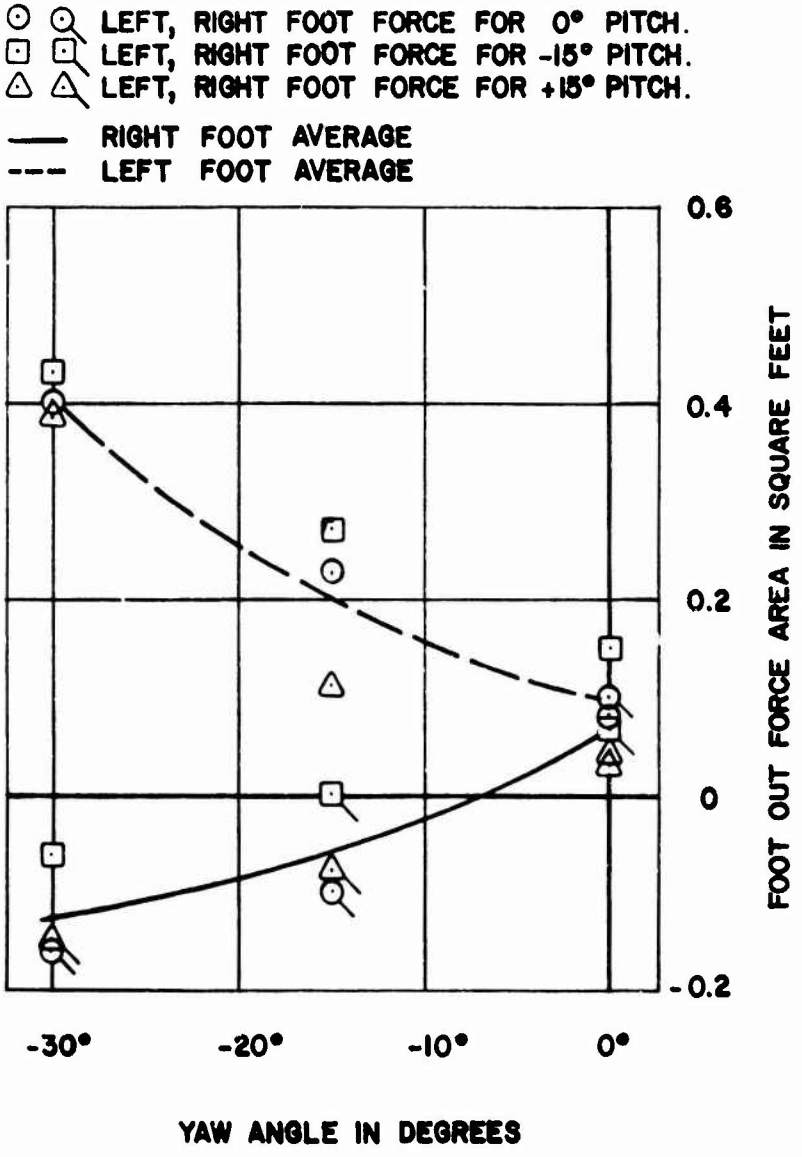

Figure 16. Variation of Foot Out Force with Yaw Angle for the ACES-II Ejection Seat.

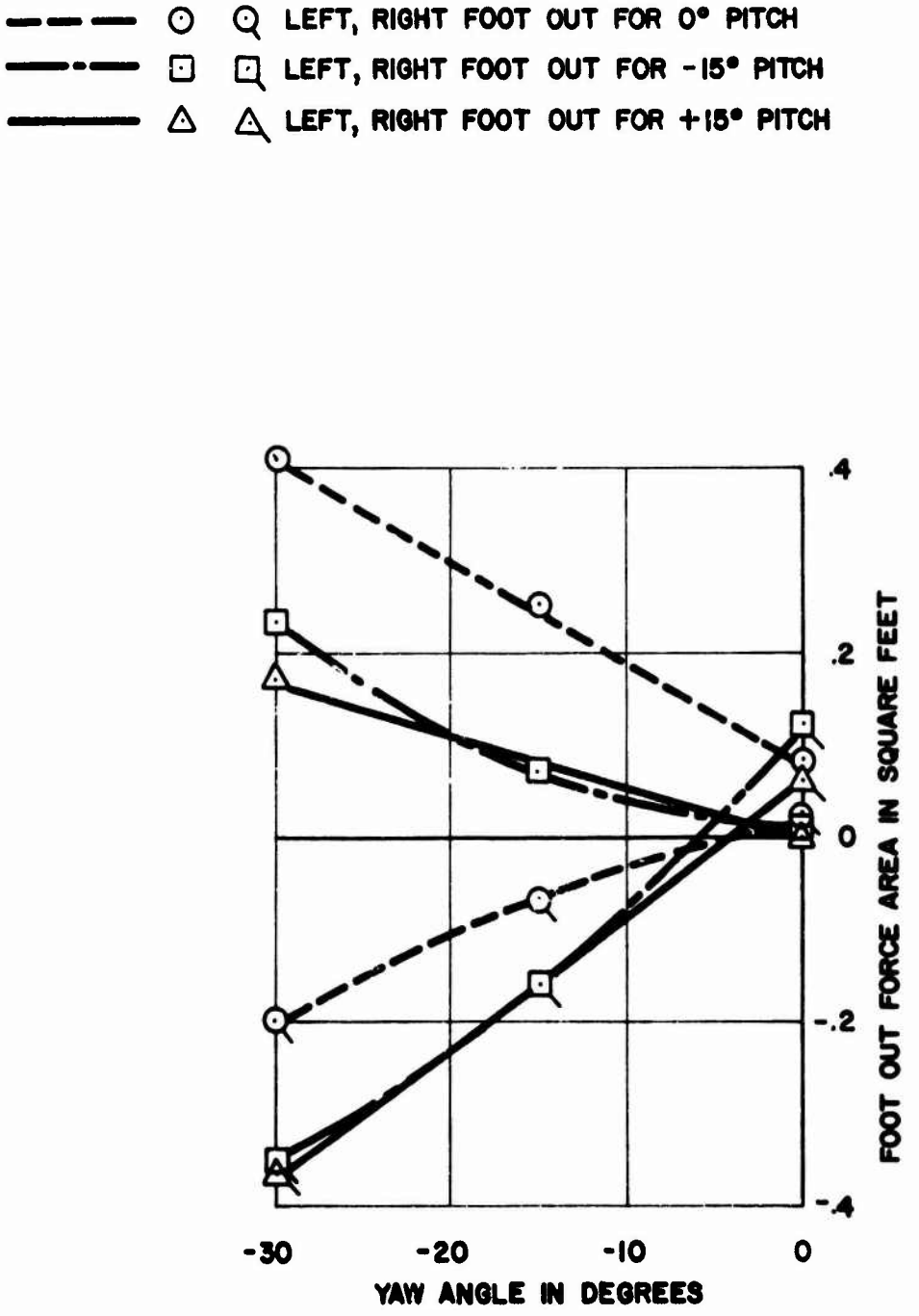

Figure 17. Effect of Pitch and Yaw Angle on the Average Outward Force on the Feet, in an F-105 Ejection Seat.

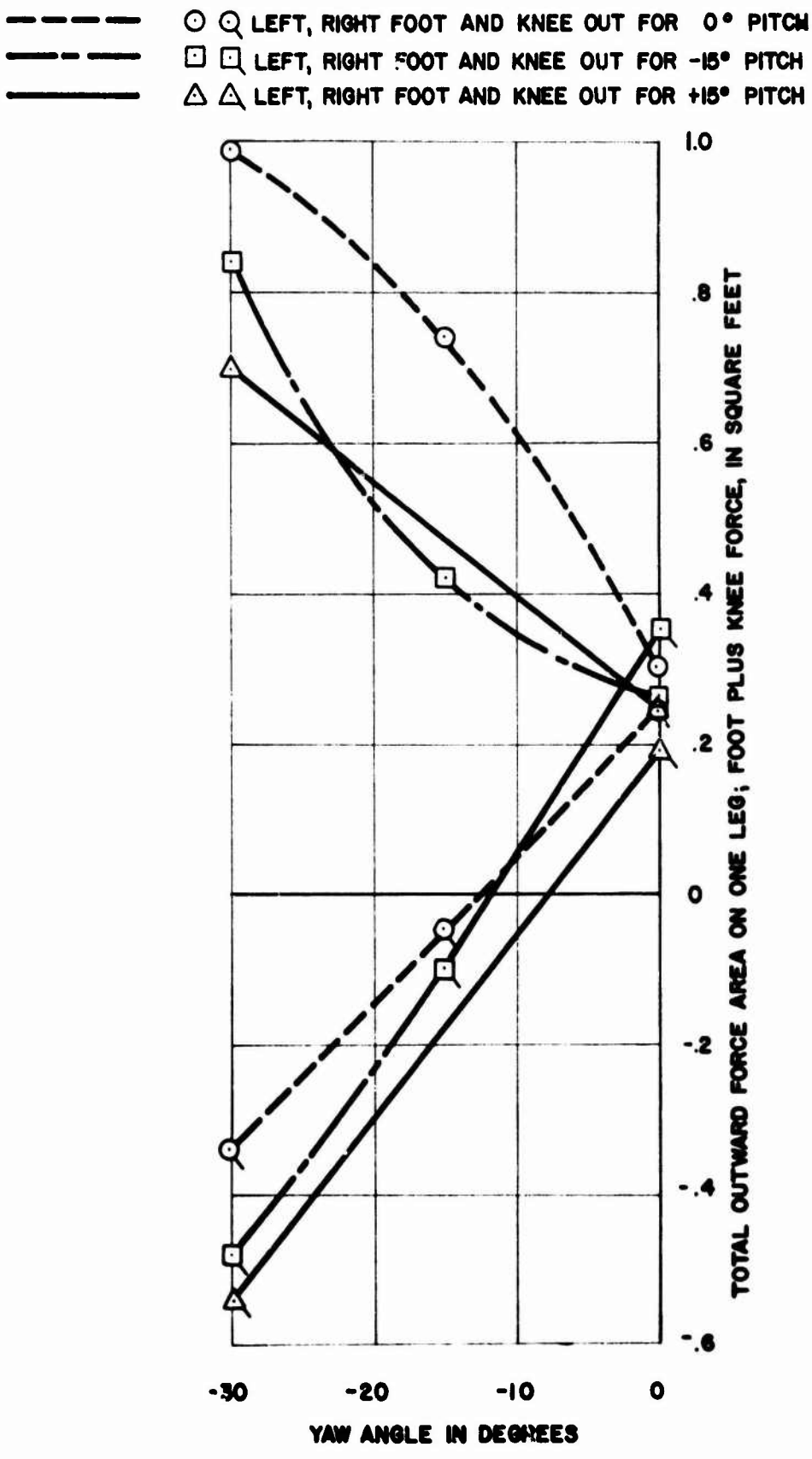

Figure 18. Effect of Pitch and Yaw Angle on the Average Outward Force on the Lower Legs (Knee Force plus Foot Force) in an F-105 Ejection Seat.

The rearward forces on the feet show a remarkable equality between the two feet, both decreasing slightly with the yaw. This appears in both seats, with the ACES-II data consistently nearly twice that of the F-105. This is not an unreasonable result if one assumes that the ACES-II exposes a greater part of the lower leg and offers less support to the calves. Figures 19 and 20 refer.

The forces on the lower arm show little or no sign of systematic variation with pitch and yaw. For comparison of the two seats we disregard the elbow restraint of the F-105 seat and take all the forearm load at the handgrip. The two components outwards and backwards are combined in a single resultant force tending to tear the hand from the grip.

Figures 21 and 22 show the resultant arm force for the two seats. There is a tendency for the load to decrease at larger angles of yaw on the ACES-II seat but this is notable only on the hand opposite to the direction of yaw. The handloads for the ACES-II seat are much higher (nearly twice) than those for the F-105 but the reduction at high yaw angles tends to bring them to the same level. The explanation may be that the arms are more exposed, less cluttered by straps or brackets, and this difference disappears as the seat is rotated relative to the wind. It would seem likely that the initial values (zero yaw) are not exceeded as the rotation develops.

The evidence suggests that the force area acting to break the grip is around 0.3 ft^2 for the ACES-II seat and about 0.20 ft^2 for the F-105. At 500 knots indicated air speed, the dynamic pressure (q) is 850 lb/ft^2, so that we are talking of forces of 255 lb. The values of Figures 21, 22a and 22b therefore look significant in relation to the probability of flail injury at such speeds.

Flail Avoidance Devices (FADs)

Considering the high degree of variation between the dislodgement forces on the individuals occupying the seats, we thought that the forces on the limbs were highly sensitive to changes in form or disposition.

Accordingly the concept of a flail avoidance device was introduced. As an experimental device, without implication as to the final form for service use if successful in reducing the limb forces, a set of spoiler wedges was attached to the limbs of one of the test subjects illustrated in Figure 23a. These appurtenances were of the same order of magnitude as the limbs to which they were attached and had been designed in the expectation that they would generate inward components of force, thus reducing the dislodgement forces.

The results are given in Table 1 and are retabulated for comparison in Table 9. They show (a) an increase generally in the backward component of force, (b) increases in outward forces at zero yaw, (c) reduction or reversal of the outward force on the limb opposite the yaw and augmentation of the outward force on the limb on the yaw (downstream) side. These effects are uneven, but on the whole adverse and strongly suggest that such devices may do more harm than good.

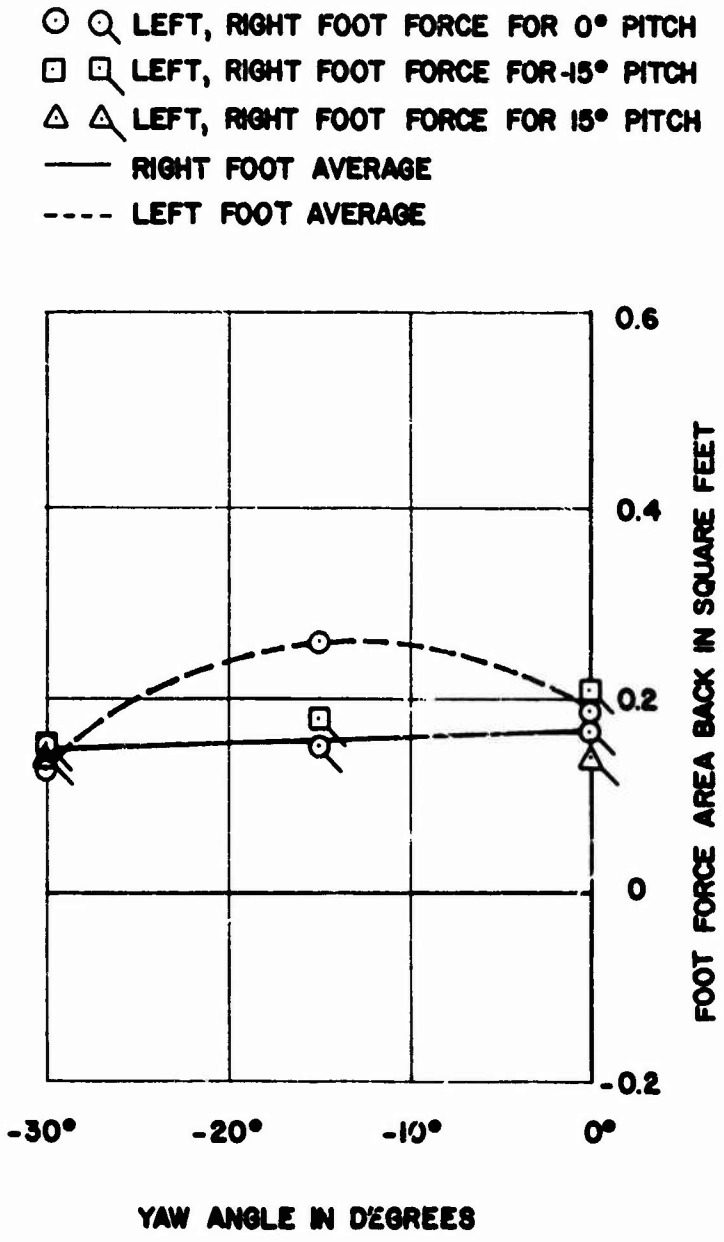

Figure 19. Variation of Foot Force Back with Yaw Angle for the F-105 Seat.
NOTE: Load cell malfunctioned, giving an incomplete range of data points.

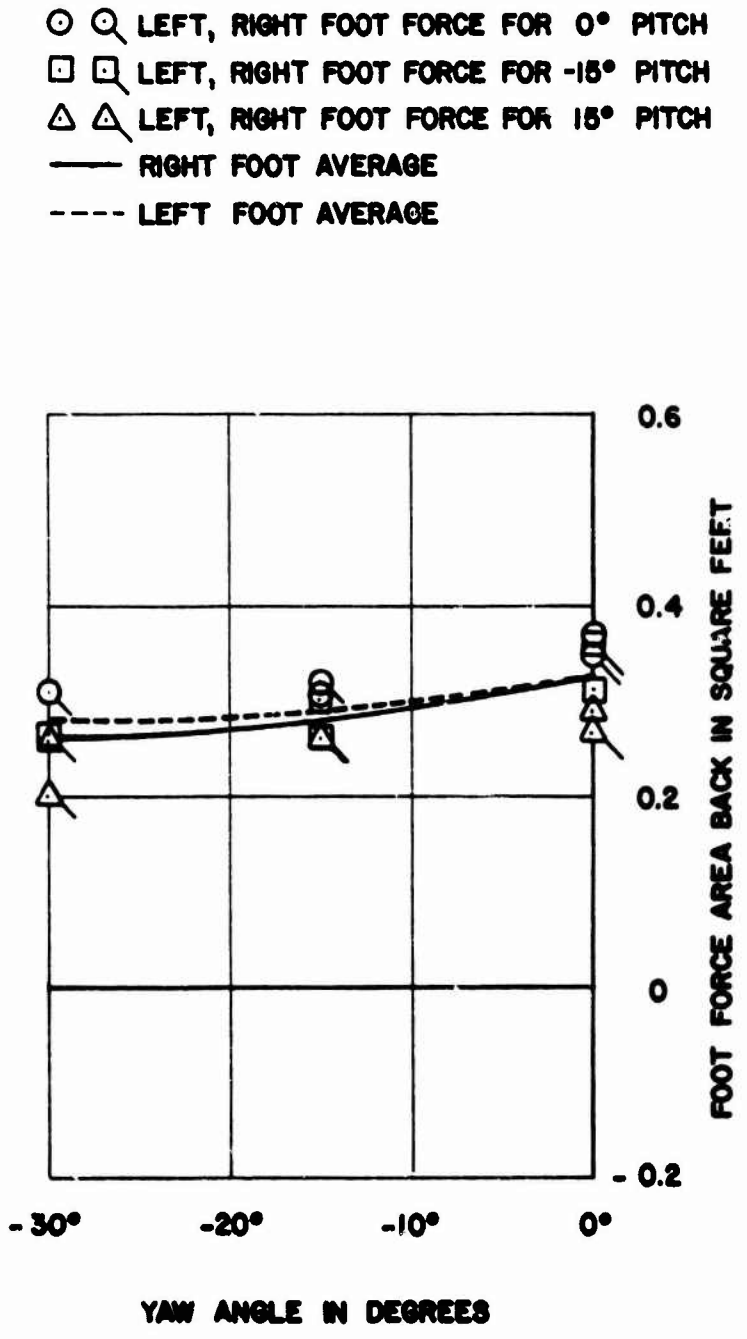

Figure 20. Variation of Foot Force Back with Yaw Angle for the ACES-II Ejection Seat.

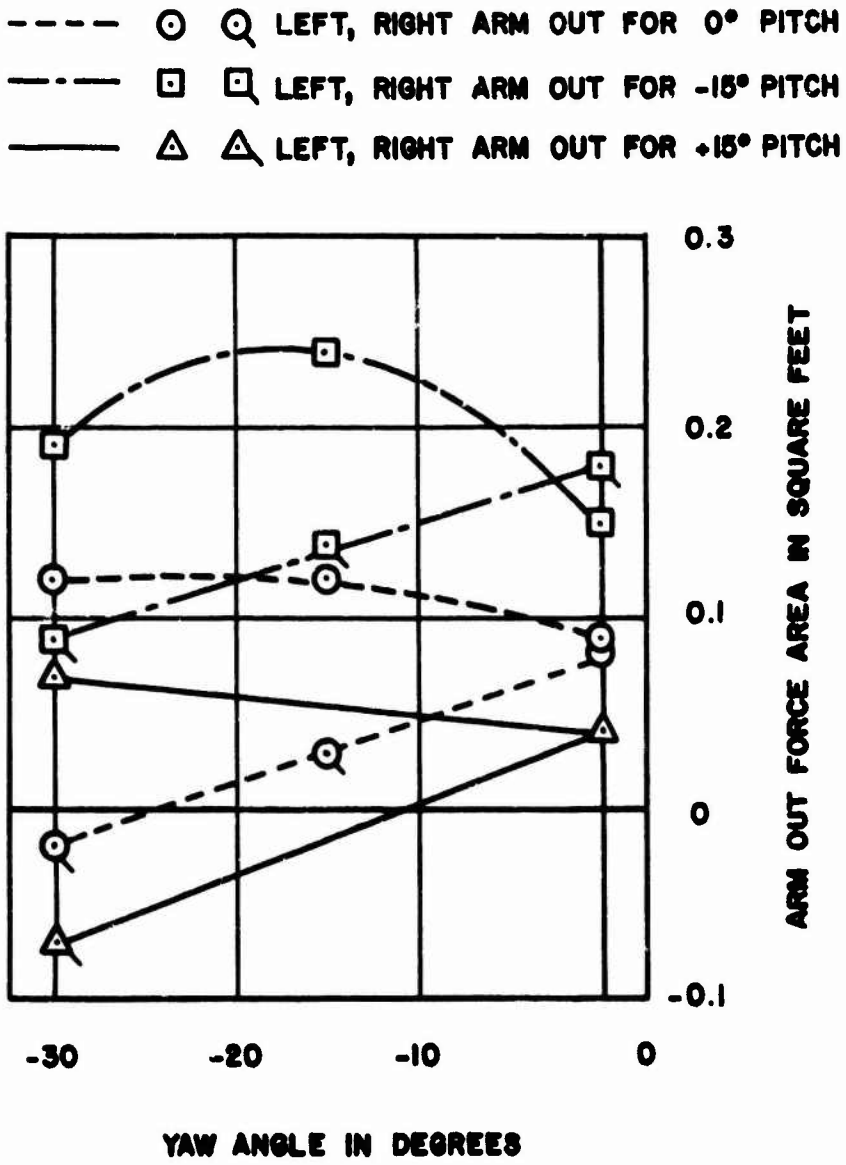

Figure 21. Effect of Pitch and Yaw Angle on the Average Outward Force on the Arms for the F-105 Seat.

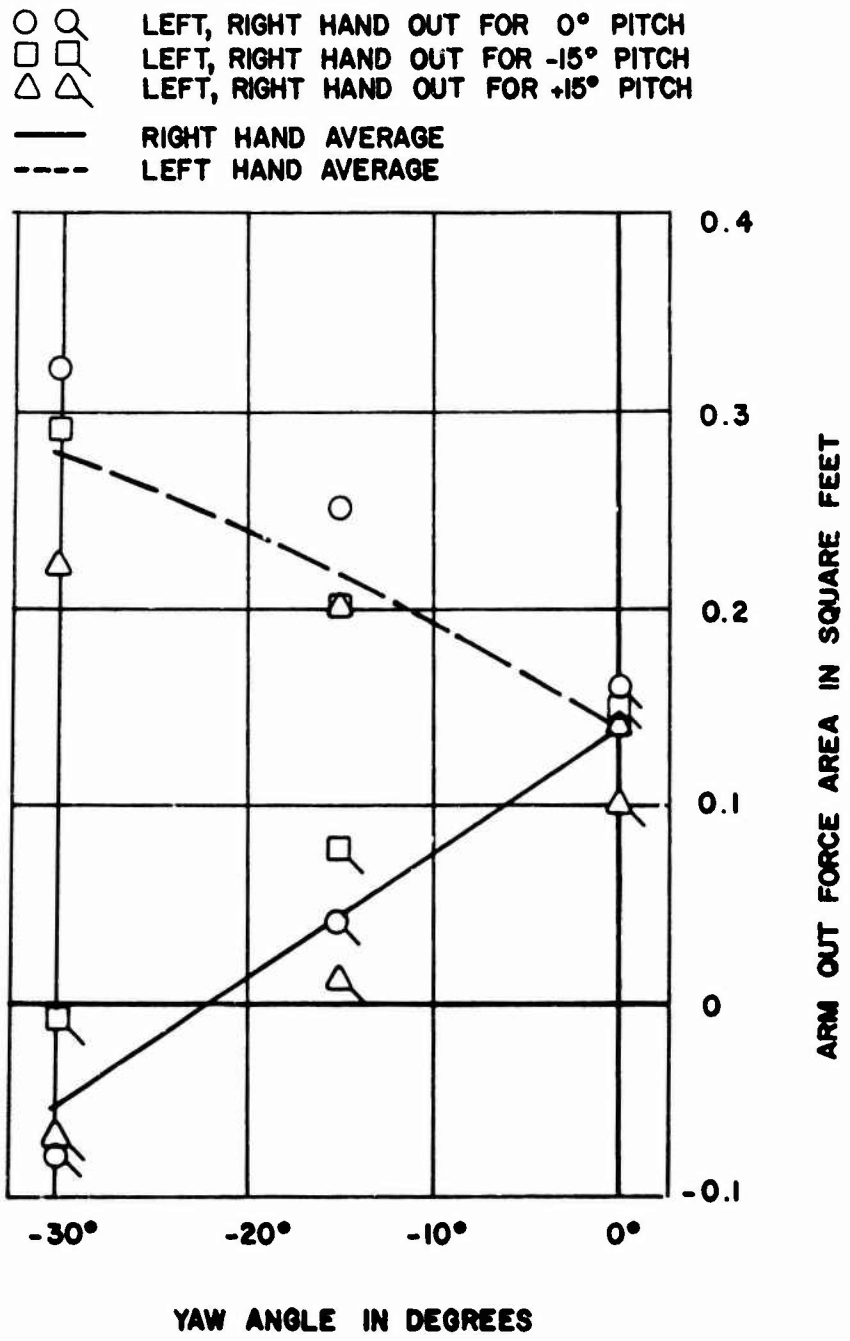

Figure 22a. The Outward Acting Hand Force Component Alone, as a Function of Yaw Angle on the ACES-II Ejection Seat.

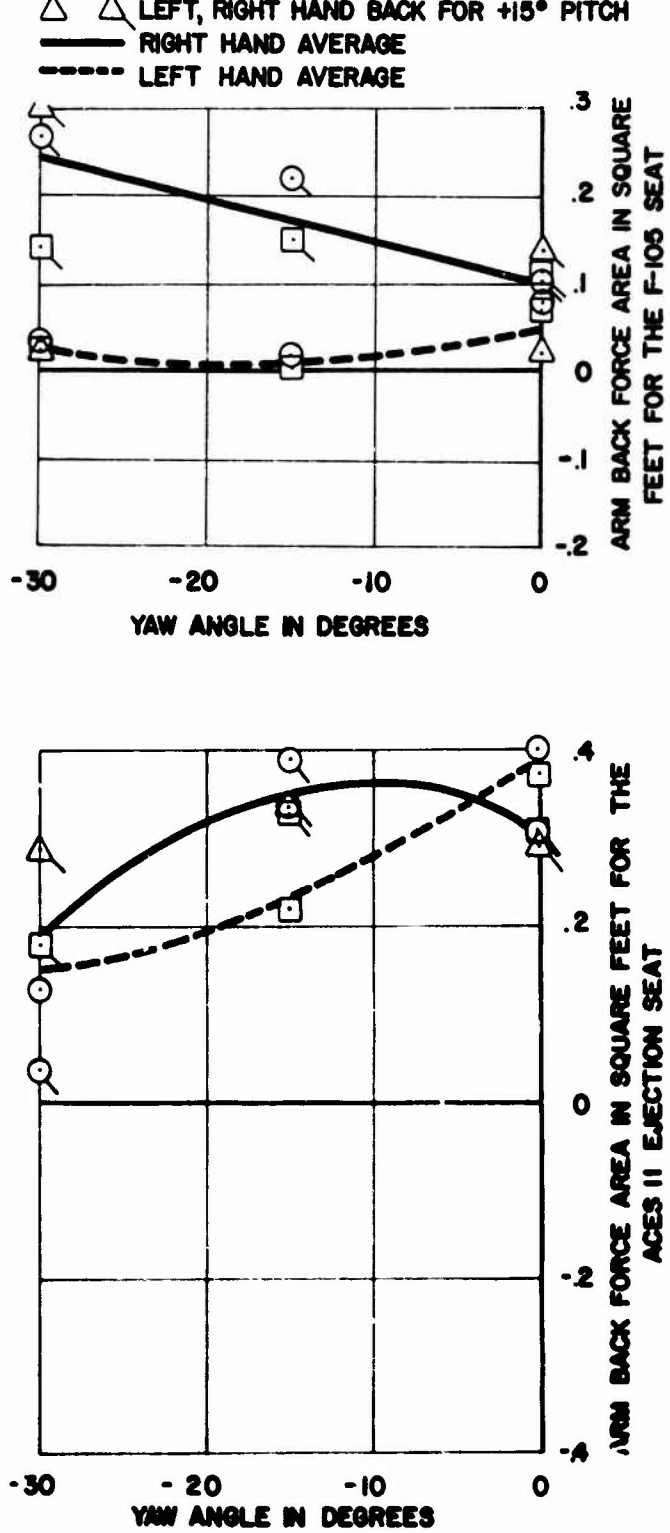

Figure 22b. Arm Back Force Areas for the F-105 and ACES-II Ejection Seats.

Figure 23a. "Spoilers" or "Wedges" Attached to Subject RM as Flow Deflectors in an Effort to Reduce Dislodgement Forces. (F-105 Seat)

Table 8. Average Outward Leg Force Areas for F-105 Seat

Yaw Angle	Pitch Angle	Left Foot Out	Left Knee Out	Total Left	Right Foot Out	Right Knee Out	Total Right
0	-15	0.01	0.25	0.26	0.12	0.23	0.35
0	0	0.08	0.22	0.30	0.02	0.22	0.24
0	+15	-0.005	0.25	0.245	0.06	0.13	0.19
-15	-15	0.07	0.35	0.42	-0.16	0.06	-0.1
-15	0	0.25	0.49	0.74	-0.07	0.02	-0.05
-30	-15	0.23	0.61	0.84	-0.35	-0.13	-0.48
-30	0	0.41	0.58	0.99	-0.20	-0.14	-0.34
-30	+15	0.17	0.53	0.70	-0.37	-0.17	-0.54
		AVERAGE FORCE AREAS WITH WEDGES (Subject RM)					
0	0	-0.1	0.19	0.09	0.01	0.31	0.32
0	-15	-0.05	0.29	0.24	0.07	0.35	0.42
0	+15	0.0	0.31	0.31	0.02	0.22	0.24
-30	+15	0.24	0.79	1.03	-0.37	-0.10	-0.47
-30	-15	0.25	0.79	1.04	-0.35	0.0	-0.35

NOTE: Average right foot out sign has been changed for -15° and -30° yaw angle because of a suspected error in the computerized data analysis.

Table 9. ACES-II Average Foot Force Areas

Yaw Angle	Pitch Angle	Right Foot Back	Left Foot Back	Right Foot Out	Left Foot Out	Right Foot Resultant	Left Foot Resultant
0°	-15°	0.36	0.31	0.07	0.15	0.37	0.34
0°	0°	0.36	0.38	0.10	0.08	0.37	0.39
0°	+15°	0.27	0.30	0.03	0.04	0.27	0.30
-15°	-15°	0.26	0.31	0.0	0.27	0.26	0.41
-15°	0°	0.32	0.31	-0.10	0.23	0.34	0.39
-15°	+15°	0.26	0.26	-0.08	0.11	0.27	0.28
-30°	-15°	0.27	0.26	-0.06	0.43	0.28	0.50
-30°	0°	0.32	0.32	-0.16	0.40	0.36	0.51
-30°	+15°	0.20	0.26	-0.15	0.39	0.25	0.47

Table 10. ACES-II Average Knee Forces

Yaw Angle	Pitch Angle	Right Knee Out	Left Knee Out
0°	-15°	0.21	0.19
0°	0°	0.20	0.20
0°	+15°	0.11	0.05
-15°	-15°	-0.01	0.47
-15°	0°	-0.03	0.46
-15°	+15°	-0.02	0.32
-30°	-15°	-0.30	0.55
-30°	0°	-0.15	0.63
-30°	+15°	-0.10	0.55

Table 11. ACES-II Average Hand Force Data

Yaw Angle	Pitch Angle	Right Hand Out	Left Hand Out	Right Hand Back	Left Hand Back	Right Hand Resultant	Left Hand Resultant
0	-15	0.15	0.14	0.31	0.37	0.34	0.40
0	0	0.16	0.14	0.31	0.40	0.35	0.42
0	+15	0.10	0.10	0.29	0.36	0.31	0.39
-15	-15	0.08	0.20	0.33	0.22	0.34	0.30
-15	0	0.04	0.25	0.39	0.34	0.39	0.42
-15	+15	0.01	0.20	0.34	0.31	0.34	0.37
-30	-15	-0.01	0.29	0.18	0.18	0.18	0.34
-30	0	-0.08	0.32	0.04	0.13	0.09	0.35
-30	+15	-0.07	0.22	0.29	0.17	0.30	0.28

Legboards

As another experiment directed to modification of the aerodynamic forces a pair of boards were set up edgewise to the wind outwards from the lower legs shown in Figure 23b. The results appear in the main table and in the following comparative tabulation.

The legboards illustrated in Figures 23b and 24 gave the following results at zero yaw and -15° pitch, for subject JP:

	Without Legboards	With Legboards
Right Foot Back	0.22	0.16
Left Foot Back	0.24	N.D.
Right Foot Out	0.09	0.13
Left Foot Out	0.11	-0.09
Right Knee Out	0.25	0.36
Left Knee Out	0.23	0.32
Right Arm Out	0.07	0.16
Left Arm Out	0.06	0.19
Right Arm Back	0.06	0.07
Left Arm Back	B.D.	0.01

It is clear that there was no significant aerodynamic benefit from the boards. The boards would act to restrain the legs. The change in sign on the left foot out reading was probably due to a misalignment of the foot. Knee and arm out forces were clearly increased by the presence of the boards.

Limb Retention Nets

At the suggestion of the program monitor, James W. Brinkley, an ad hoc test was made of a system of nets arranged to protect the limbs from injury by restricting their movement. This is in concept an ancillary equipment intended to reinforce the limbs rather than relieve the loading but it is necessary to show that such an arrangement can be effective without introducing disagreeable aerodynamic side effects.

This experiment, by its nature, did not yield quantitative data. Although, obviously, refinement in detail is to be desired, the nets were completely satisfactory in restraining the limbs throughout the test range of pitch and

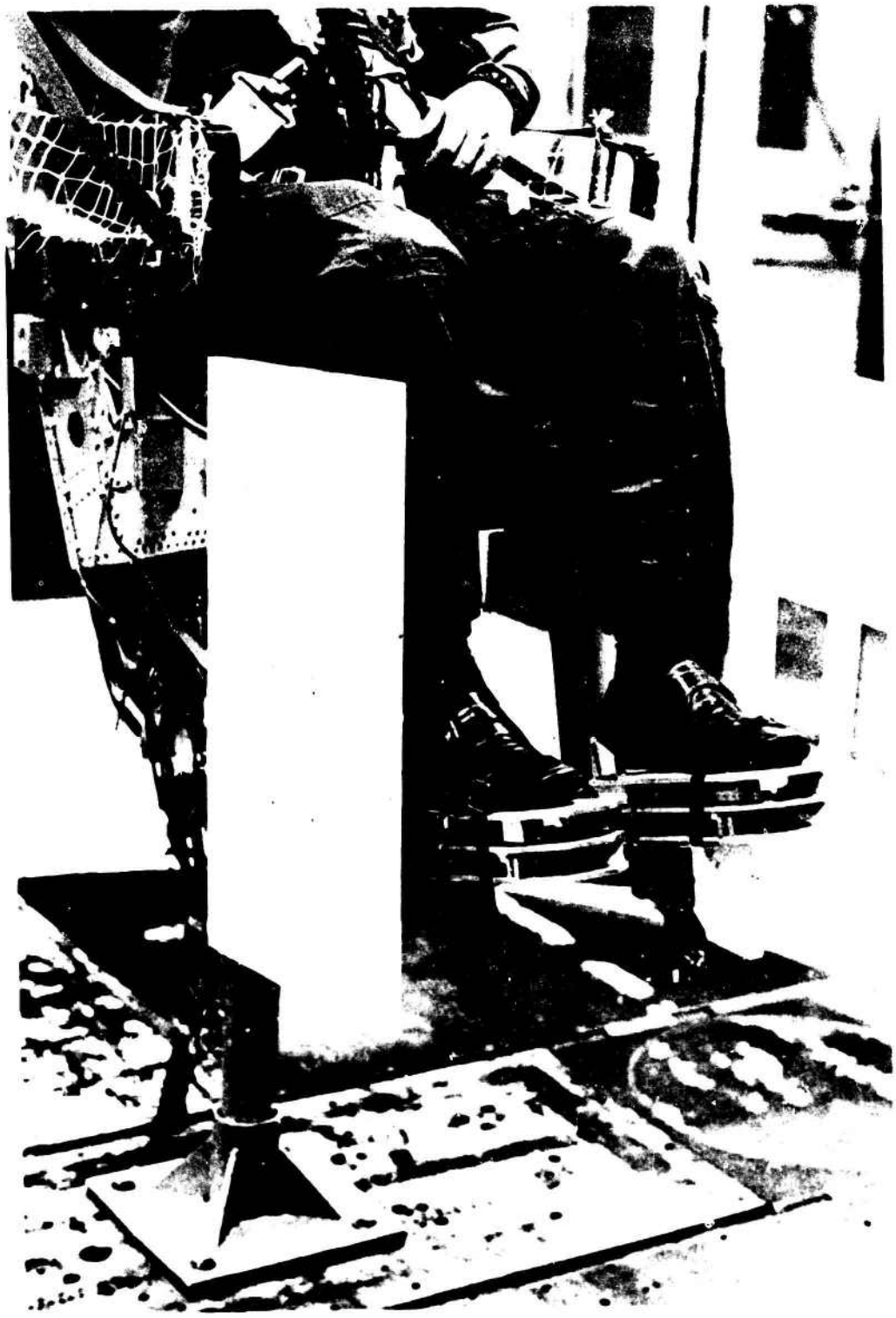

Figure 23b. The "First Mod" Legboards Were Mounted One Inch Out From the Side of the Seat.

yaw angles. It seems likely that this approach to flail prevention will provide an acceptable solution applied to an aerodynamically stable ejection seat. The nets would be stowed out of the way of normal operations and would be deployed automatically prior to ejection. The arm system, as tested for the F-105 seat, is shown in Figures 24 and 25 and the lower leg system in Figure 26.

The arm and leg restraining nets were further developed for the ACES-II ejection seat. These nets, as shown in Figures 27 and 28 provided a realistic operational simulation. Major Ray Madson, test subject from the Aerospace Medical Research Laboratory, systematically evaluated the restraining nets. At high angles of attack the leg nets were judged less effective because of the lift on the legs. The arm nets should be higher than the underarms for positive retention of the arms. The restraining leg and arm nets were judged to be satisfactory in capturing the limbs if the seat were to fly in a stable configuration.

Static Stability

In the initial stages the motion of an ejection seat and occupant after leaving the aircraft is characterized by high resultant velocity derived from the forward speed of the aircraft and of the ejection velocity relative to it. The resultant velocity, referred to the seat axis, is forward and upwards; the lateral velocity, angular rate of roll, and of yaw, are all those of the aircraft at the moment of separation and are conveniently thought of as small. This permits the simplification of treating the motion as two dimensional involving only the resultant velocity and the angle of pitch or yaw. The attempt is made to analyze the motion in the general case of ejection with arbitrary conditions in the six degrees of freedom; however, some of the effects of asymmetry may be allowed for to some degree by inserting sideslip (yaw) into the initial conditions by checking upon the magnitude of rolling moments for a range of values in pitch and yaw.

In the present series of tests, measurements were made on the ACES-II seat of the overall aerodynamic forces (using the tunnel balance system) to express the three moments (roll, pitch, yaw) as volumes (M/q) over a range of values of pitch and yaw attitudes. This data, with the lift, drag and side force data, is presented in Tables 2, 6, 7 and Figures 29 - 36.

By extending the range of measurement to $\pm 180°$ we would expect to plot a quasi-sinusoidal curve which intersected the axis at two points in the cycle. This would apply to both pitch and yaw. The pitch range is somewhat difficult to set up experimentally because of support problems but the complete rotation in yaw is easily arranged. Figures 29 and 30 present sample curves for the ACES-II seat. Evidently, intersections with negative slope ($M = 0$, $\partial M/\partial \theta = 0$) alternate with positions of positive slope. A position with negative slope is statically stable because a small displacement from the position of zero moment generates a restoring moment; likewise a positive slope generates a moment promoting the displacement.

Figure 24. A Combination of a Low Net and Lateral Straps to Entrap the Arms and Prevent Dislodgement. (F-105 Seat)

Figure 25. A Close-Up Detail of the Arm Retention Flail Avoidance Device on the F-105 Ejection Seat.

Figure 26. The Lower Leg Entrapment Net for the F-105 Ejection Seat

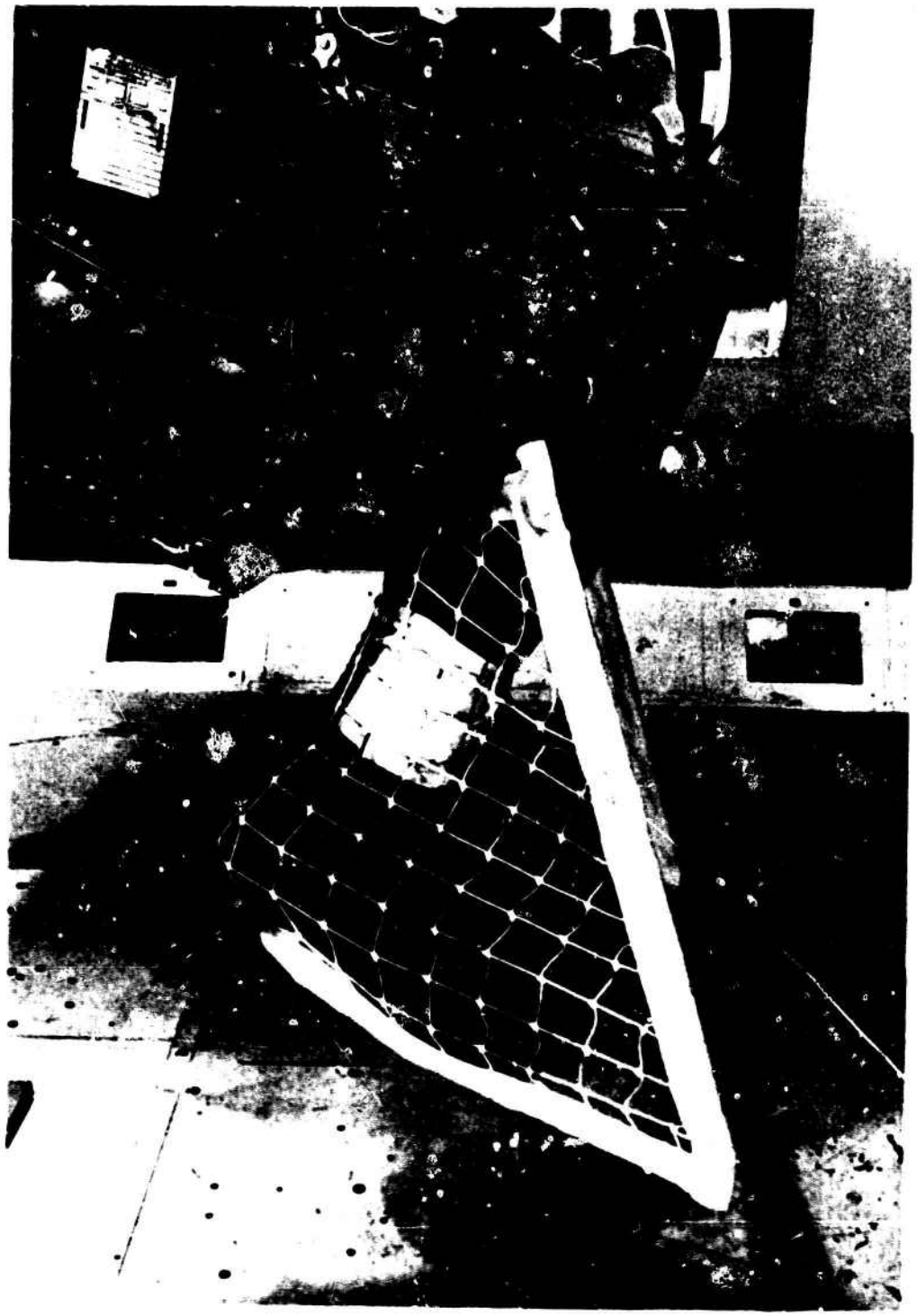

Figure 27. Leg Restraint Nets Tested on the ACES-II Ejection Seat.

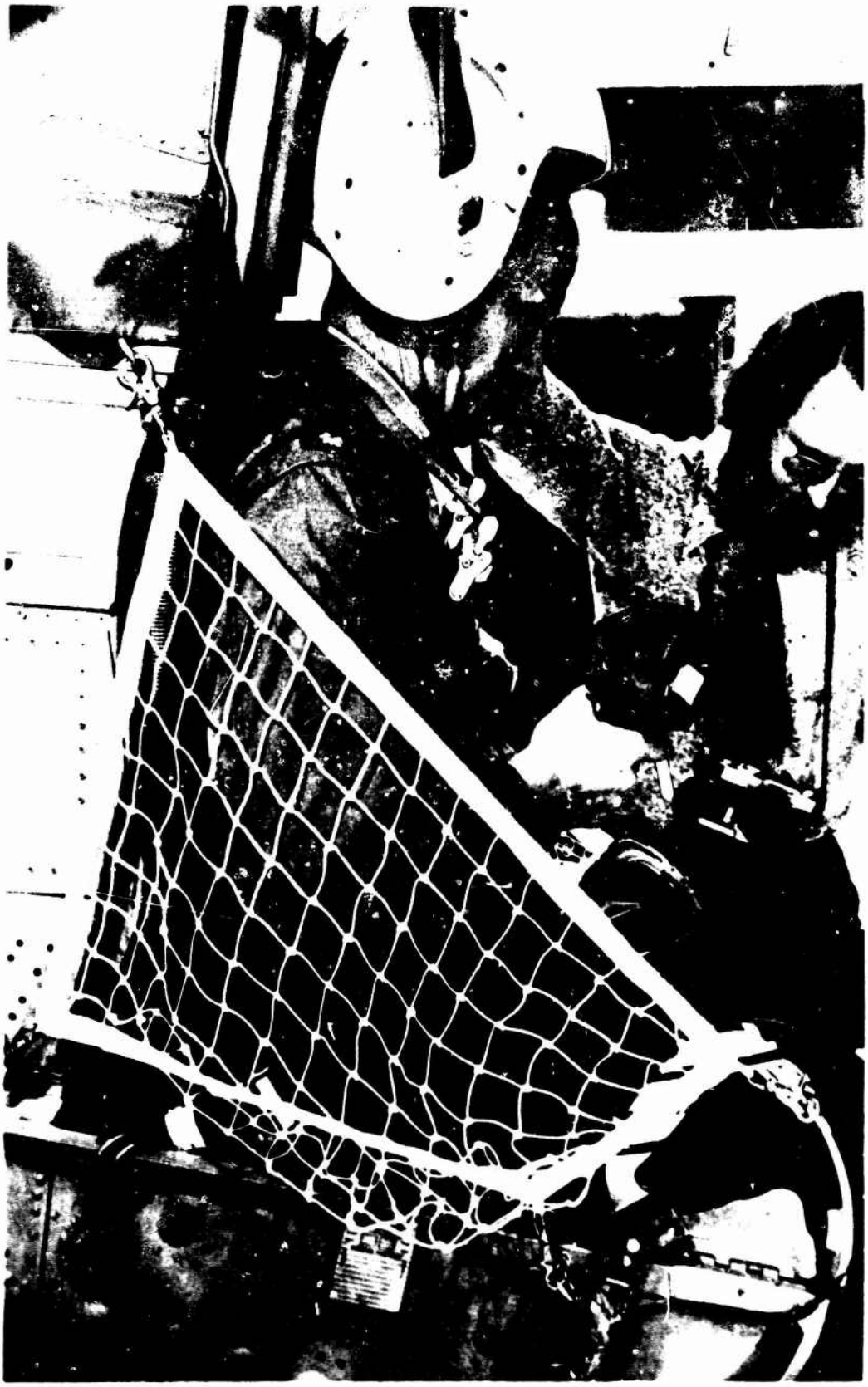

Figure 28. Arm Restraint Nets Tested on the ACES-II Ejection Seat.

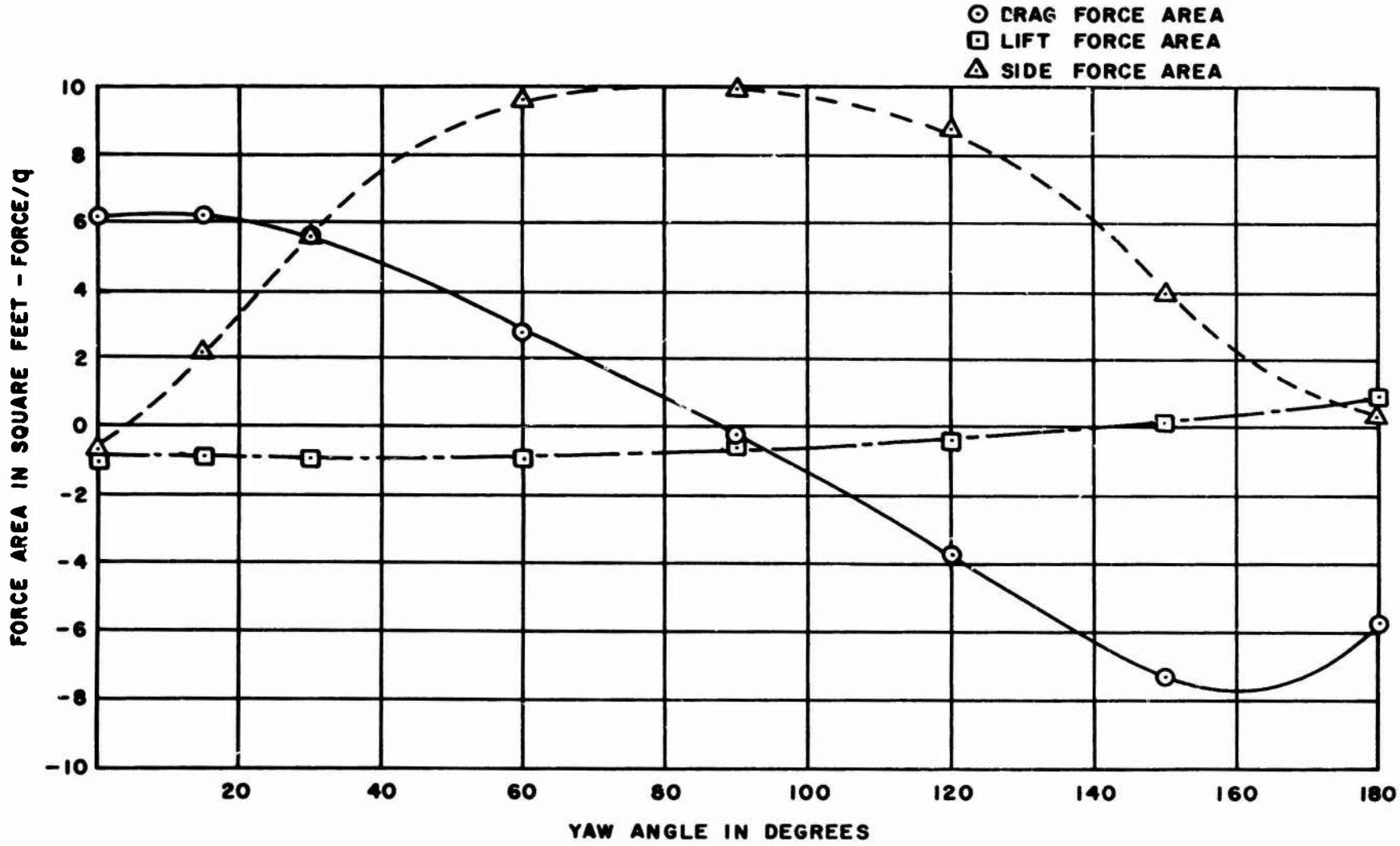

Figure 29. ACES-II Seat Forces as a Function of Yaw Angle Relative to Body Axis for Zero Pitch Angle. Subject: FWH.

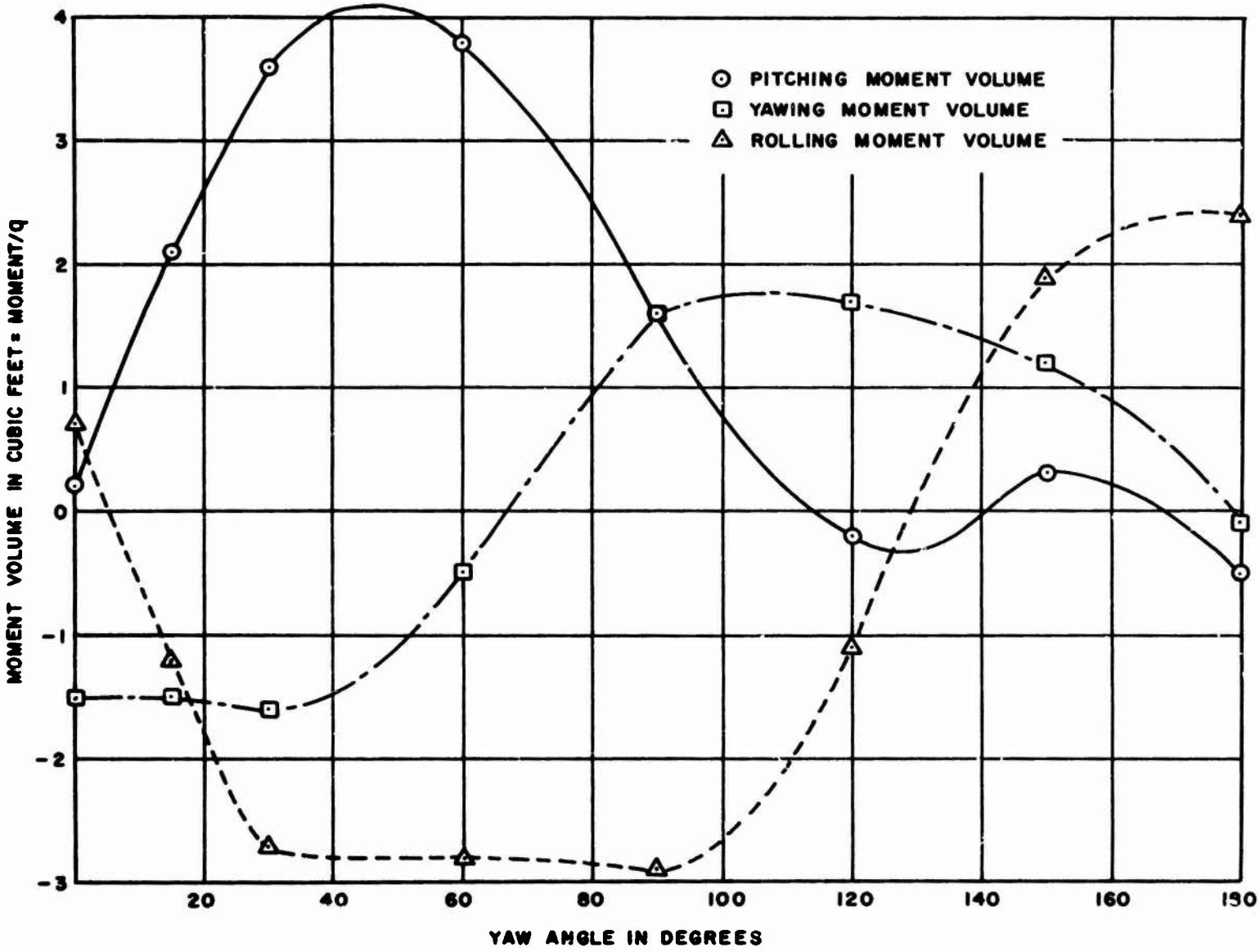

Figure 30. ACES-II Seat Moments Relative to Body Axis for Zero Pitch as a Function of Yaw Angle. Subject: FWH.

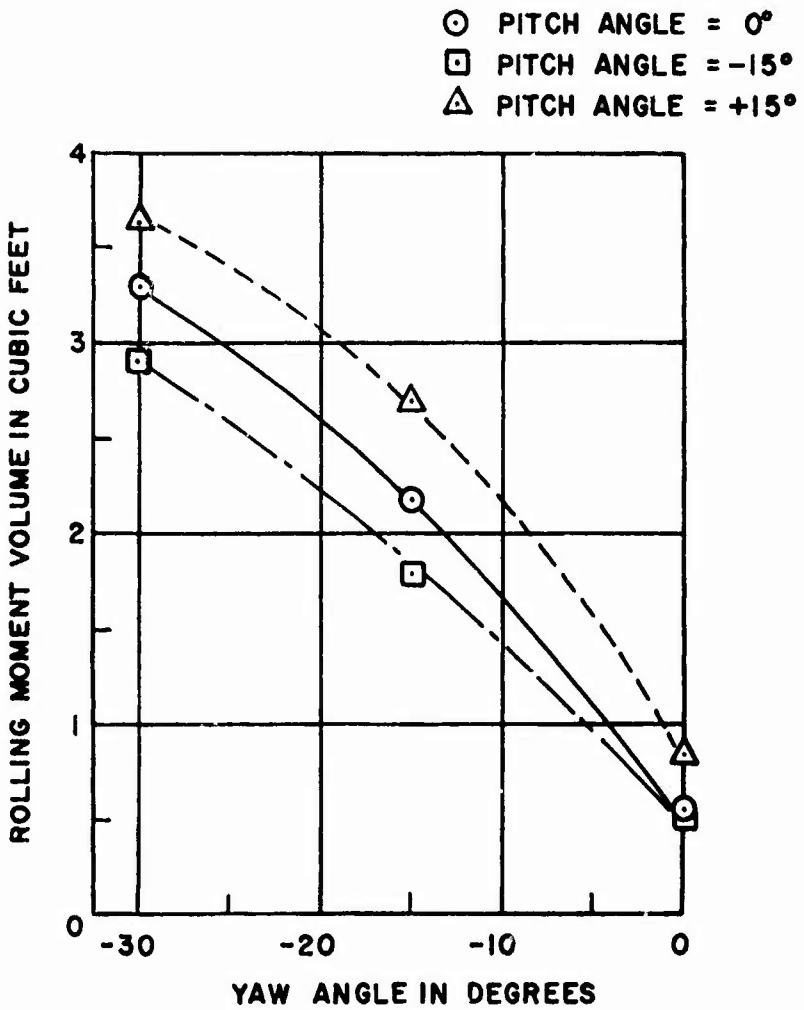

Figure 31. Average Rolling Moment Volume as a Function of Yaw Angle for the ACES-II Ejection Seat. (All Subjects)

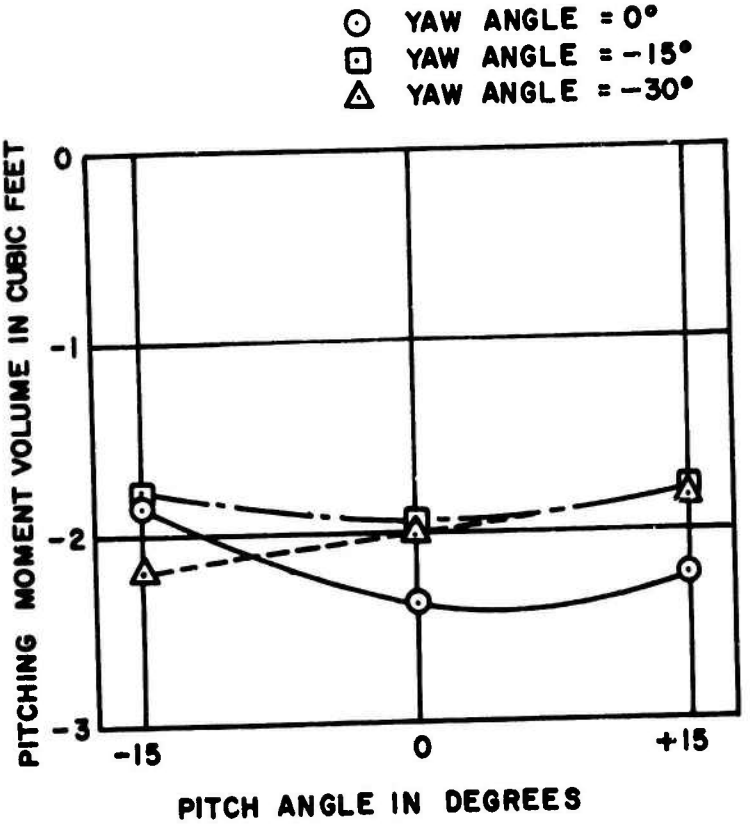

Figure 32. Average Pitching Moment Volume as a Function of Pitch Angle for the ACES-II Ejection Seat. (All Subjects)

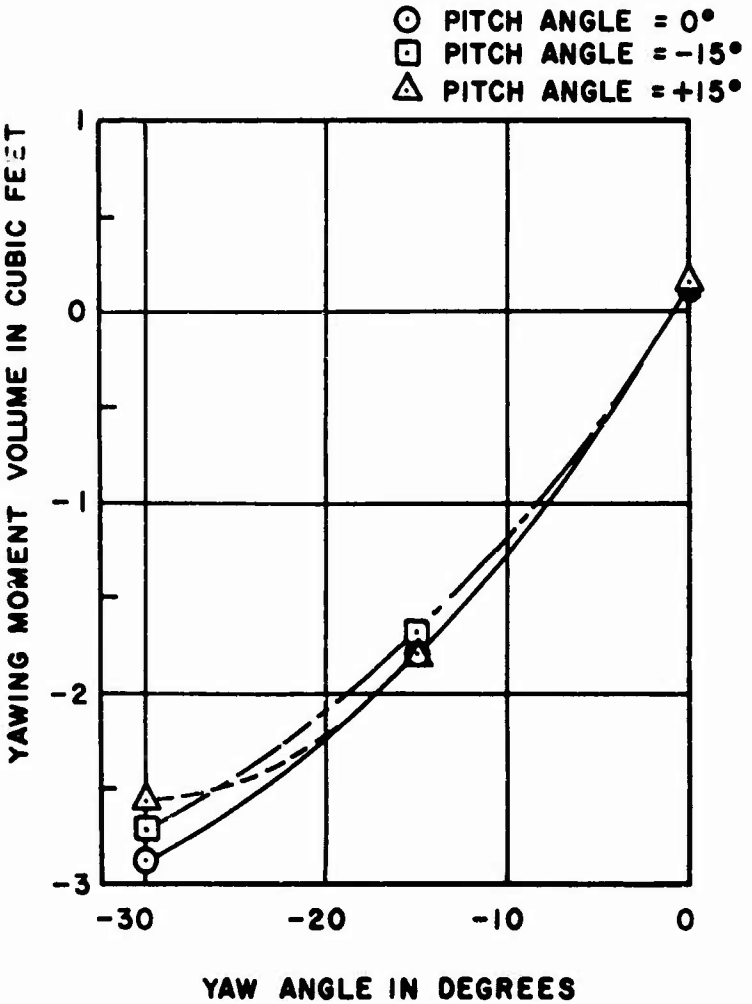

Figure 33. Average Yawing Moment Volume as a Function of Yaw Angle for the ACES-II Ejection Seat. (All Subjects)

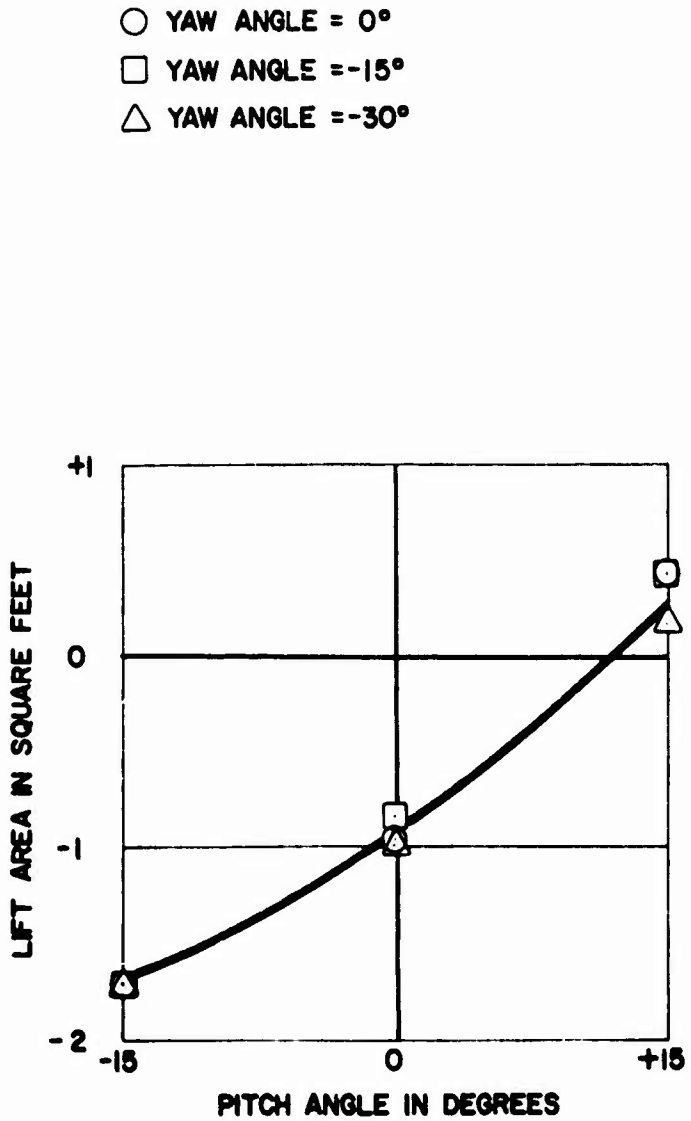

Figure 34. Average Lift Area as a Function of Pitch Angle for the ACES-II Ejection Seat. (All subjects)

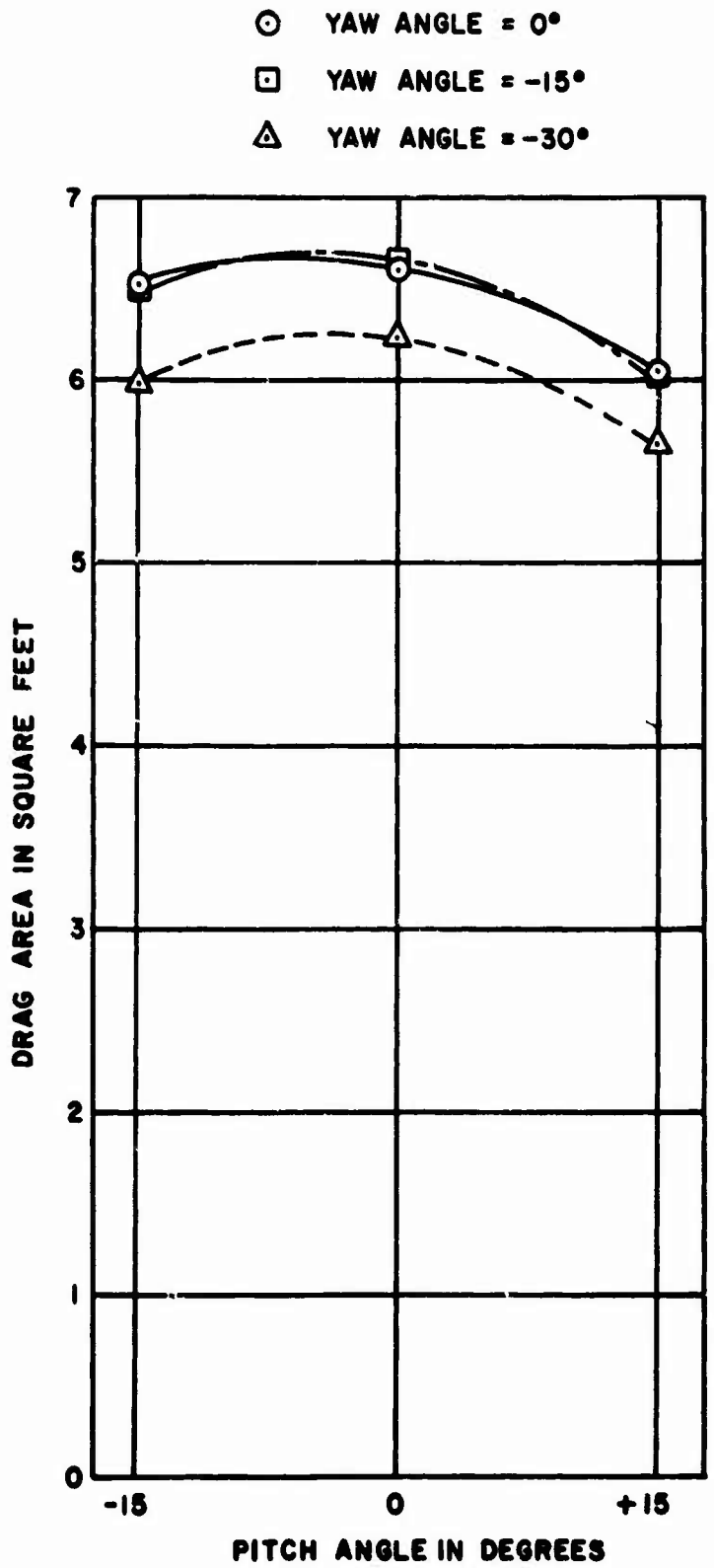

Figure 35. Average Drag Area as a Function of Pitch Angle for the ACES-II Ejection Seat. (All Subjects)

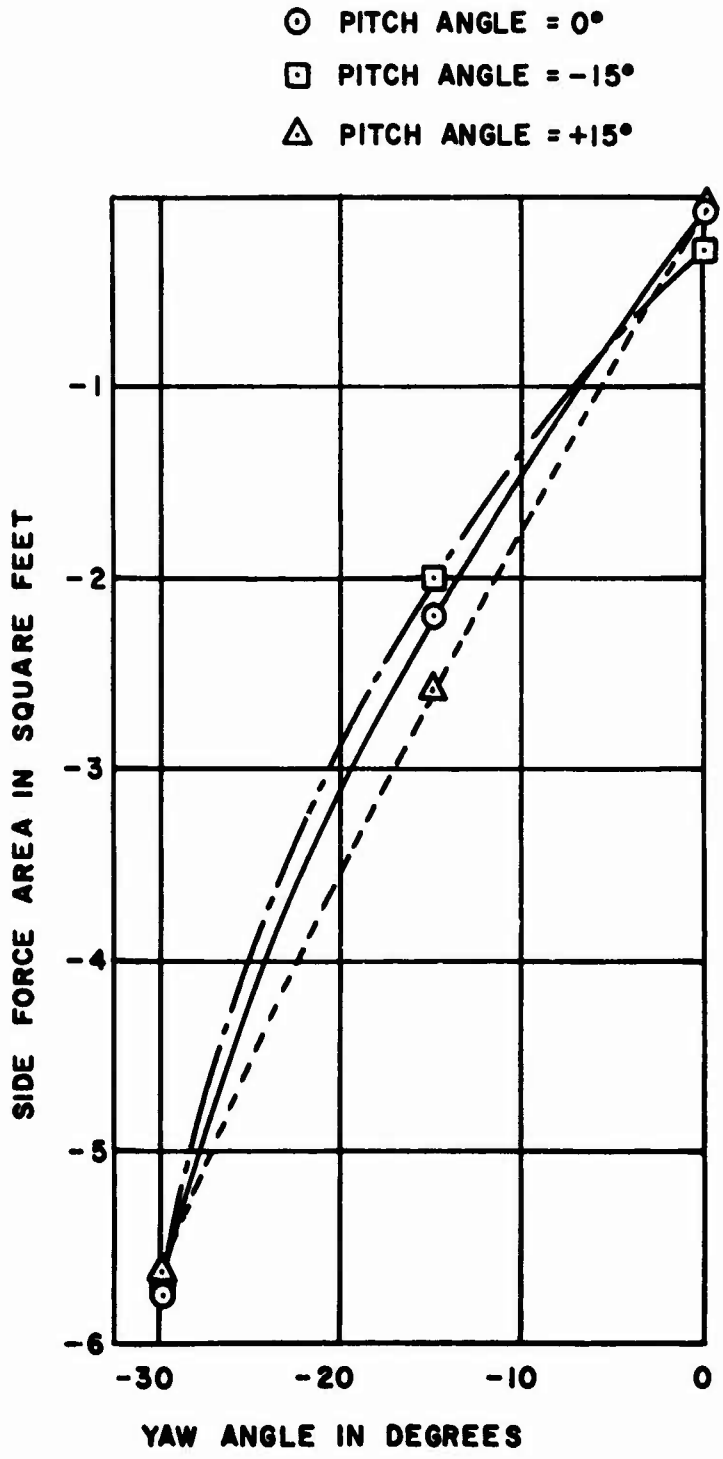

Figure 36. Average Side Force Area as a Function of Yaw Angle for the ACES-II Ejection Seat. (All Subjects)

A seat is judged to be statically stable in pitch and yaw if the launch attitude is close to moment zeros with negative slope on both pitch and yaw moment curves.

Force and Moment Data for the F-105 Seat

Table 3 presents the force and moment data for the empty F-105 seat. Moments are referred to the seat datum point, which closely approximates center of mass for the seat plus the median occupant, as defined in Figure 3. It will be observed that, for each angle of pitch (+15°, 0°, -15°) the pitching moment M is negative and the slope $\partial M/\partial\theta$ is positive. Considering the large drag force the moment could be trimmed to zero by a small downward movement of the C.G. with little effect upon the positive slope. This shows that the seat is statically unstable in pitch in this range of pitch and yaw angles. (Figures 37 - 42.)

Tables 4 and 5 give the force and moment data for the F-105 seat occupied in turn by each of the test subjects (Figures 43 through 48). For comparison with the empty seat the arithmetic means of the values for the subjects have been taken as the best available data for the median man. The comparison shows that the presence of the occupant

1. reduces the negative lift substantially
2. has little effect on drag
3. slightly increases the side force
4. destabilizes in yaw (the yawing moment decreases with the yaw angle)
5. slightly reduces the rolling moment produced by yaw angle

These results clearly indicate that the occupied F-105 seat is statically unstable in pitch for the range of physical dimensions of the occupants tested and especially for the median of the test subjects. There is indication also of static instability in yaw which is just as important as pitch instability. (Yaw instability by itself would lead to spinning like a top; even if limited to the first 180°, it could complicate drogue release and introduce disagreeable, perhaps intolerable, rotary accelerations under drogue forces.)

Force and Moment Data for the ACES-II Seat

The ACES-II seat with three of the above mentioned occupants was examined in similar fashion in a later series of tests. Results are given in Tables 6 and 7. The pitch stability is summarized by Figure 32 which shows negative values of the moment with the slope going from slightly stable at zero yaw to about slightly unstable at -30° yaw. After trimming to zero moment this would indicate a more or less neutral static stability ($\partial M/\partial\theta \approx 0$) over the yaw angles but the information is not sufficient basis for any more precise statement.

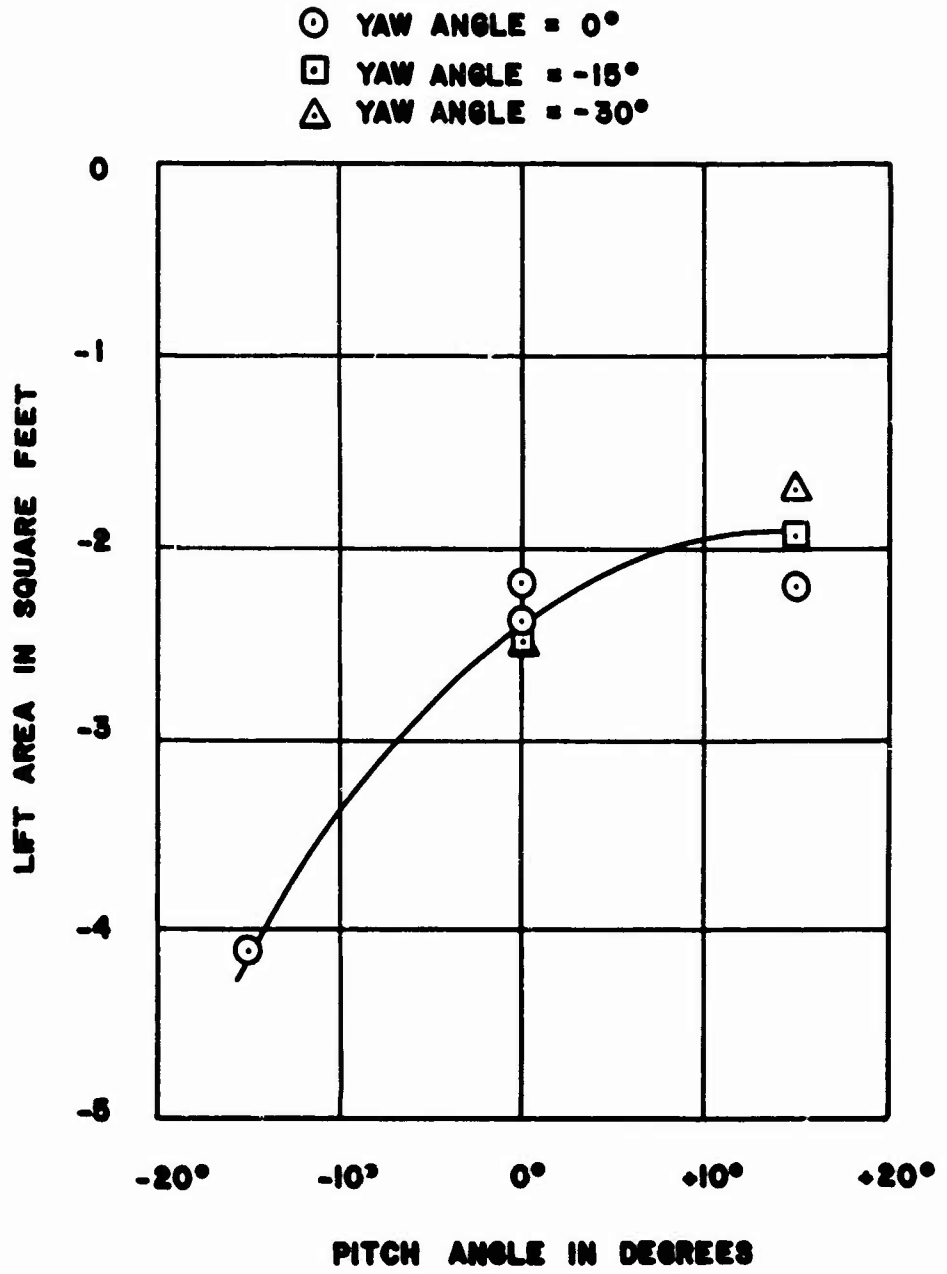

Figure 37. Empty Seat Lift Area, as a Function of Pitch Angle, for the F-105 Ejection Seat.

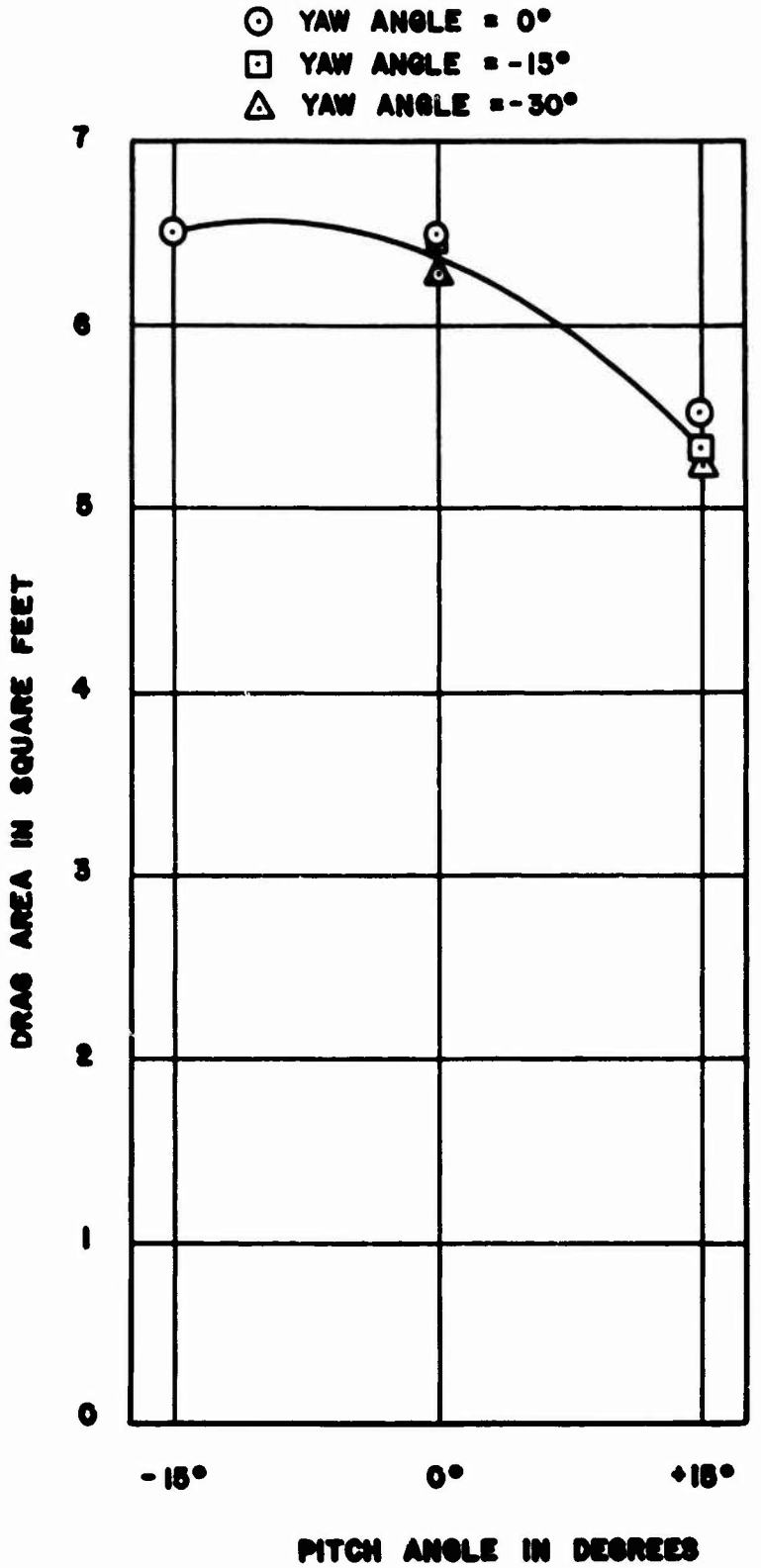

Figure 38. Empty Seat Drag Area, as a Function of Pitch Angle, for the F-105 Ejection Seat.

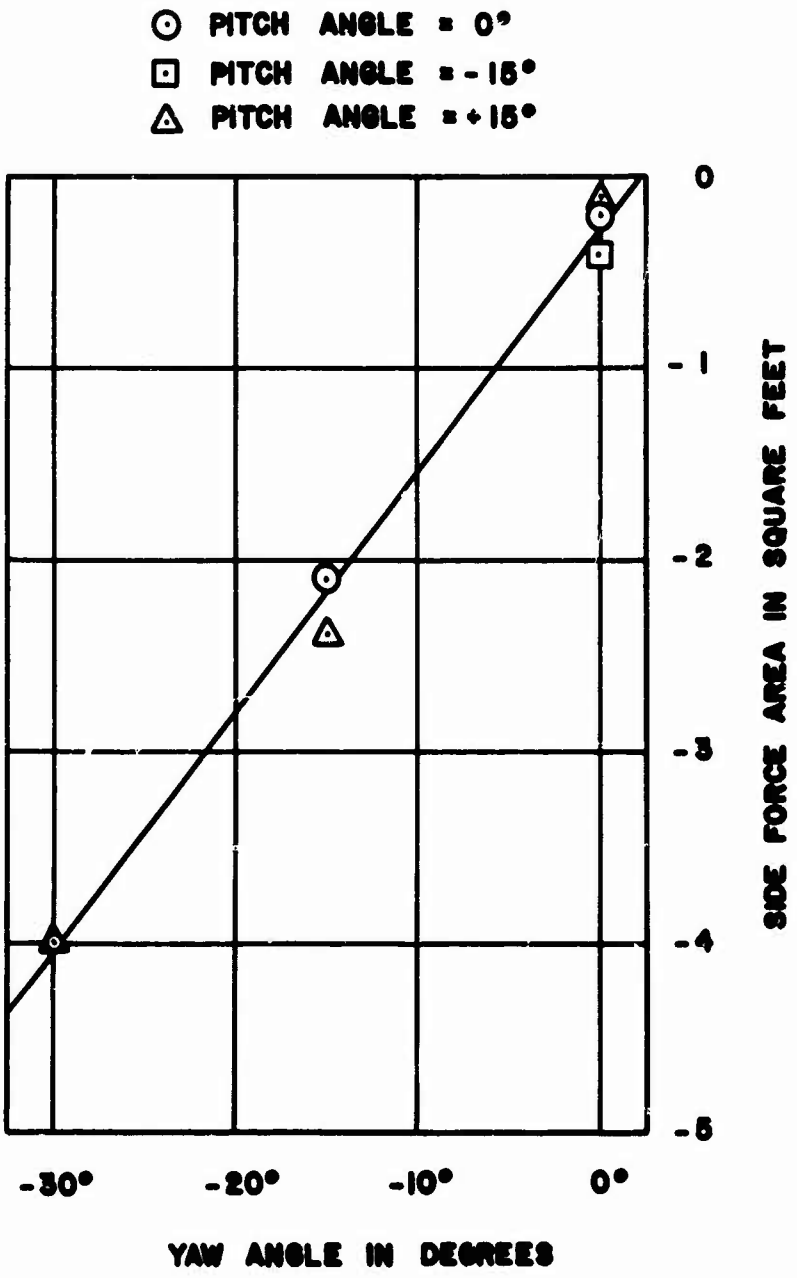

Figure 39. Empty Seat Side Force as a Function of Yaw Angle, for the F-105 Ejection Seat.

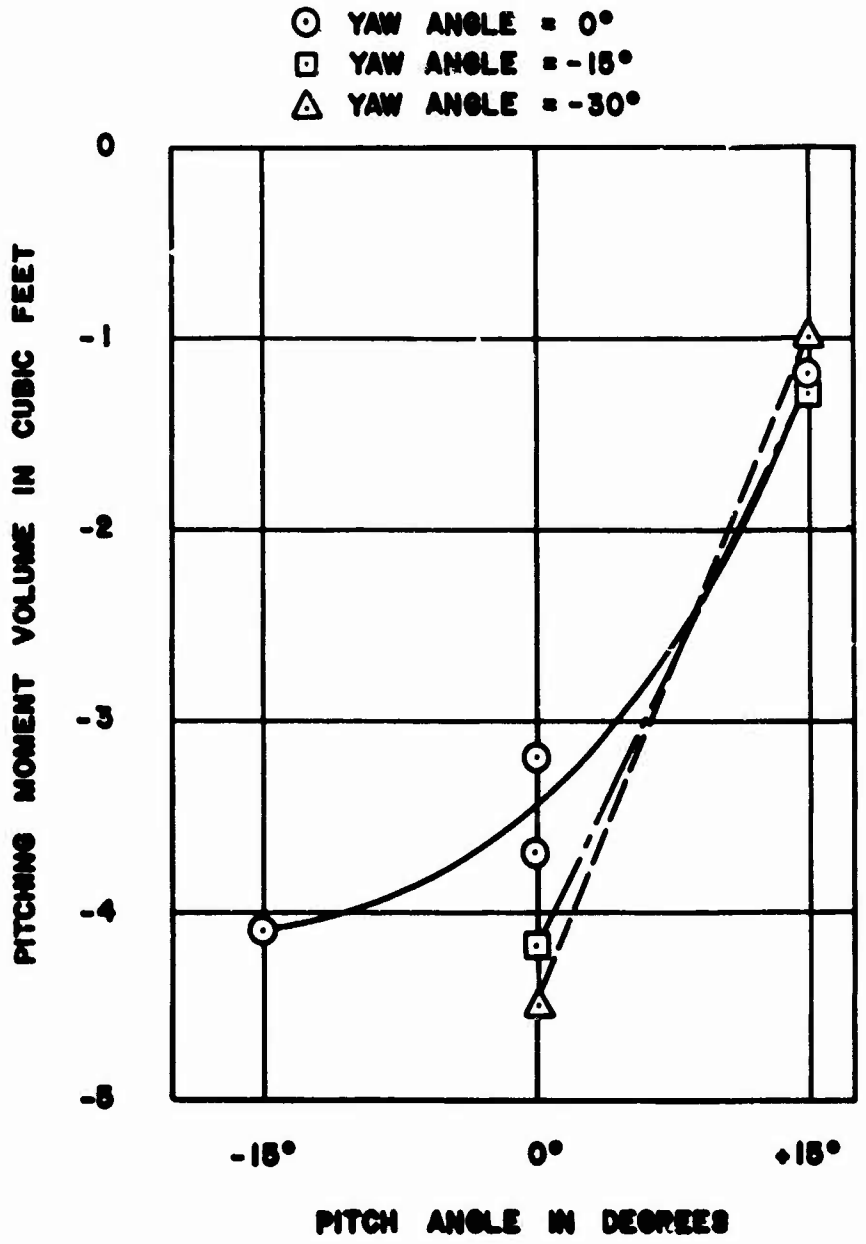

Figure 40. Empty Seat Pitching Moment, as a Function of Pitch Angle, for the F-105 Ejection Seat.

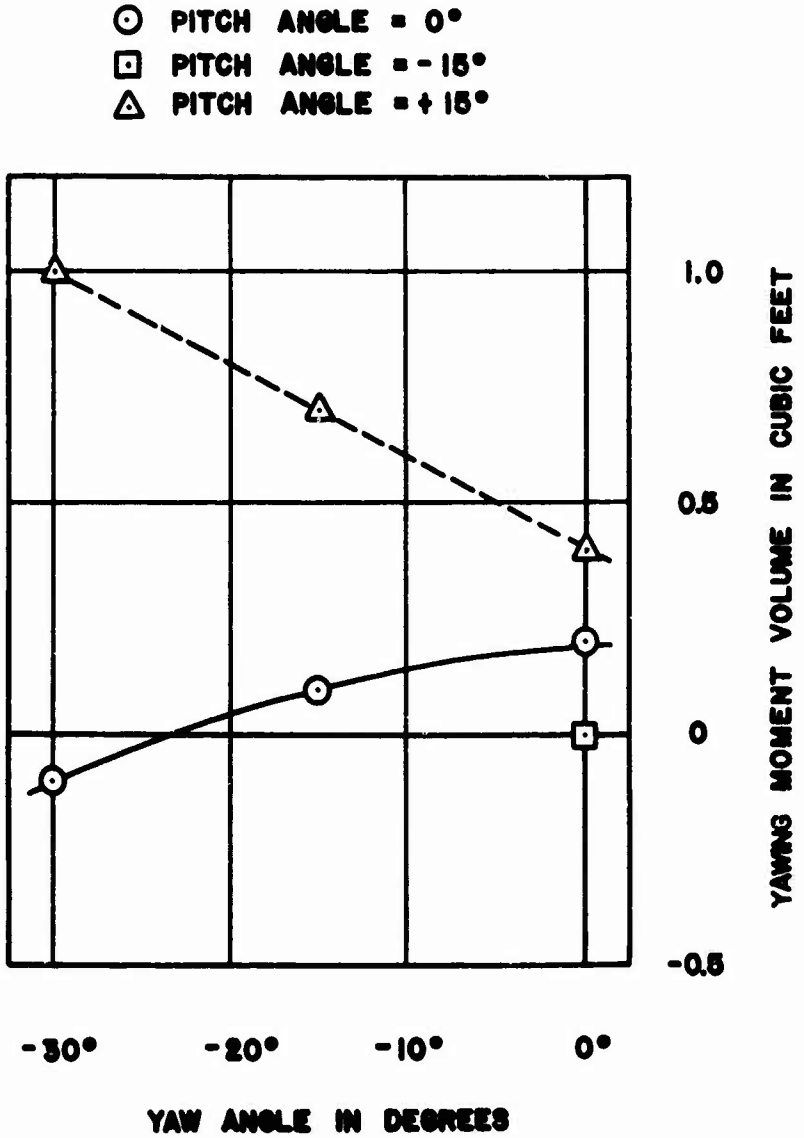

Figure 41. Empty Seat Yawing Moment as a Function of Yaw And Pitch Angle for the F-105 Seat.

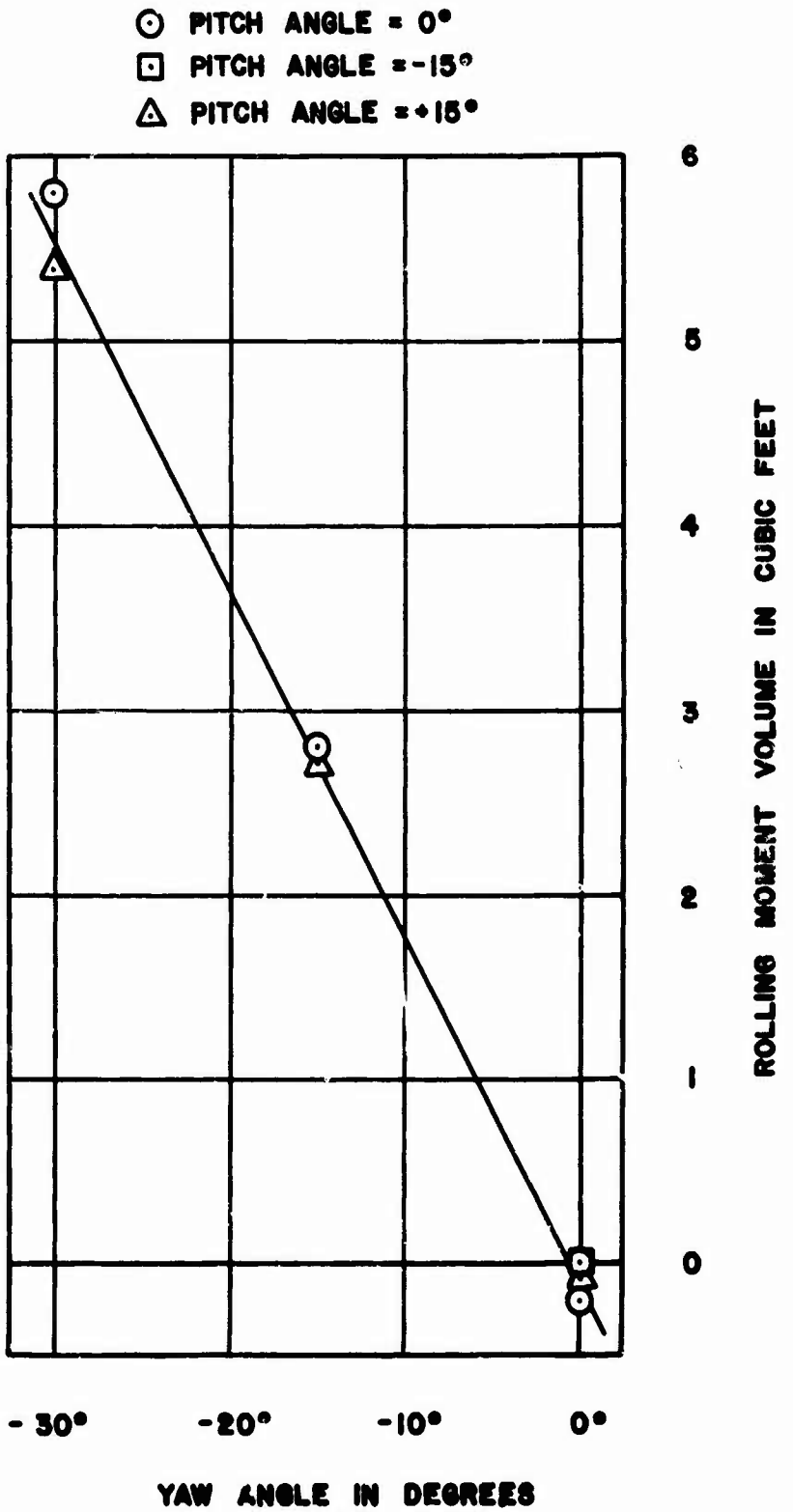

Figure 42. Empty Seat Rolling Moment, as a Function of Yaw Angle, for the F-105 Ejection Seat.

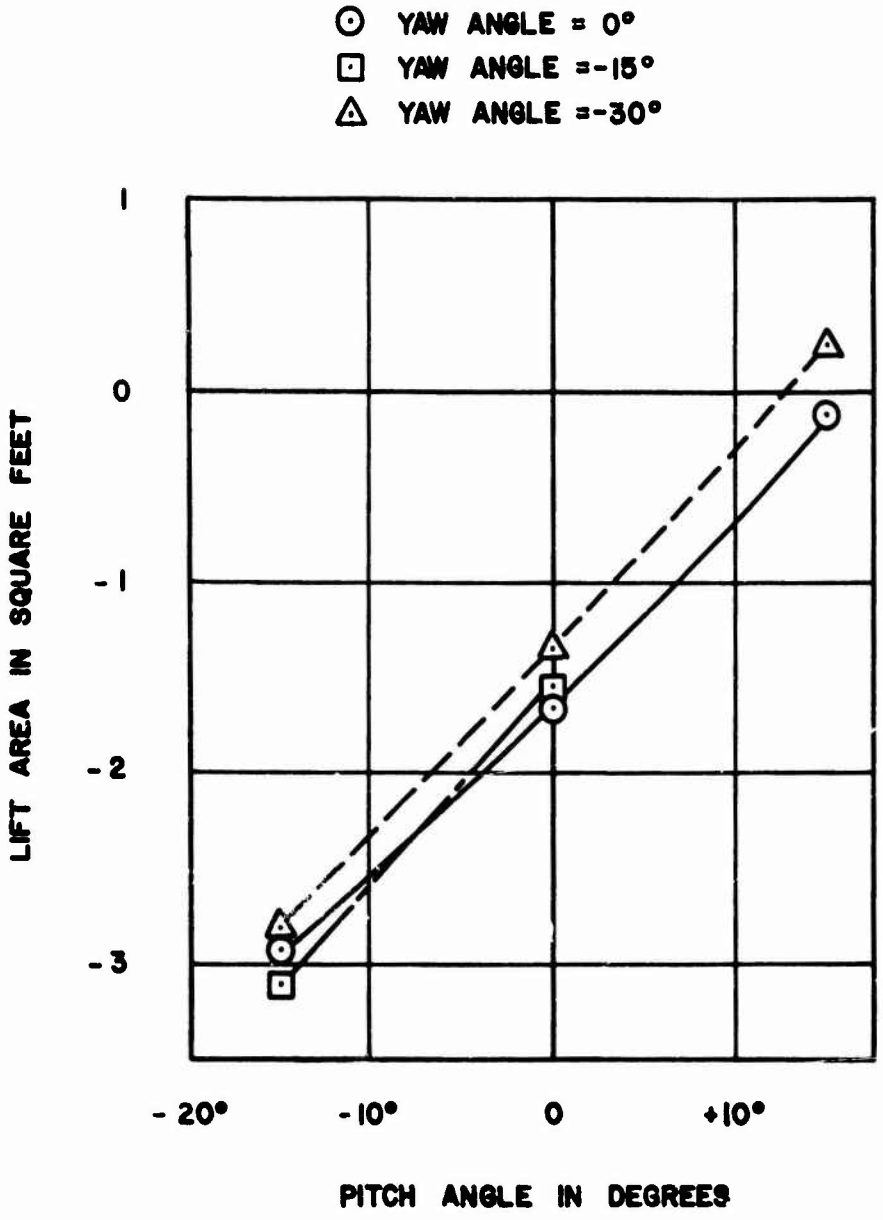

Figure 43. Average Lift Force (All Subjects), as a Function of Pitch Angle, for the Standard Side-Arm Configuration, for the F-105 Ejection Seat.

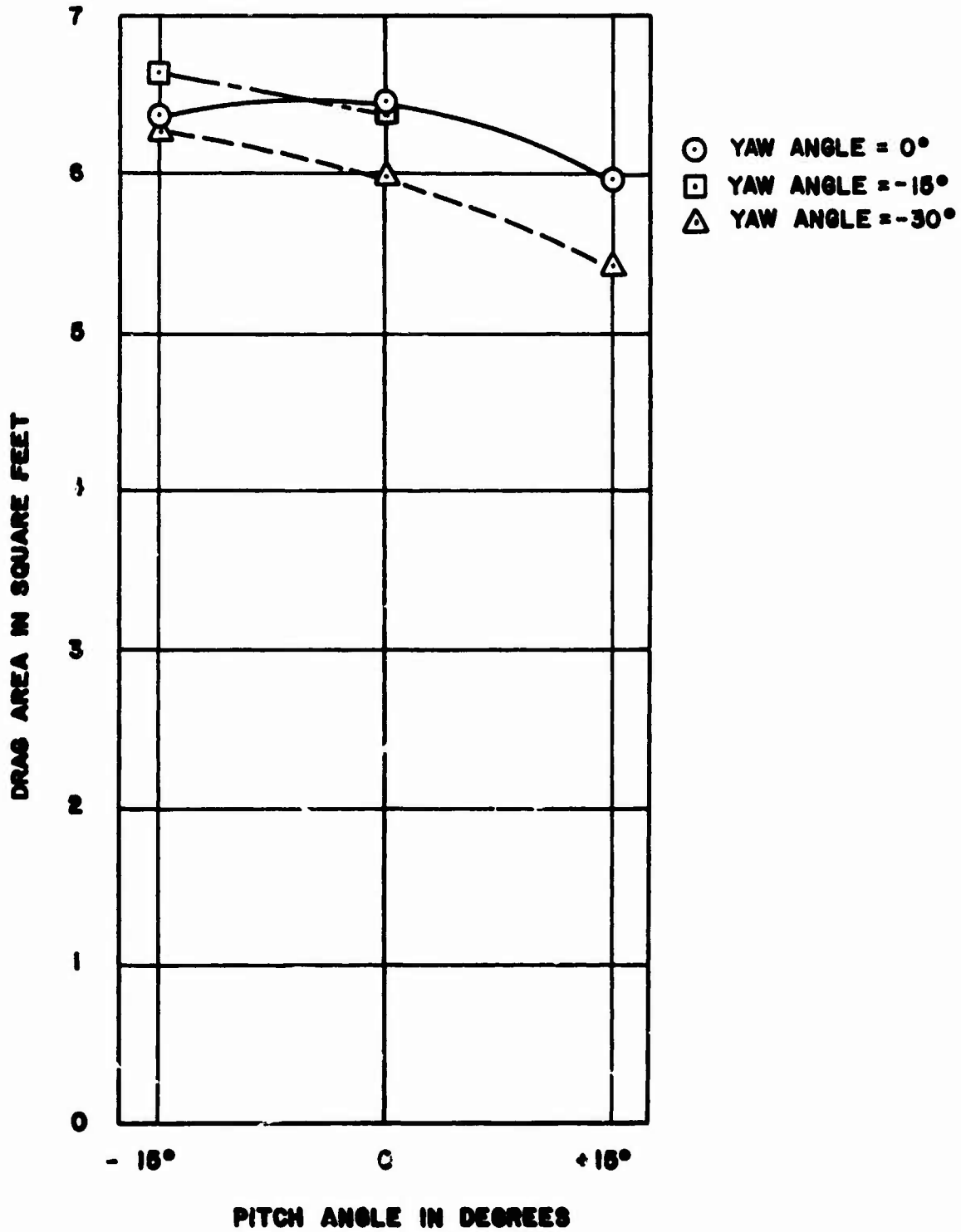

Figure 44. Average Drag Force (All Subjects) as a Function of Pitch Angle, for the Standard Side-Arm Configuration for the F-105 Ejection Seat.

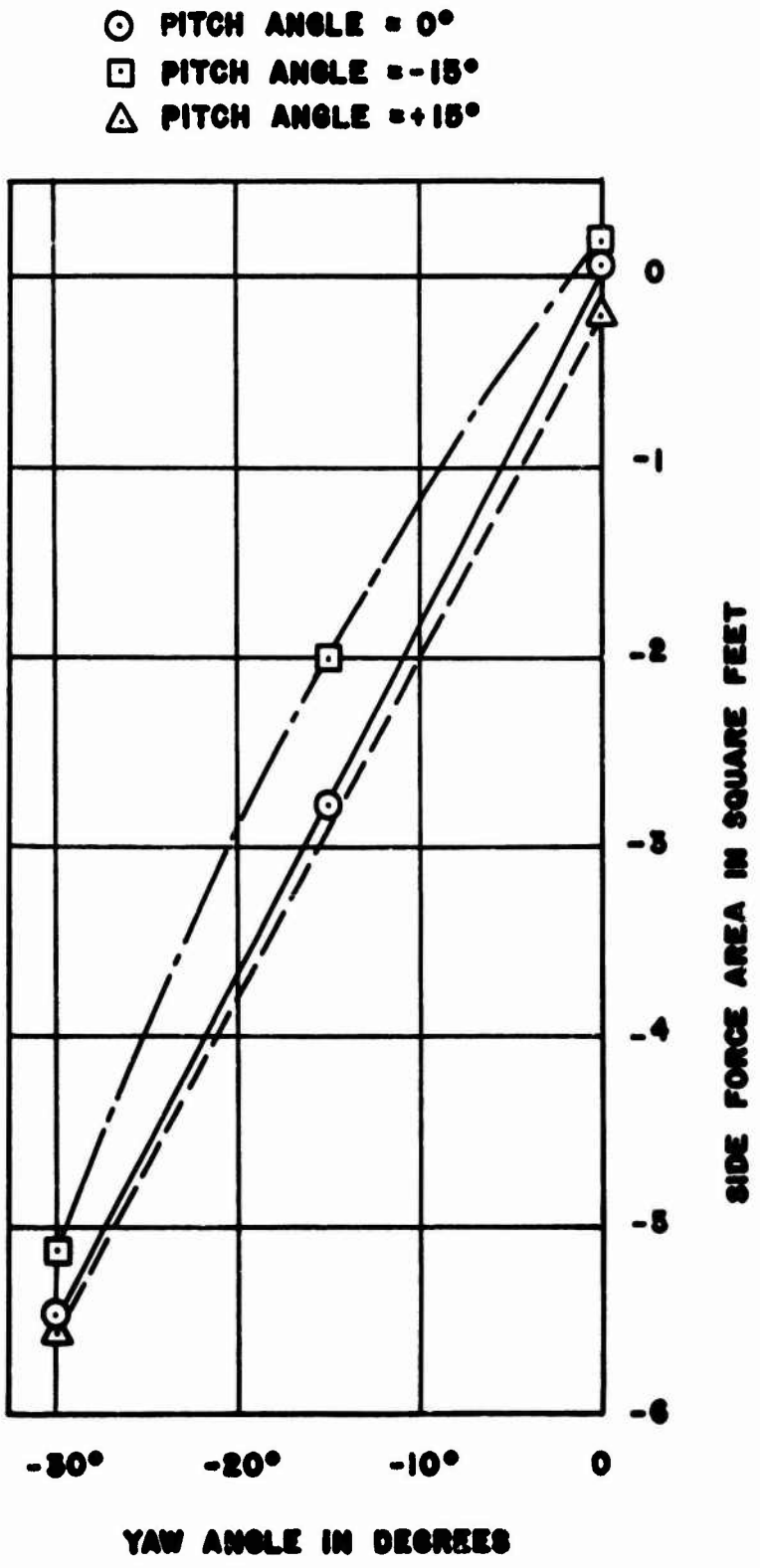

Figure 45. Average Side Force (All Subjects) as a Function of Yaw Angle, for the Standard Side-Arm Configuration for the F-105 Ejection Seat.

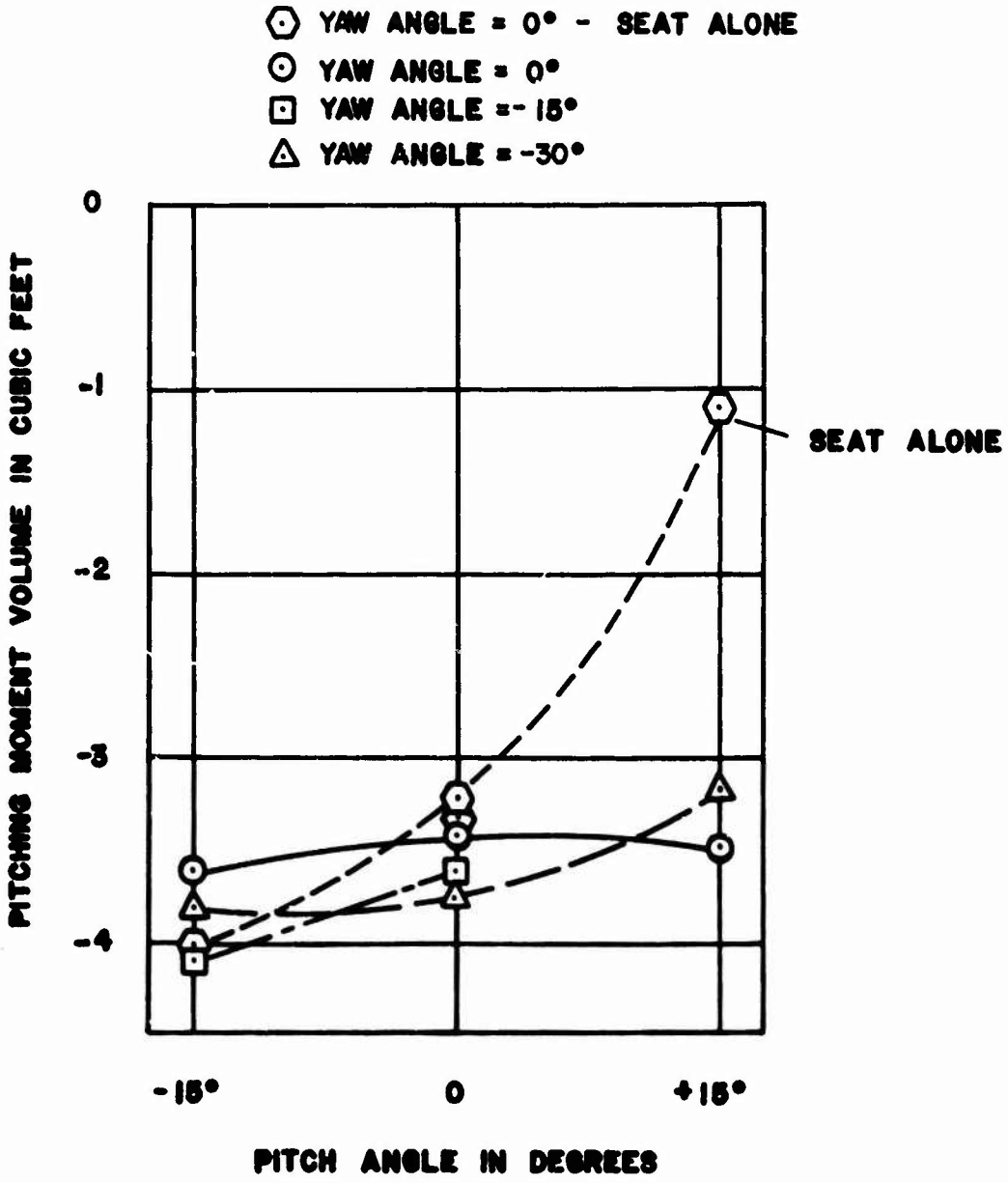

Figure 46. Average Pitching Moment (All Subjects) as a Function of Pitch Angle, for the Standard Side-Arm Configuration for the F-105 Ejection Seat.

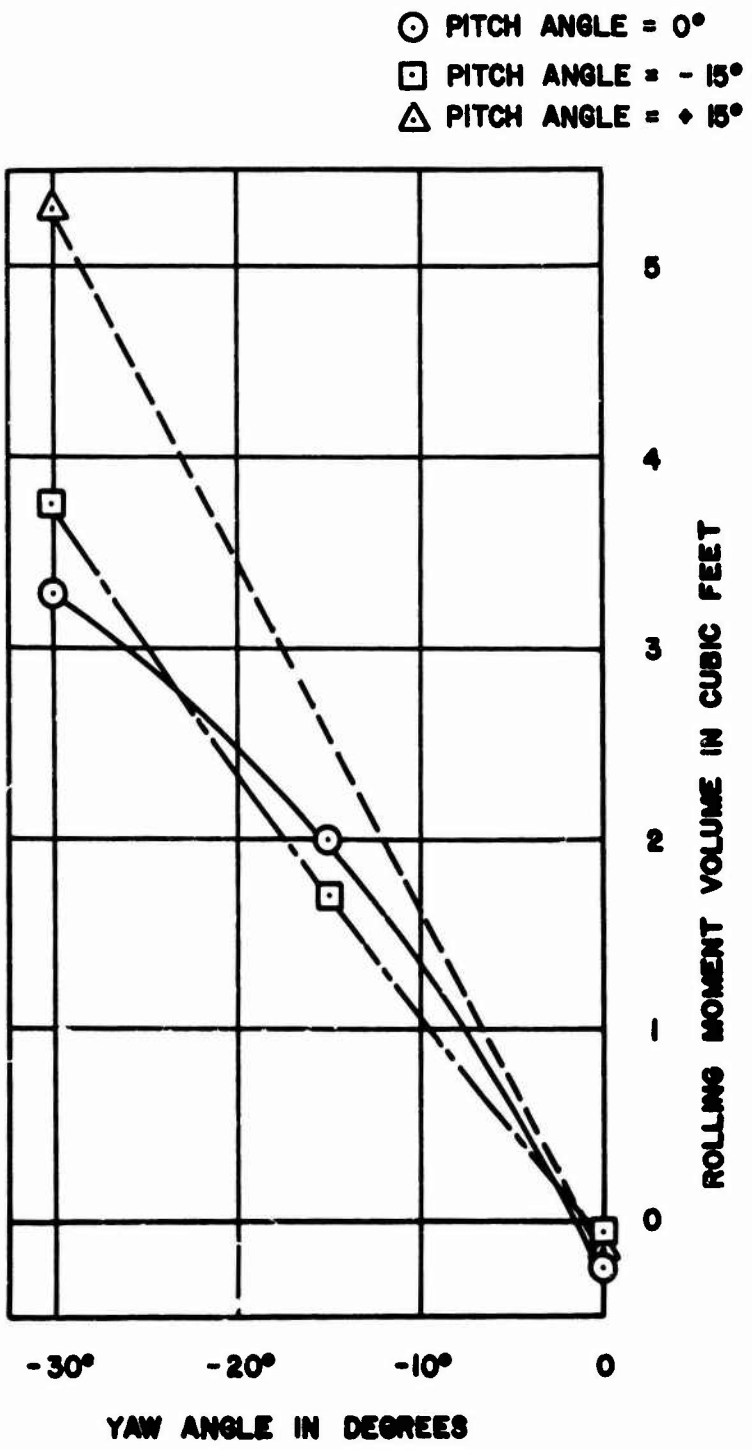

Figure 47. Average Rolling Moment (All Subjects) as a Function of Yaw Angle, for the Standard Side-Arm Configuration for the F-105 Ejection Seat.

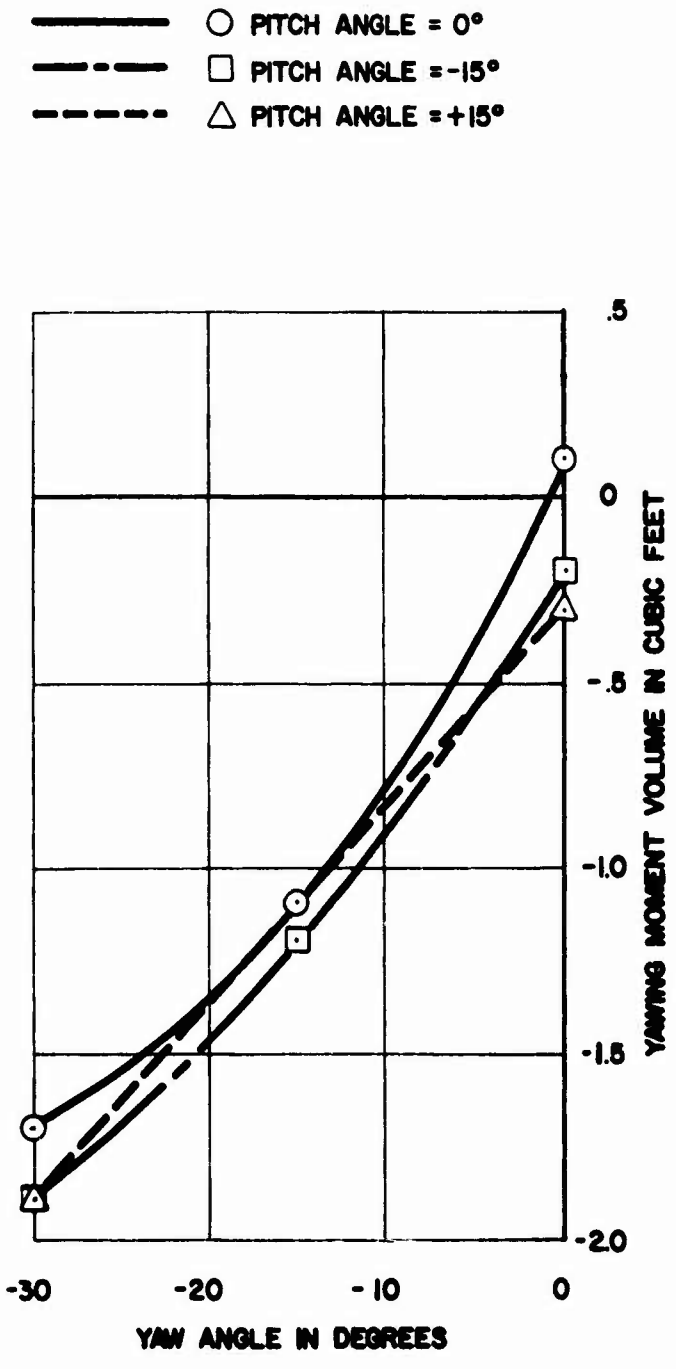

Figure 48. Average Yawing Moment (All Subjects) as a Function of Yaw Angle, for the Standard Side-Arm Configuration for the F-105 Ejection Seat.

The yaw instability is quite marked (Figure 33). This topic was investigated in greater detail in the subsequent work reported in Reference 4, Figures 33 and 34. Measurements through 180° of yaw angle show that the stable slopes occur near to ±90° of yaw with strong instability in the vicinity of 0° (face forward) and a weak ill-defined condition of instability at -180° (seat first). In the same series the pitch near-neutral stability was confirmed (Reference 4, Figures 31 and 32) with dummy occupants, but repetition of the tests with human subjects indicated rather more marked instability in pitch. The conclusion is that, in the present context at least, the seat is statically unstable in the pitch range in which ejection is initiated.

Tests of an In-Plane Stabilizer on the F-105 Seat

The in-plane stabilizer concept was first reported in Reference 3, based on theoretical considerations and drop testing of simple models. One purpose of the present wind tunnel test program was to obtain experimental verification of the theoretical predictions.

Since the pitching and yawing moments of the F-105 seat were not known, and since the stabilizer clearly had to be fabricated before the testing started, it was deliberately made over-size. It was also made so that four, one or two plates could be attached to the seat, as shown in Figures 49, 50, and 51.

The geometry of the stabilizer is defined in Figure 52.

The test results are given in Table 12 and plotted in Figures 53 through 56. Pitching and yawing moments are obtained over a range of pitch and yaw angles, in the same manner as for the basic seat. The results, especially the plots of Figures 54 and 55, show strong negative slope to the moment curves in the test range, indicating that a high degree of static stability has been attained. A lesser, but still adequate, degree of stabilization would have been provided with smaller plates.

It will be noted from Figure 56 that the drag areas have been increased appreciably, roughly by the projected area of the added plates. A conventional drogue would have the same effect, of course.

Tests of an In-Plane Stabilizer on the ACES-II Seat

The arrangement of the stabilizers for the ACES-II seat is shown in Figure 57, which shows the three configurations actually tested.

The test results are given in Figures 64 and 65 (Configuration 3); Figures 62 and 63 (Configuration 2); Figures 60 and 61 (Configuration 1); and, for comparison, Figures 58 and 59 (no stabilizer).

Figure 49. Rear View of the Full In-Plane Stabilizer Array on the Seat, Yawed at -30°. (F-105 Seat)

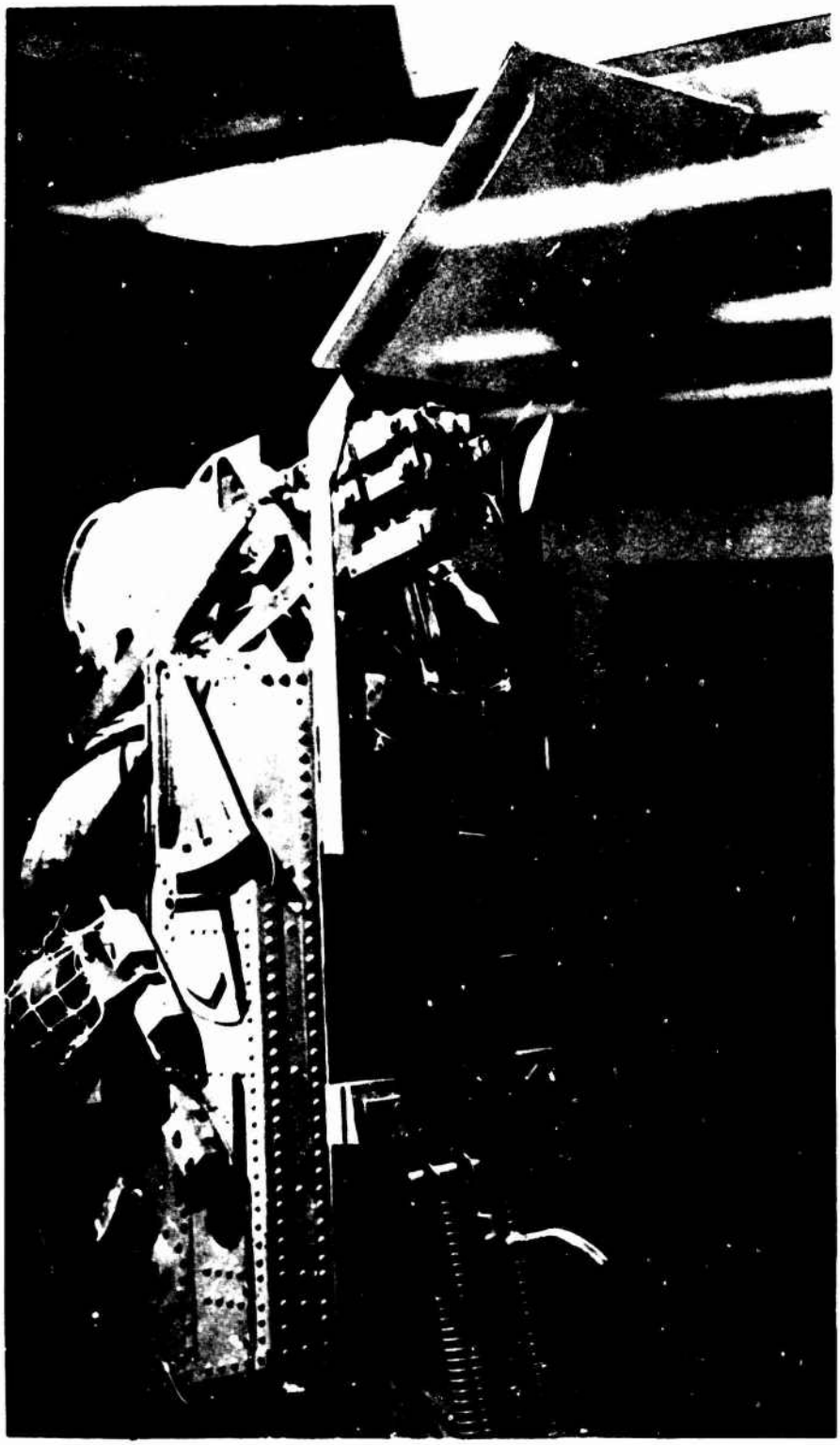

Figure 50. The Single Plate In-Plane Stabilizer Configuration on the F-105 Seat.

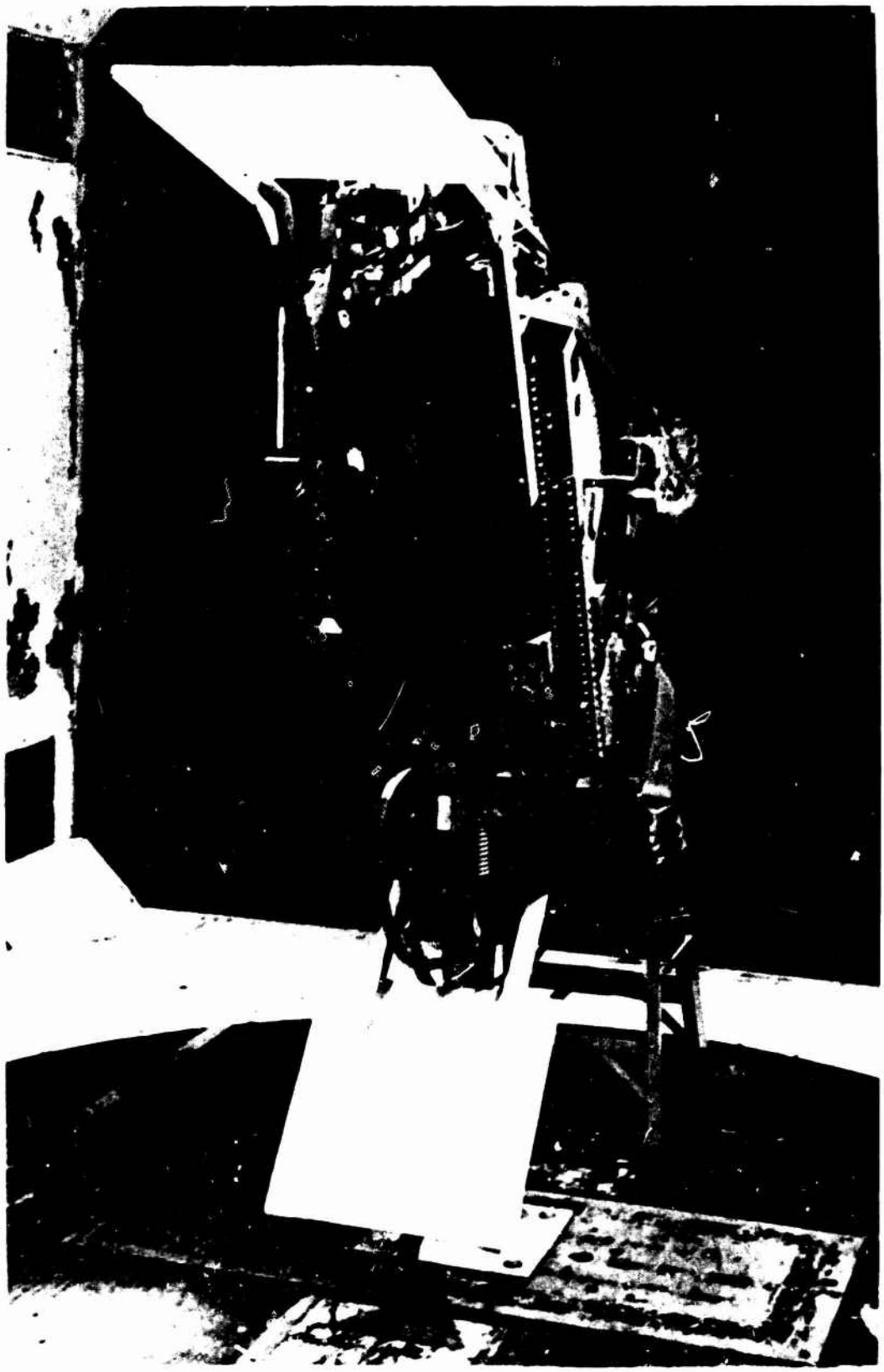

Figure 5?. The Two Plate In-Plane Stabilizer Configuration on the F-105 Ejection Seat.

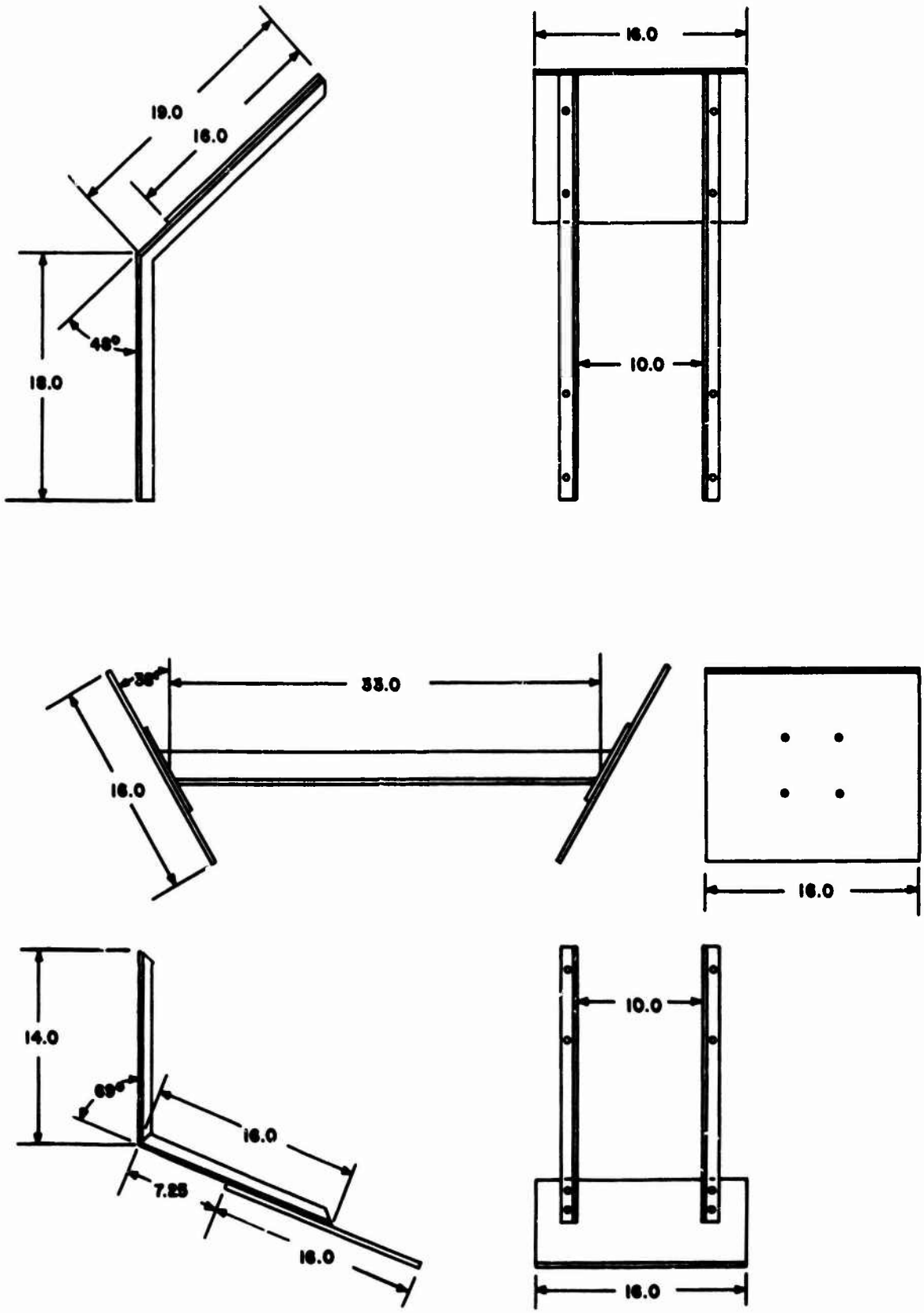

Figure 52. F-105 In-Plane Stabilizers Geometry.

Table 12. FORCES AND MOMENTS WITH IN-PLANE STABILIZER PLATES IN POSITION, NET RESTRAINTS (F-105 EJECTION SEAT)

Yaw Angle	Pitch Angle	Run No.	Subject	Lift Area	Drag Area	Side Force Area	Pitch Moment Volume	Yaw Moment Volume	Roll Moment Volume
					TOP PLATE ONLY				
0°	+15°	48	RM	-0.5	6.21	0.0	-3.1	0.5	-0.2
0°	0°	48	RM	-3.0	7.34	0.2	0.7	0.4	-0.3
0°	-15°	48	RM	-4.9	8.40	0.2	4.9	0.4	0.1
					ALL PLATES				
0°	+15°	50	RM	0.2	9.86	0.3	-8.9	0.0	-0.7
0°	0°	50	RM	-2.4	10.92	0.5	-4.1	0.0	-1.0
0°	-15°	50	RM	-4.7	9.08	0.2	3.3	0.4	-0.7
-15°	+15°	51	RM	0.5	9.22	-4.8	-8.8	2.0	4.7
-15°	0°	51	RM	-2.6	10.28	-4.3	-4.7	1.8	3.4
-15°	-15°	51	RM	-4.6	9.60	-3.9	1.4	2.6	2.6
-30°	+15°	52	RM	0.3	8.29	-9.4	-8.1	3.5	7.6
-30°	0°	52	RM	-1.9	9.30	-8.9	-4.9	3.4	5.2
-30°	-15°	52	RM	-4.1	9.47	-8.7	0.0	3.5	4.2
					NO PLATES				
-30°	+15°	53	RM	-0.1	5.69	-5.3	-3.4	-1.4	5.6
-30°	0°	53	RM	-1.1	6.17	-5.1	-4.6	-1.3	4.6
-30°	-15°	53	RM	-2.3	6.97	-4.3	-4.2	-1.9	3.8
-15°	+15°	54	RM	0.4	6.09	-2.6	-4.0	-1.2	3.3
-15°	0°	54	RM	-1.0	6.90	-2.1	-3.7	-1.1	2.7
-15°	-15°	54	RM	-2.3	7.19	-1.2	-4.7	-0.9	1.7

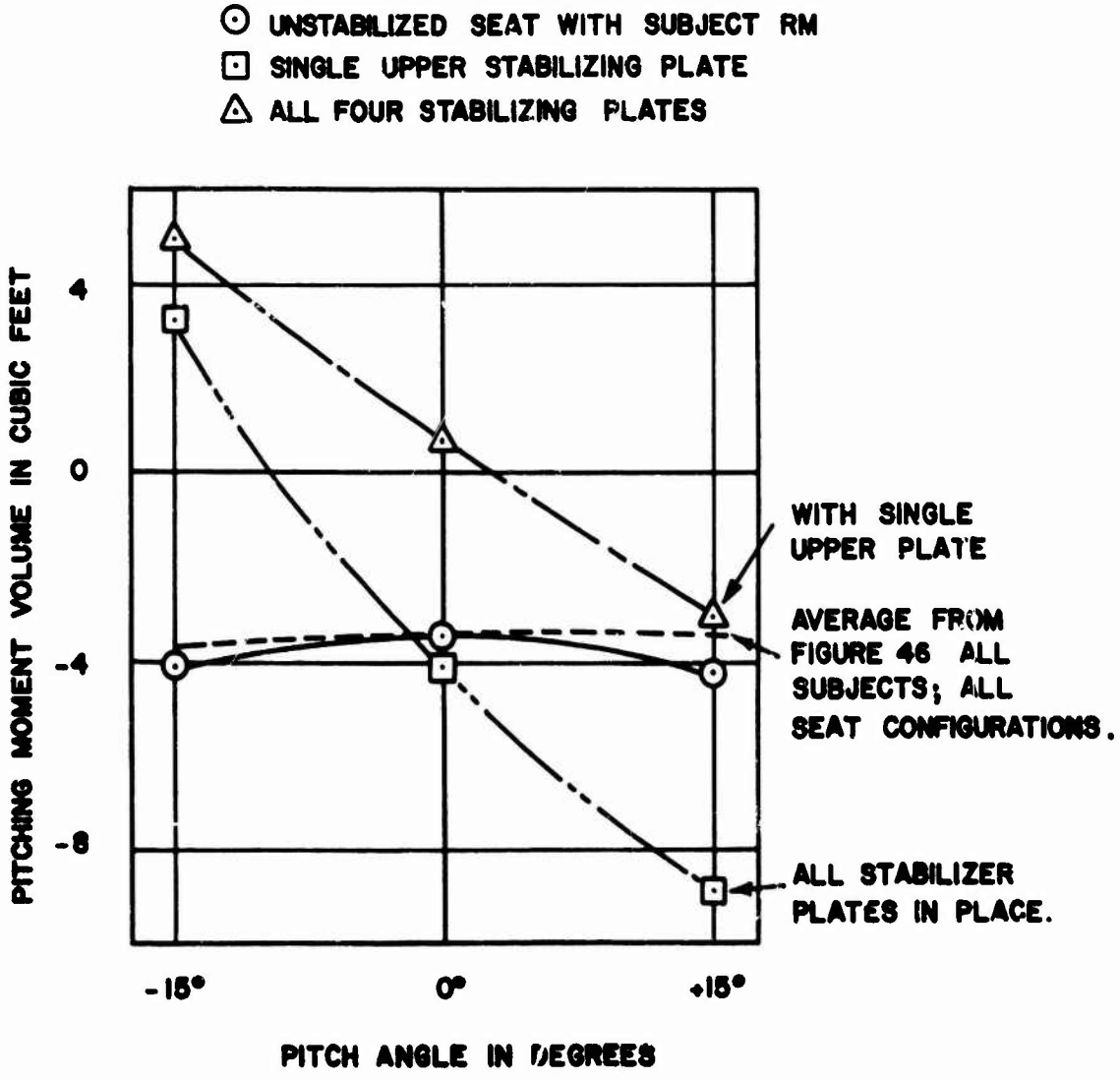

Figure 53. Pitching Moment at Zero Yaw, With and Without In-Plane Stabilizer Plates. Subject RM with arm and leg restraint nets. Results are not corrected for tunnel wall proximity. (F-105 seat).

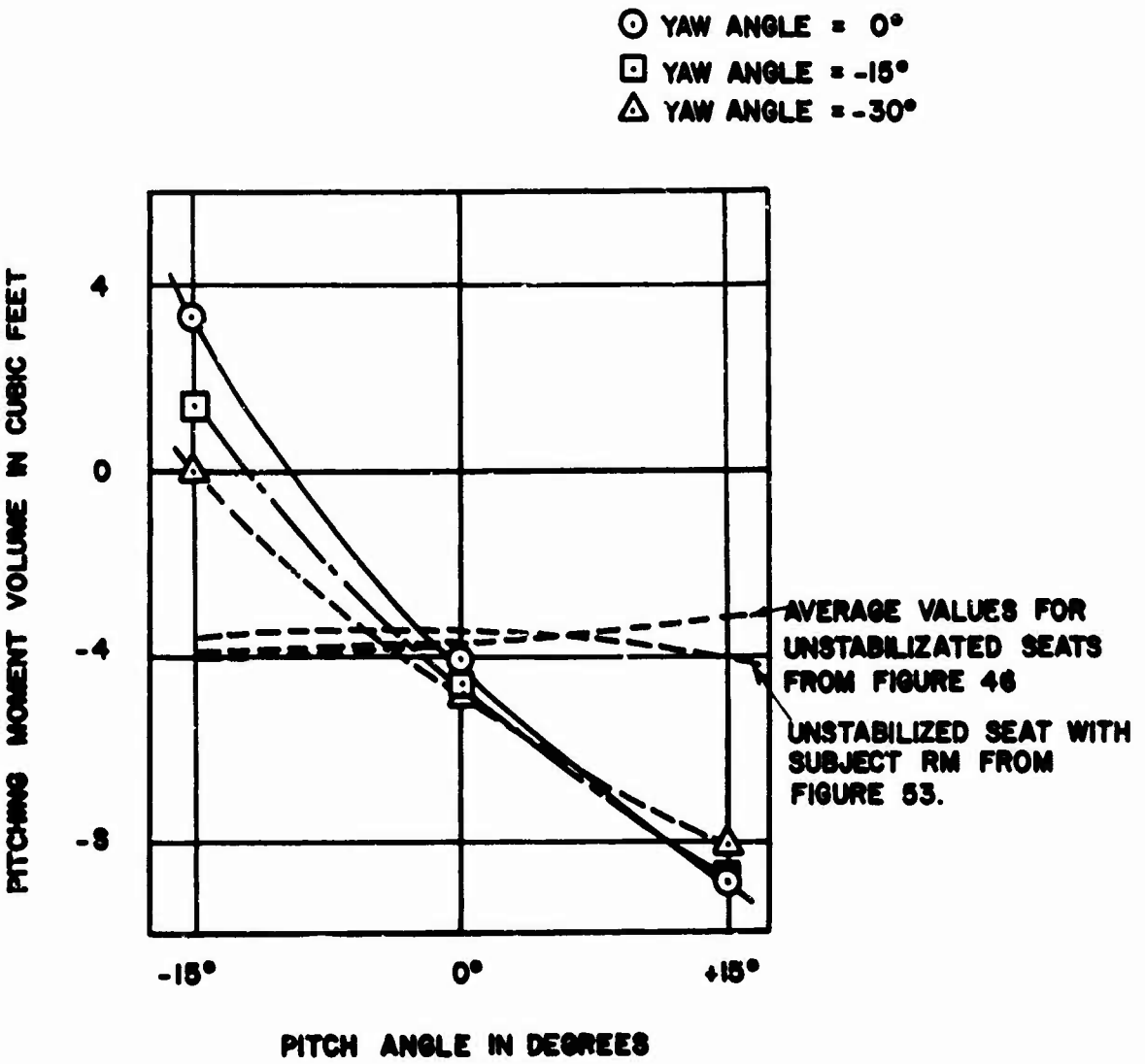

Figure 54. The Effect of Yaw upon the Seat Pitching Moment When Equipped with all Four Stabilizer Plates. Subject RM with arm and leg restraint nets. Results are not corrected for tunnel wall proximity. (F-105 seat).

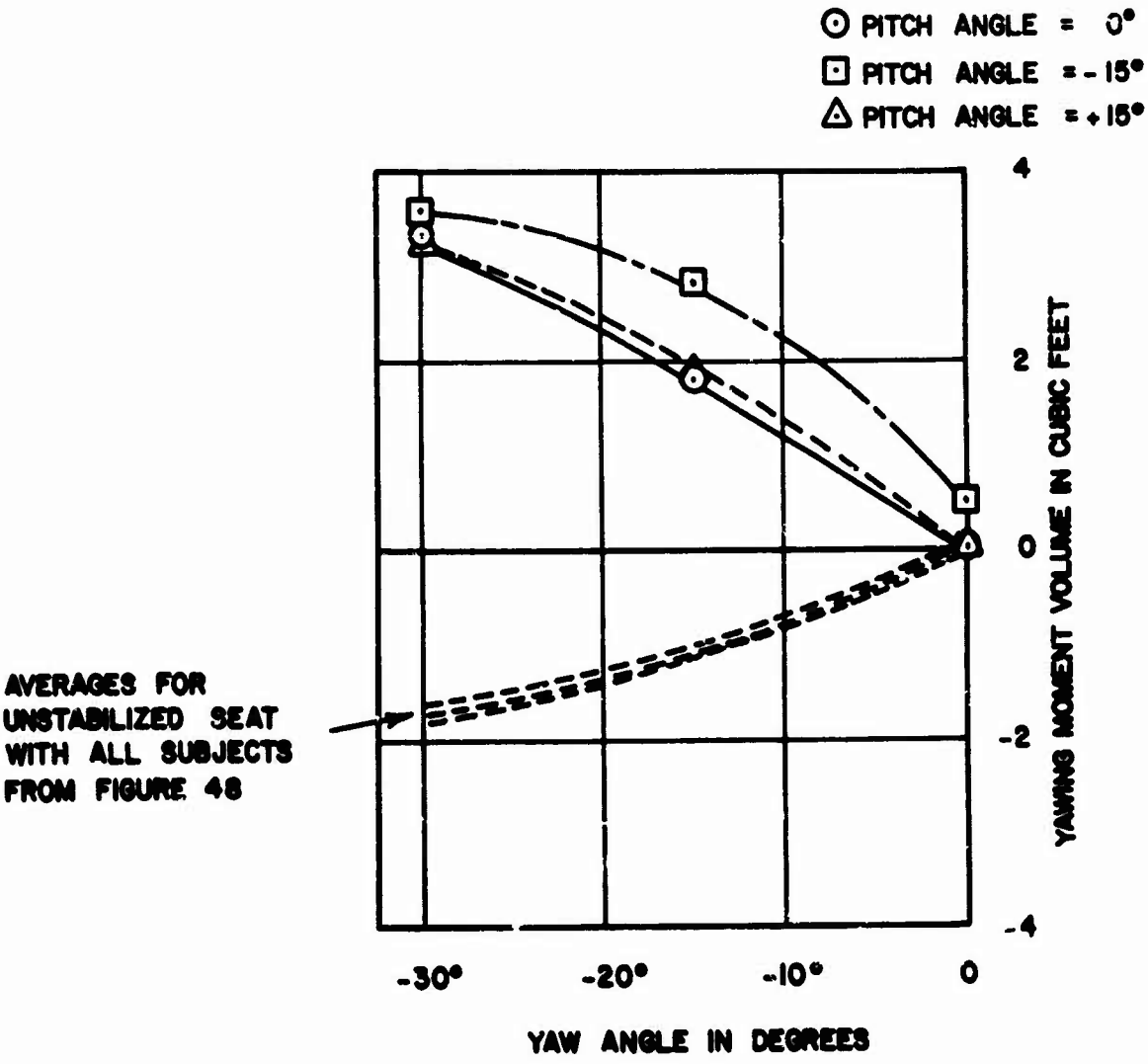

Figure 55. Yaw Volume with Subject RM When the In-Plane Stabilizer was in Place.

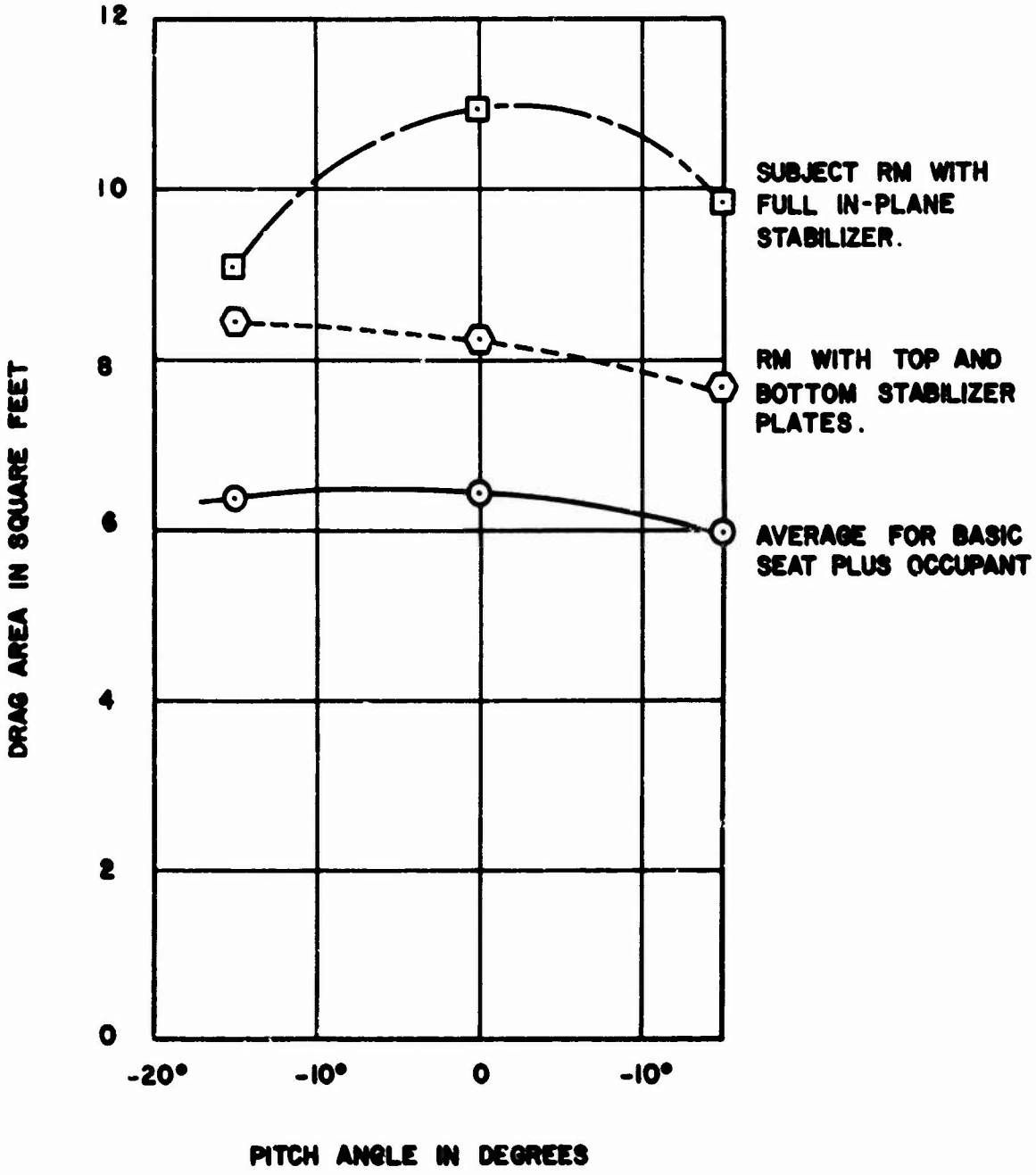

Figure 56. Some Drag Area Measurements for the F-105 Ejection Seat, as a Function of Pitch Angle, for Zero Yaw.

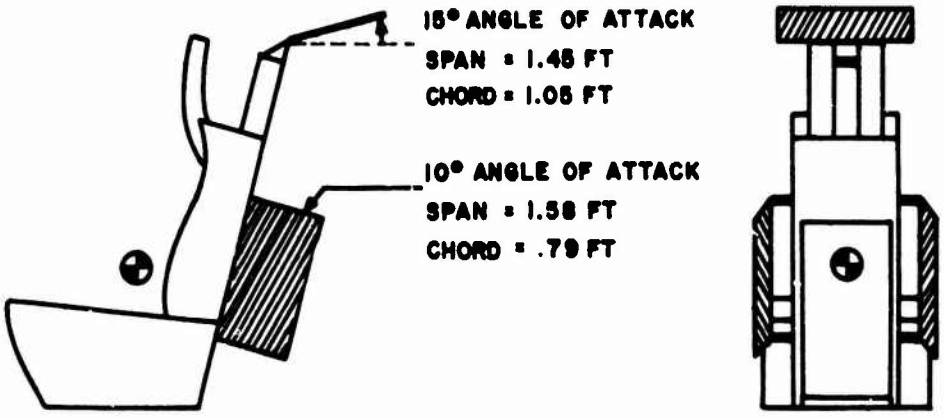

Configuration 1. Foldable Euler Design, Reference 8.

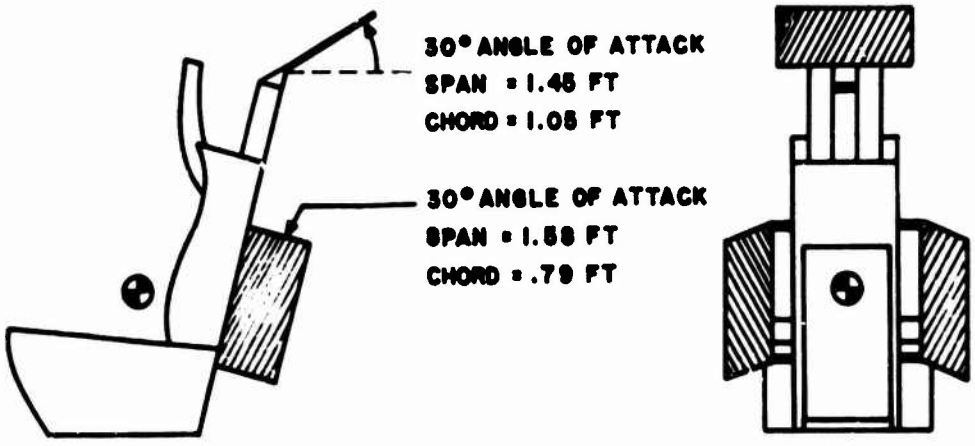

Configuration 2. Foldable Euler Design With Plate Angles Arbitrarily Increased.

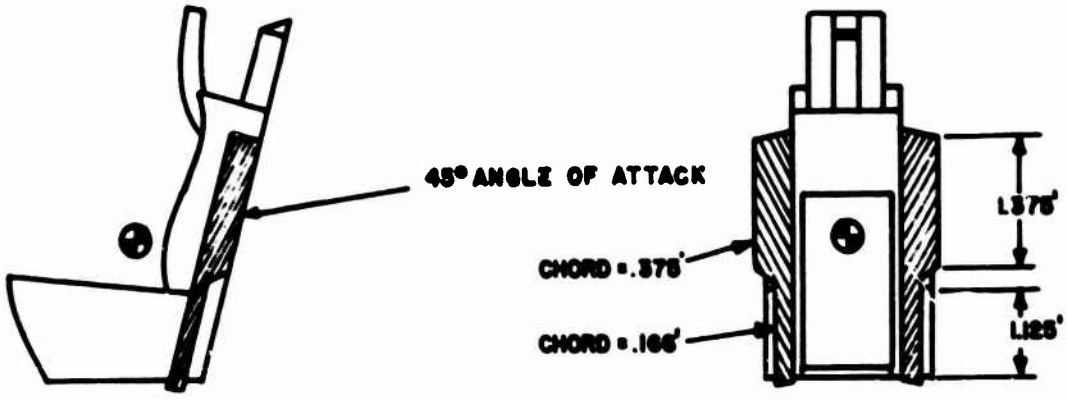

Configuration 3. McDonnell-Douglas "Largest Possible" Fixed Plate Design for Yaw Only.

Figure 57. In-Plane Stabilizer Configurations for the ACES II Seat.

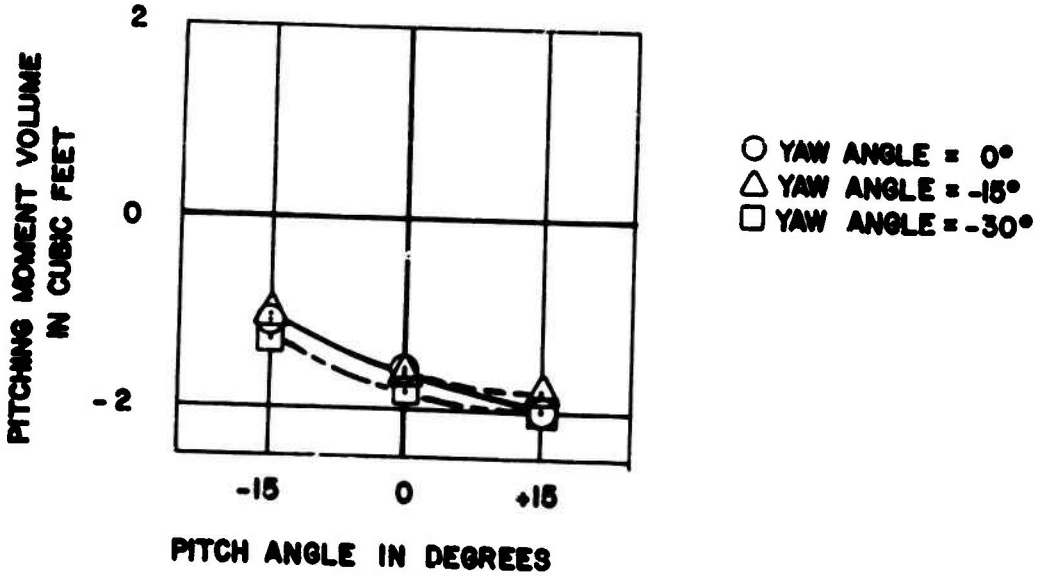

Figure 58. ACES-II Seat Pitching Moment Volume as a Function of Pitch Angle for Various Yaw Angles, with No Stabilizer Plates. Subject: 95% Anthropomorphic Dummy, $q = 30$ lb/ft^2.

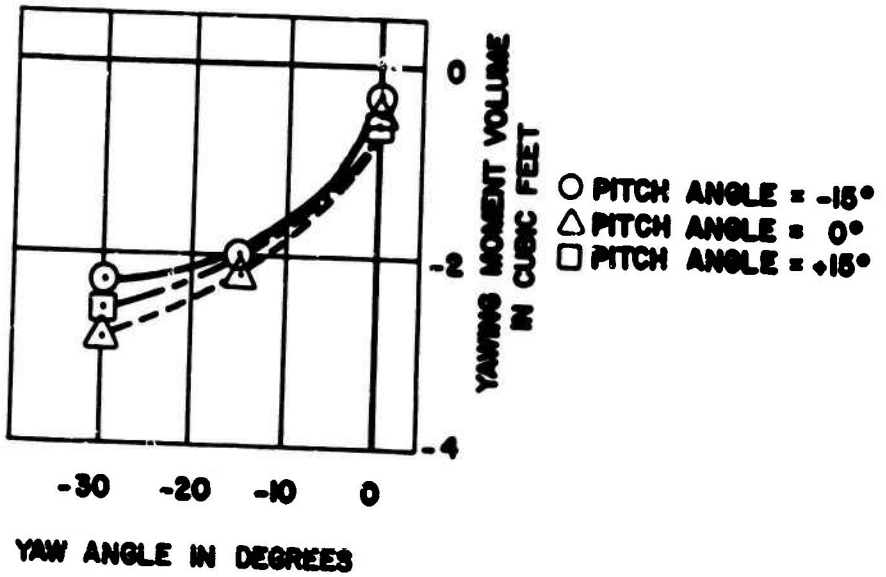

Figure 59. ACES-II Seat Yawing Moment as a Function of Yaw Angle for Various Pitch Angles, with No Stabilizer Plates. Subject: 95% Anthropomorphic Dummy; $q = 30$ lb/ft^2.

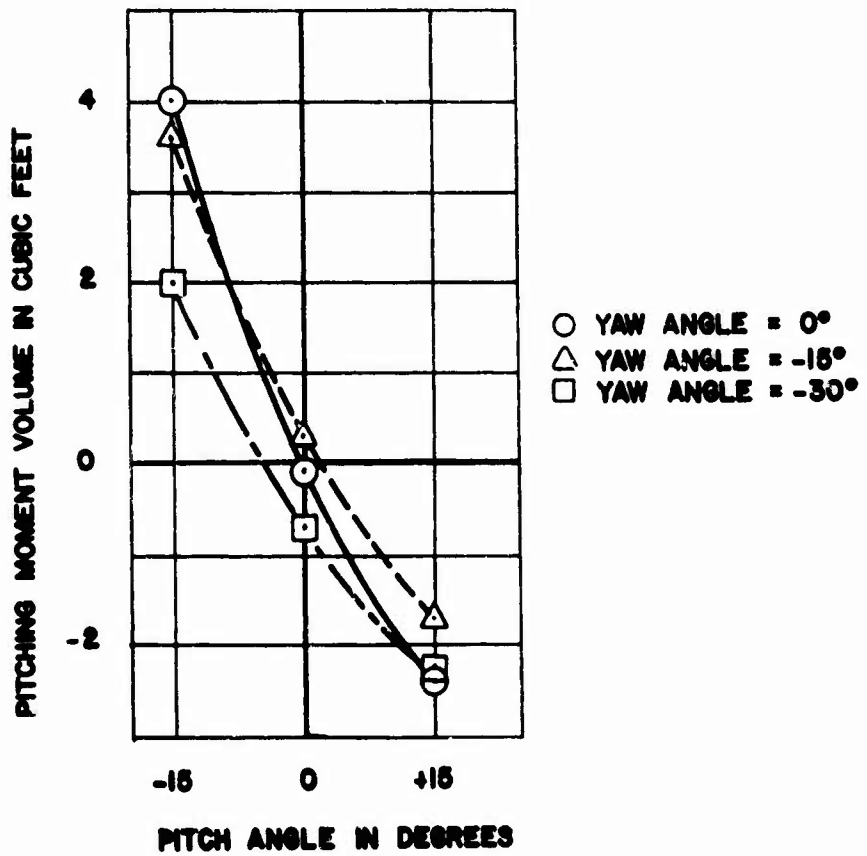

Figure 60. ACES-II Seat Pitching Moment Volume as a Function of Pitch Angle for Various Yaw Angles, With Configuration 1 Stabilizer Plates. Subject: 95% Anthropomorphic Dummy; q = 30 lb/ft^2.

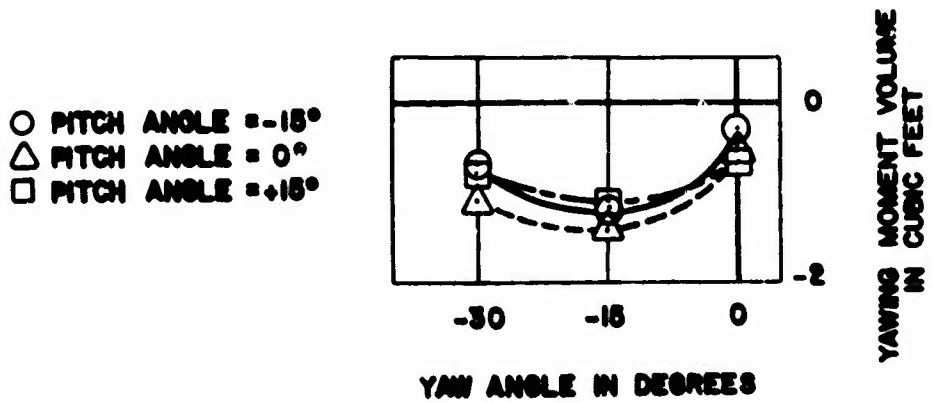

Figure 61. ACES-II Seat Yawing Moment as a Function of Yaw Angle for Various Pitch Angles, With Configuration 1 Stabilizer Plates. Subject: 95% Anthropomorphic Dummy; q = 30 lb/ft^2.

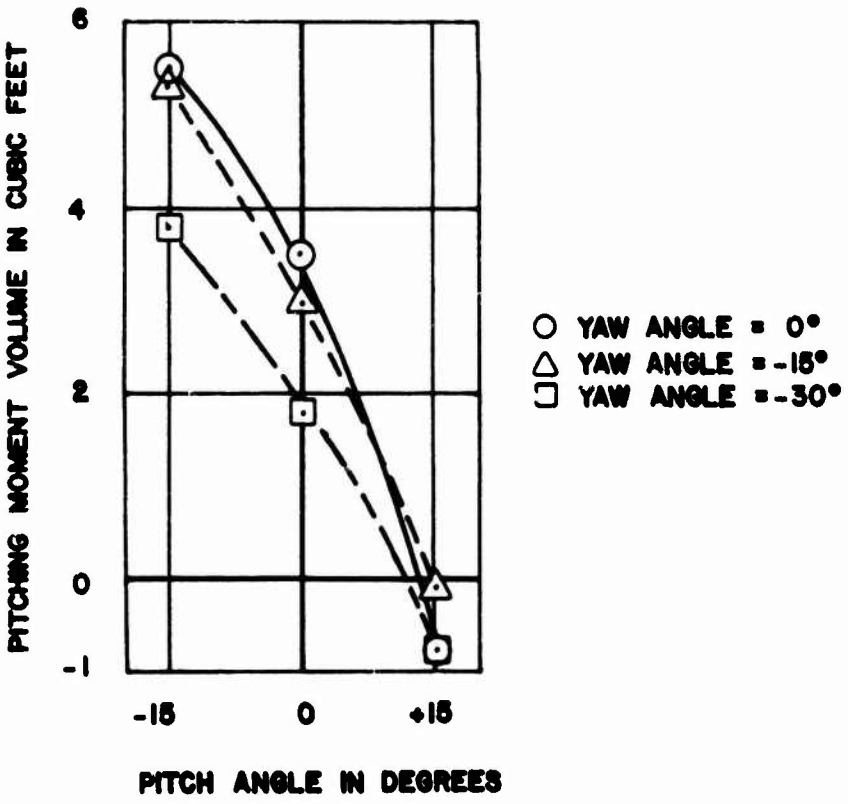

Figure 62. ACES-II Seat Pitching Moment as a Function of Pitch Angle for Various Yaw Angles with Configuration 2 Stabilizer Plates. Subject: 95% Anthropomorphic Dummy; q = 30 lb/ft^2.

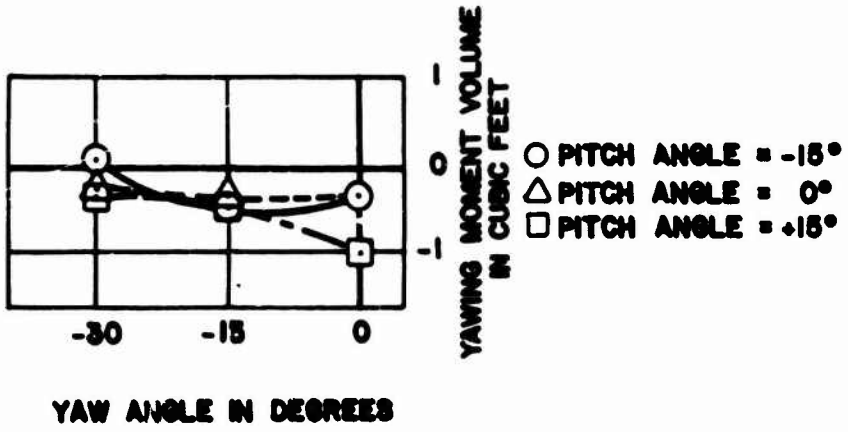

Figure 63. ACES-II Seat Yawing Moment Volume as a Function of Yaw Angle for Various Pitch Angles with Configuration 2 Stabilizer Plates. Subject: 95% Anthropomorphic Dummy; q = 30 lb/ft^2.

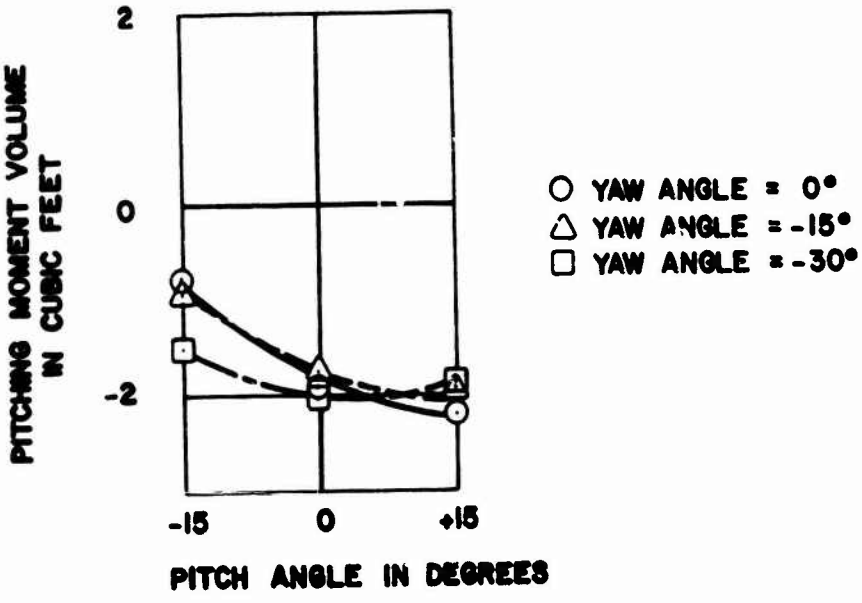

Figure 64. ACES-II Pitching Moment Volume as a Function of Pitch Angle for Various Yaw Angles, with Configuration 3 Stabilizer Plates. Subject: 95% Anthropomorphic Dummy; q = 30 lb/ft^2.

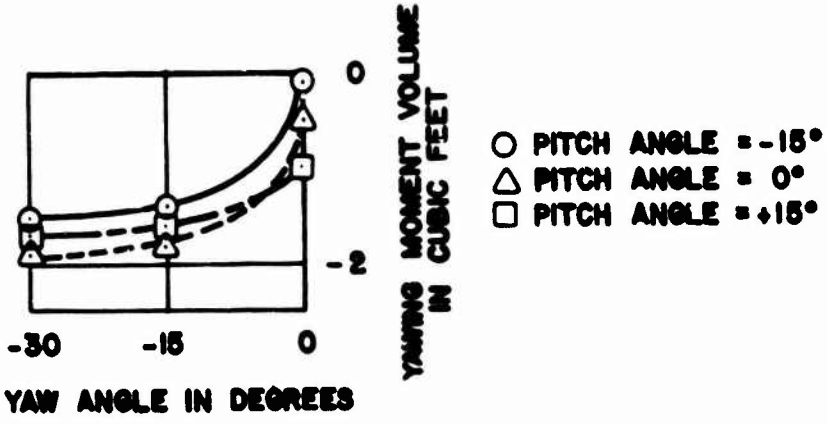

Figure 65. ACES-II Seat Yawing Moment Volume as a Function of Yaw Angle for Various Pitch Angles, with Configuration 3 Stabilizer Plates. Subject: 95% Anthropomorphic Dummy; q = 30 lb/ft^2.

Figure 58 shows a fair degree of stable slope over the range of pitch angle offered in the comparison, but a significant absolute value of the pitching moment. The trim angle would be less than -20° and therefore the seat would be driven in that direction at arrival into the free stream, and would overshoot trim, probably to start a spin.

The pitch stability is augmented by the stabilizer in all three configurations, somewhat weakly by #3, but very strongly by #2 and #1. The trim angle is zero only in configuration #1. This is the ideal case since the trim angle would approximate the angle at which the ejectee would emerge into the free stream.

The yaw instability is less strongly affected. Figure 65 (#3) still shows instability, though appreciably reduced; Figure 63 (#2) is slightly stable; Figure 51 (#1) shows stable, neutral, unstable slope over the range.

These results firmly establish the technique as a means of promoting static stability.

Comparison of Ejection Seats in Terms of Force and Moment Data

On the basis of the data presented, a comparison may be made of the F-105 and ACES-II seats, also comparing with three other designs of seat for which data is available in the literature (References 5, 6, 7).

In the comparison, all the pitch zero angles are with the ejection rails 13° aft of vertical for the F-105 and ACES-II seats. The other seats are specified in Table 13.

The lift, drag, and side forces are shown in Figures 66, 67, and 68. There is a high degree of similarity in these results, which may be considered to be remarkable, having regard to the differences in configuration. To a first approximation the force areas are proportional to actual areas which is to be expected.

The moments, which result from a finite distance between the C.G. and the appropriate force center, are more variable. This is particularly so in the case of pitching moment, plotted in Figure 69. The NASA model seat has a nose up pitching moment at all angles, which does not vary much with pitch angle. The ACES-II seat has a small pitching moment, which presumably is of considerable help to the performance of its vernier rocket pitch stabilization system. In contrast, the F-105 seat has a large nose down pitching moment, again almost invariant with pitch angles, (over the limited range tested) which presumably could result in tumbling at high speed, prior to drogue chute deployment. The ARO model and the F-101 seats have almost as large nose down moments near zero angle.

This rather large variability in pitch is presumably due to the fact that a relatively small shift in drag area center, relative to the C.G., gives a relatively large change in moment. Comparison of Figures 67 and 69 at zero pitch gives the following table.

Seat	Drag Center Vertical Offset from C.G.	
ACES-II	-0.30 ft	Zero yaw, Zero pitch
F-105	-0.54 ft	
F-101	-0.56 ft	
ARO Model	-0.48 ft	
NASA Model	+0.12 ft (M = 0.8)	

This calculation does not allow for any contribution due to lift force offset, but reference to Figure 66 shows that this is likely to have an order of magnitude less effect.

Yawing moment is less variable. The side-force center offsets at 30° yaw and as follows

Seat	Side Force Center Distance Forward of C.G.	
ACES-II	0.51 ft	At 30° yaw, 0° pitch
F-105	0.30 ft	
F-101	0.39 ft	
ARO Model	0.69 ft	(-13° pitch, 30° yaw)
NASA Model	0.36 ft	(at 9° yaw)

Zero pitch rolling moment (Figure 71) is also quite consistant between the various seats. If we assume that it is due only to side force, then the side force offset is as follows

Seat	Side Force Center Distance Above C.G.	
ACES-II	0.58 ft	At 30° yaw, 0° pitch
F-105	0.61 ft	
F-101	0.78 ft	
ARO Model	0.66 ft	(-13° pitch, 30° yaw)
NASA Model	0.42 ft	(at 9° yaw)

The first four of these offsets are remarkably consistent, and if the NASA model test had extended to 30° yaw, it might well have shown a very similar value.

Table 13. Ejection Seats

	Seat Type	Mach No.		Seat Back Angle During Tests When Angle of Attack = 0°
A[1]	Model Seat	0.4	Reference 5	0°
A	Model Seat	0.8	Reference 5	0°
C	Model Seat	0.6	Reference 6	0°
D	F101 Seat	0.2	Reference 7	6°
B	F105 Seat	≈.16		13°
E	ACES II Seat	≈.16		13°

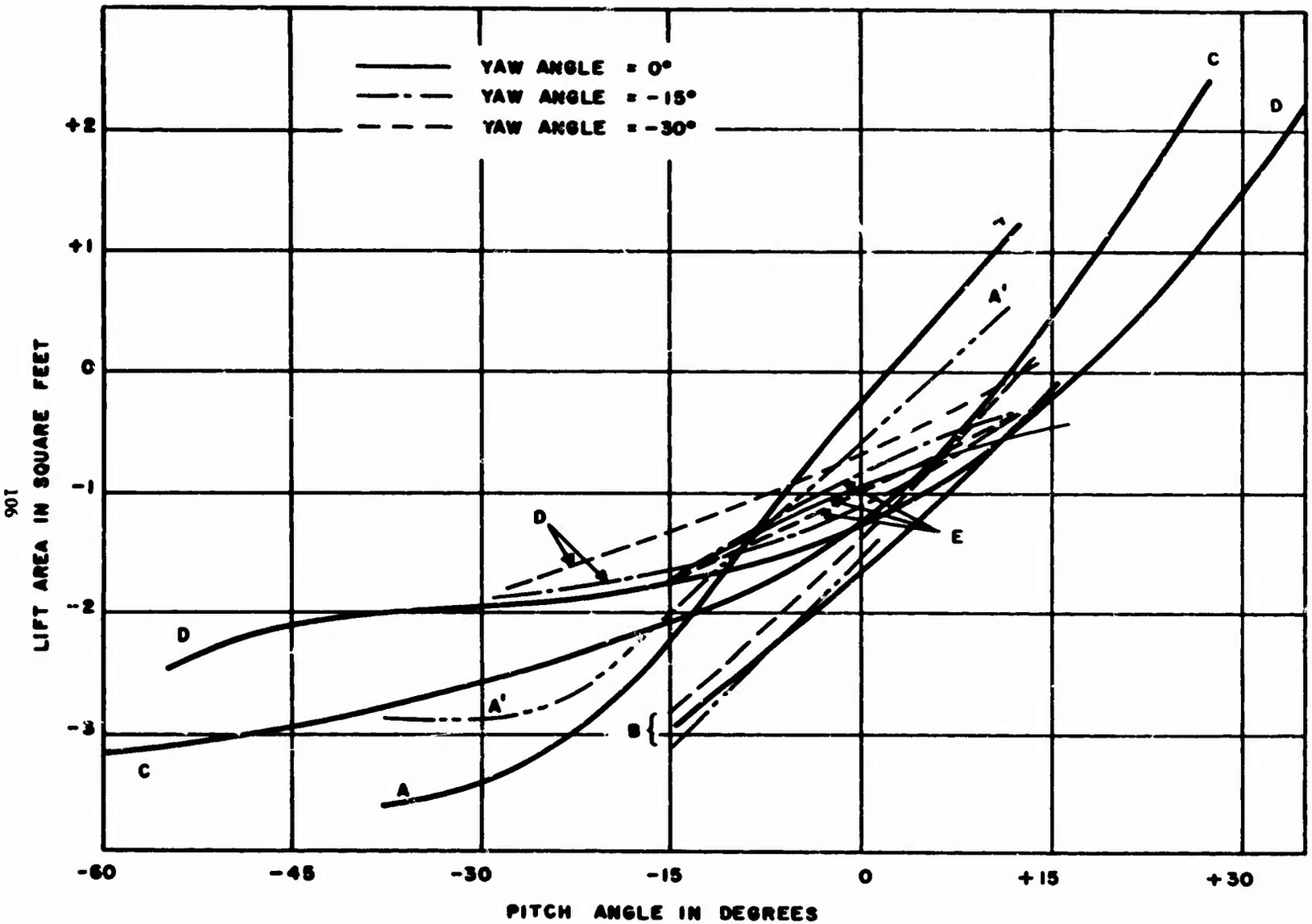

Figure 66. Lift Area Versus Pitch Angle for Five Different Ejection Seats

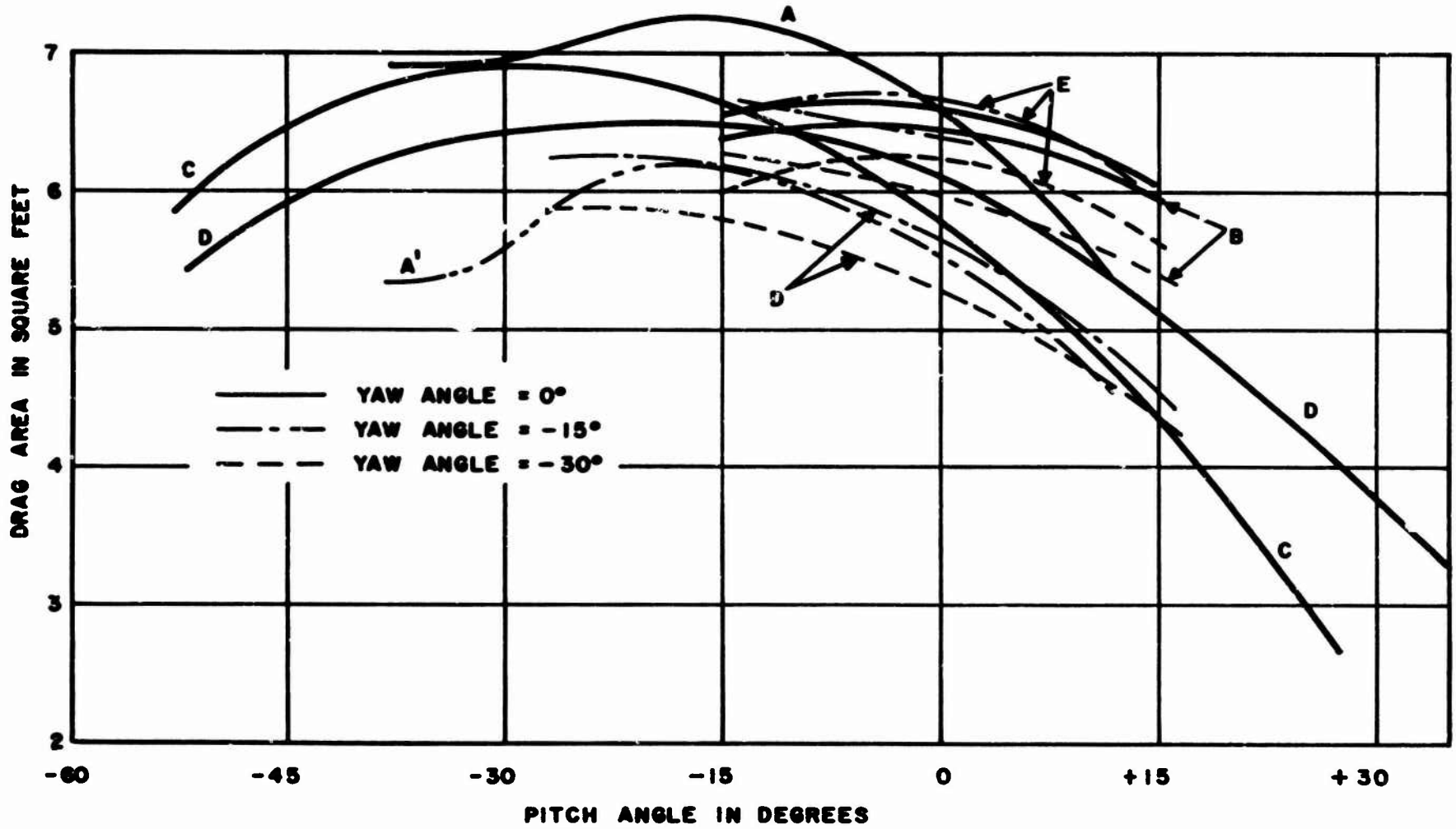

Figure 67. Drag Area Versus Pitch Angle for Five Different Ejection Seats.

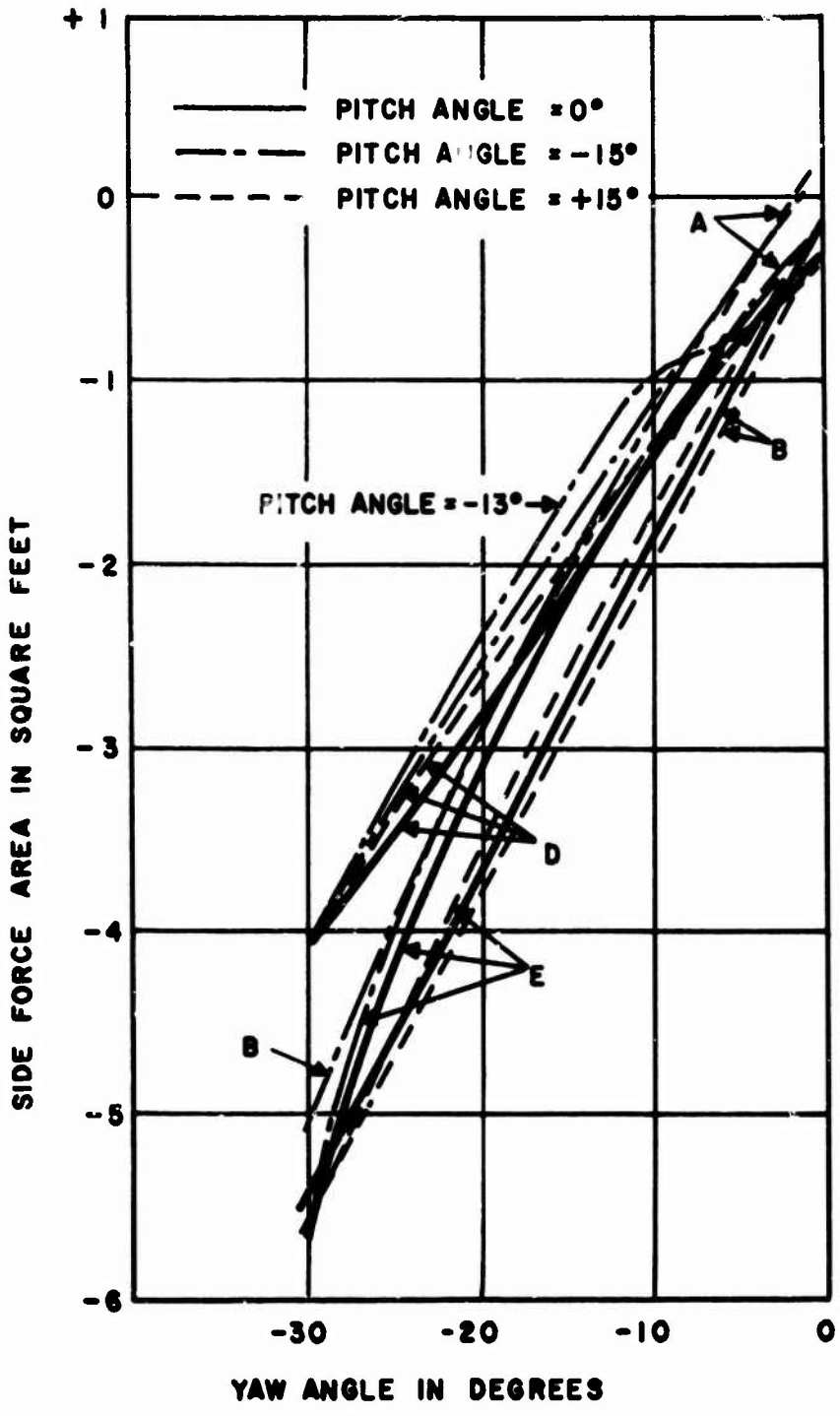

Figure 68. Side Force Versus Yaw Angle for Five Different Ejection Seats.

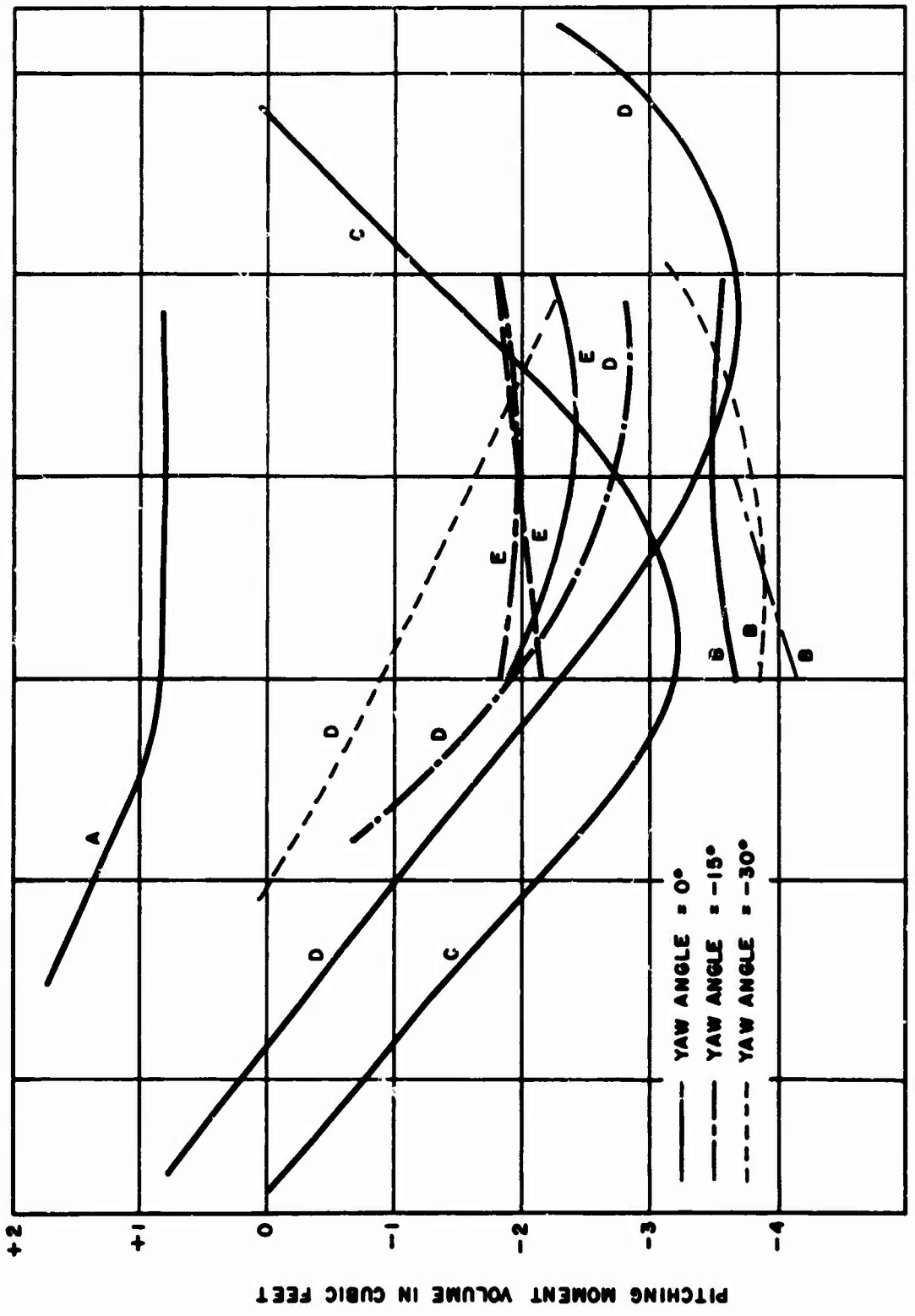

Figure 69. Pitching Moment Volume Versus Pitch Angle for Five Different Ejection Seats.

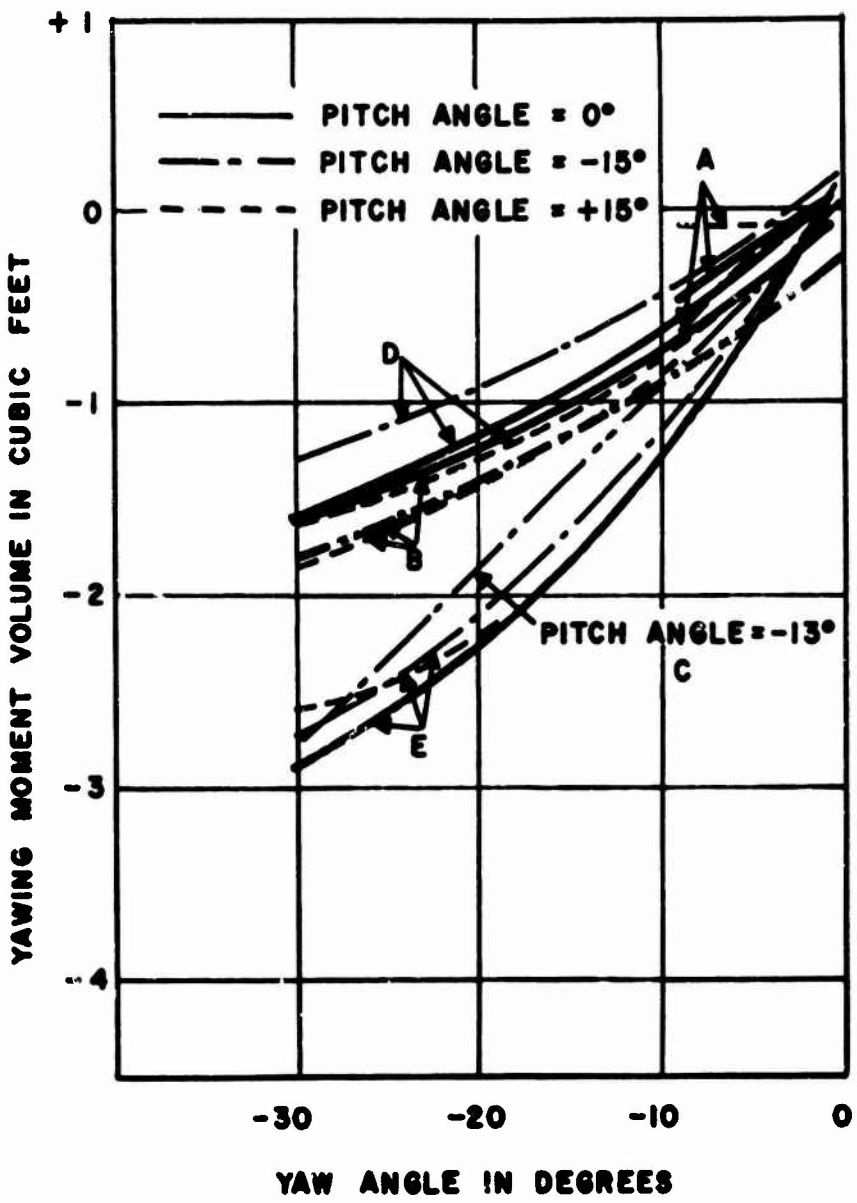

Figure 70. Yawing Moment Volume Versus Yaw Angle for Five Different Ejection Seats.

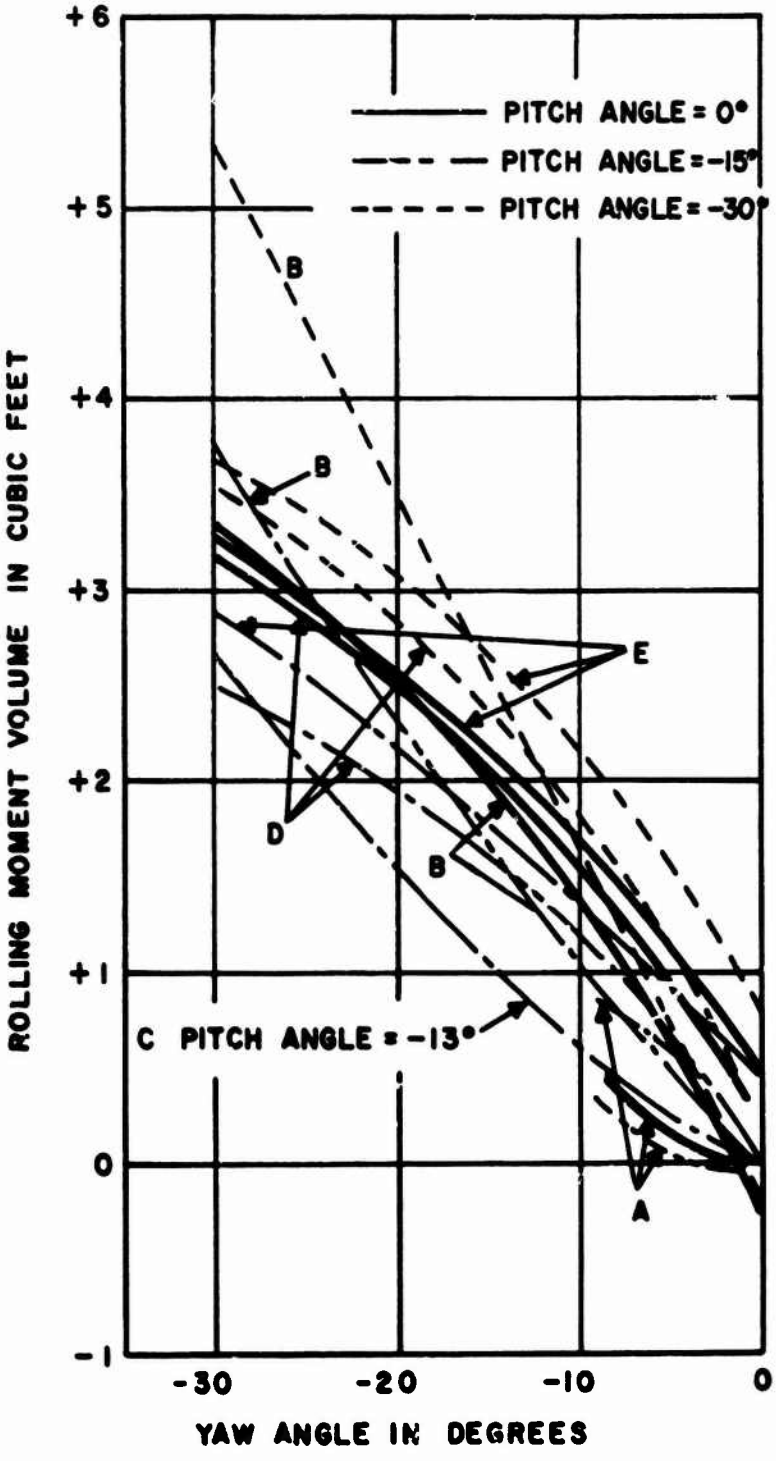

Figure 71. Rolling Moment Volume Versus Yaw Angle for Five Different Ejection Seats.

CONCLUSIONS

The forces which dislodge the limbs from their "stowed" positions vary considerably between individuals. Larger samples than were available during these tests would be required to establish distribution over the population of potential occupants. Values averaged from the results for those tested have been compared over ranges of yaw and pitch angles for the two seats tested. Outward force at the knee shows good systematic variation with angle and good equality between the seats. Forces on the lower leg and on the arm show less plottable variation and less agreement between the seats. Generally, hand and foot forces on the ACES-II seat are greater than those on the F-105 seat and are quite high enough to account for limb dislodgement at high speeds.

Devices to reduce the forces were rated unsuccessful because they reduced some of the forces while increasing others. Passive protection in the form of the net entrapment devices proposed by Brinkley are a practical solution to the problem of flail injury provided, of course, that the seat is stable in its face-forward attitude.

Forces tending to remove the helmet arise from external low pressure, not from internal positive pressures. They are large enough to ensure loss of helmet at high speed, or to cause neck injury if the helmet retention strap is strong enough to withstand these loads. A helmet flow spoiler reduced the lift-off force to a negligible amount and appears to offer a possible solution to the problem of helmet loss.

The basic F-105 seat plus occupant was found to be statically unstable in pitch and yaw attitudes. The addition of over-size in-plane stabilizer plates made it strongly stable in both directions. This result suggests that a satisfactory stabilizer of this type is feasible if acceptable compact hardware can be developed.

The ACES-II seat plus occupant was also found to be statically unstable in yaw and neutral to unstable in pitch. The addition of the best tested in-plane stabilizers made the pitching moment stable and reduced the yawing moment.

As shown in Appendix II, the degradation of seat stability (or instability) due to deceleration, is negligible.

APPENDIX I

PRESSURE AND FORCE MEASUREMENTS ON THE STANDARD USAF FLIGHT HELMET WITH AND WITHOUT AERODYNAMIC ADDENDA

As mentioned in the description of the test set-up, arrangements were made to measure forces and pressures acting on the helmet. This is a separate subject, not necessarily related to the incidence of flail injury, but since helmet loss is not uncommon following ejections, it seemed appropriate to add these measurements to the program for greater utilization of the tunnel facility.

Instead of being attached to the subject's head, the helmet was supported by a sting attached to the headrest. The sting was strain-gauged to measure the lift, side and drag forces and the pitching and yawing moments of the helmet. The F-105 seat was used in this series of tests.

Fourteen (14) static pressure taps were fitted to the helmet to obtain evidence of the pressure distribution on the helmet. Ten (10) were used to measure the static pressure outside the helmet and four (4) were used to measure the static pressure inside the helmet. These are shown in Figure I-6. The helmet support bracket is seen in Figure I-7, and a view from above, during an actual run, in Figure I-8.

The basic experimental data obtained with the standard USAF flight helmet is given in Table I-1. Average values of the three helmet forces are plotted in Figure I-1 to I-3, and the pitching and yawing moment averages in Figures I-4 and I-5. The scatter of the individual data points is again considerable, but as for the case of the limb forces, the trend of the means is reasonable. The average lift area of 0.38 ft^2 at zero yaw, zero pitch, is somewhat higher than the figure of 0.28 ft^2 reported in Reference 1*. This lift force is very powerful and makes helmet loss inevitable during high speed escape.** A force area of 0.38 ft^2, for example, corresponds to a lift of about 460 lb at 600 knots.

The lift force is mainly due to suction on the outside of the helmet, rather than ram pressure inside. The data from the static pressure tap measurements show that the pressure coefficient C_p can be as low as -1.0 on the outside but rarely exceeds +0.2 inside (Table I - 3).

The definition of C_p is

$$C_p = \frac{p - p_\infty}{\frac{1}{2}\rho u_o^2}$$

where

p is the local static pressure

p_∞ and u_o are the undisturbed pressure and velocity

ρ is the undisturbed air density.

---

*Accuracy of the Reference 1 helmet force measurement was known to be poor.

**That is, for USAF helmets, where the retention strap is designed to "let go" at relatively low loads.

From Bernoulli, it follows that, for incompressible flow

$$C_p = 1 - \left(\frac{u}{u_o}\right)^2 \quad \text{or} \quad \frac{u}{u_o} = \sqrt{1 - C_p}$$

Thus $C_p = -1.0$ implies $u/u_o = \sqrt{2}$. Locally, the flow velocity over the helmet is 40% greater than the free-stream flow.

In an effort to reduce lift, the "crested spoiler" shown in Figures I-9 and I-10 was tried, with results recorded in Table I-2. As can be seen, the results were disappointing.

The winged helmet configuration of Figures I-11 and I-12 was then evaluated, for zero yaw and pitch only, due to test scheduling limitations. As can be seen from Table I-2 and Figures I-1 and I-4, the wings were very successful in reducing both lift and pitching moment, without adverse effect on the other forces. We believe that a "second generation" winged helmet, having small swept back wings at a greater negative angle might achieve zero lift and not impede the helmet wearer significantly. More experimental work in the tunnel is clearly necessary before we can recommend an optimum configuration.

In concluding this section, it is of interest to note that one subject - the one with the fullest face - experienced some discomfort at high speed because of waves developed in the soft tissue of his cheeks by the wind. The mechanism is presumably the same by which the wind develops waves in the sea, even though the "fetch" is only a few inches. Similar waves developed on the upper arms and thighs of a naked subject in previous tests (Reference 1), but not to such a marked extent as to cause discomfort. Waves of this general class have sometimes been ascribed to distributed parameter response to acceleration in the past, during rocket sled experiments with live human subjects. If the subject is not completely shielded from windblast, it seems possible that they might instead be wind generated, or that both factors might have an influence.

Table I - 1. STANDARD HELMET FORCES AND MOMENTS

(Forces are expressed as equivalent area in square feet; moments as volumes in cubic feet)

Yaw Angle	Pitch Angle	Run No.	Subject	Lift Area	Side Force Area	Drag Area	Pitch Moment Volume	Yaw Moment Volume
0°	-15°	23	RM	B.D.	B.D.	0.249	B.D.	B.D.
		25	JP	0.134	-0.061	0.210	0.232	-0.072
		32	JS	0.336	B.D.	0.472	0.450	B.D.
0°	0°	7	BC	0.455	B.D.	0.348	0.685	B.D
		8	RM	0.471	0.044	0.289	0.702	0.072
		11	JP	0.372	B.D.	0.279	0.605	B.D.
		14	JS	0.211	B.D.	0.211	0.347	B.D.
		17	JB	0.400	B.D.	0.330	0.646	B.D.
0°	+15°	20	RM	0.374	0.086	0.168	0.581	0.126
		28	JP	0.454	0.137	0.095	0.725	0.220
		29	JS	0.420	0.068	0.244	0.649	0.112
-15°	-15°	24	RM	0.298	0.164	0.274	0.463	0.235
-15°	0°	9	RM	0.294	0.111	0.244	0.561	0.212
		12	JP	0.310	0.087	0.335	0.492	0.173
		15	JS	0.295	0.106	0.245	0.496	0.230
		16	JB	0.312	0.066	0.263	0.558	0.141
-30°	-15°	22	RM	0.323	0.376	-0.100	0.508	0.643
		26	JP	B.D.	0.386	B.D.	B.D.	0.704
		31	JS	0.208	0.501	B.D.	0.301	0.835

Table I-1. STANDARD HELMET FORCES AND MOMENTS (continued)

Yaw Angle	Pitch Angle	Run No.	Subject	Lift Area	Side Force Area	Drag Area	Pitch Moment Volume	Yaw Moment Volume
-30°	0°	10	RM	0.284	0.284	B.D.	0.451	0.456
		13	JP	0.296	0.212	0.205	0.464	0.391
		16	JS	0.358	0.306	-0.100	0.599	0.566
		19	JB	0.353	0.332	0.099	0.566	0.614
-30°	+15°	21	RM	0.306	0.290	0.193	0.527	0.447
		27	JP	0.350	0.194	-0.060	0.571	0.346
		30	JS	0.281	0.271	0.127	0.437	-.478

Table I-2. FORCES AND MOMENTS FOR HELMETS WITH SPOILERS

Yaw Angle	Pitch Angle	Run No.	Subject	Lift Area	Side Force Area	Drag Area	Pitch Moment Volume	Yaw Moment Volume
CRESTED SPOILER								
0°	0°	35	RM	0.284	B.D.	0.60	0.493	B.D.
0°	-15°	36	RM	0.288	B.D.	0.50	0.388	B.D.
0°	+15°	37	RM	N.D.	0.131	0.37	N.D.	0.167
-30°	+15°	38	RM	0.406	0.374	0.12	0.610	0.598
-30°	-15°	39	RM	0.233	0.486	0.12	0.351	0.871
VIKING WINGS								
0°	0°	42	JS	0.070	0.035	0.32	0.139	0.093

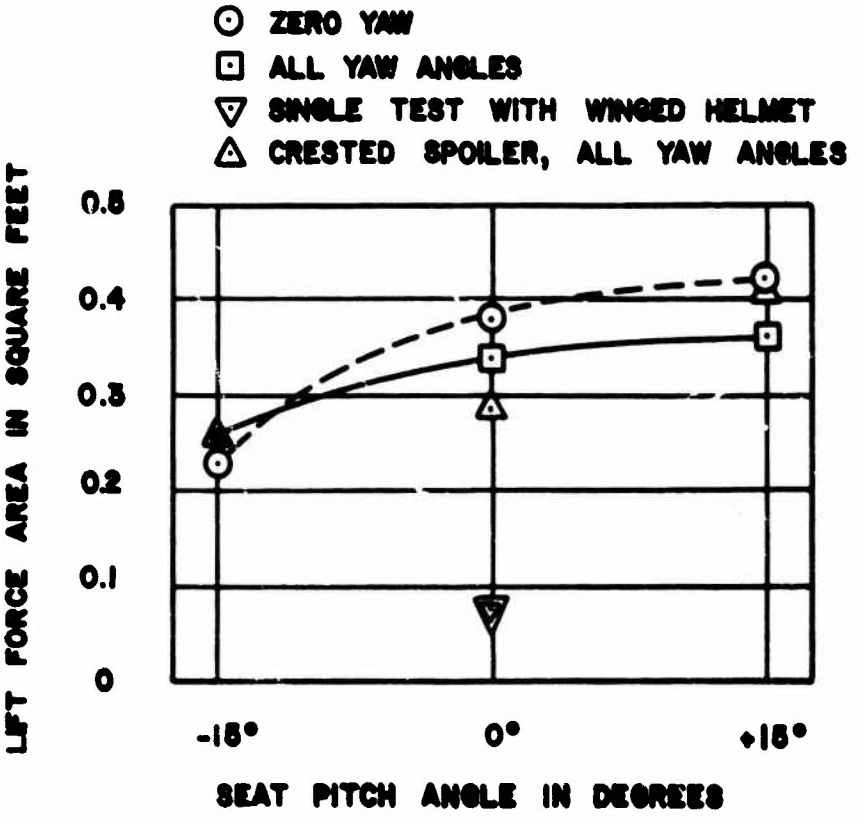

Figure I - 1. Average Helmet Lift as a Function of Seat Pitch Angle (Helmet Axes).

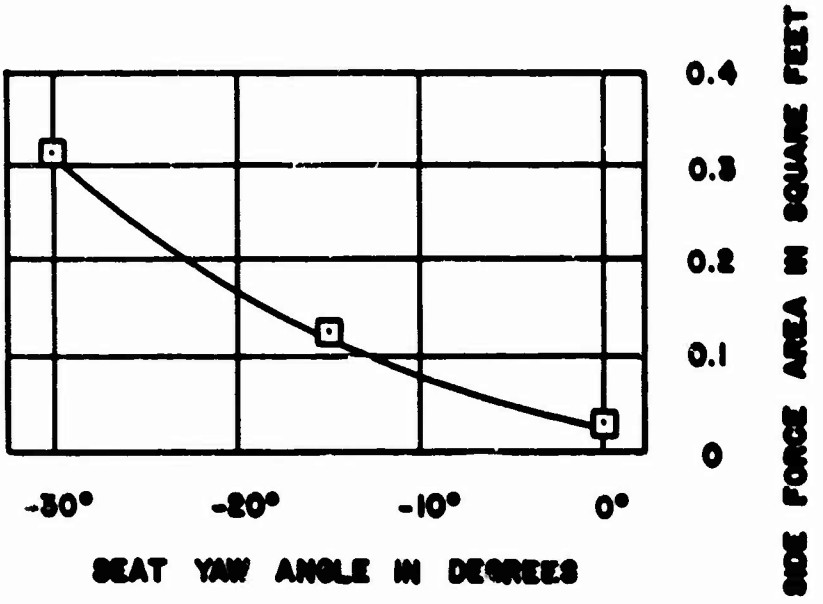

Figure I - 2. Average Helmet Side Force, For all Pitch Angles, as a Function of Seat Yaw Angle (Helmet Axes).

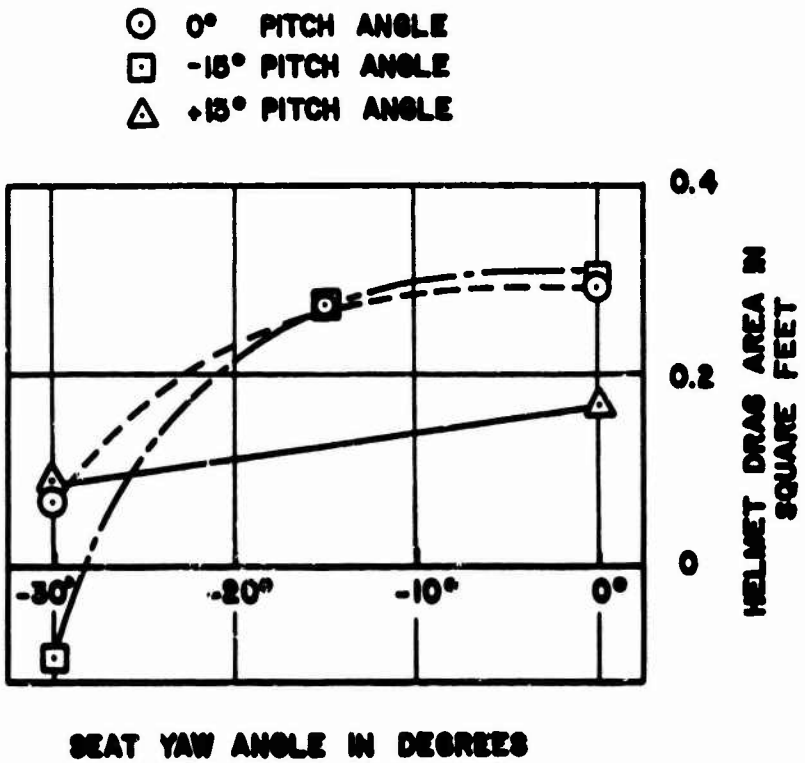

Figure I - 3. Helmet Drag Area, as a Function of Pitch and Yaw Angle (Helmet Axes).

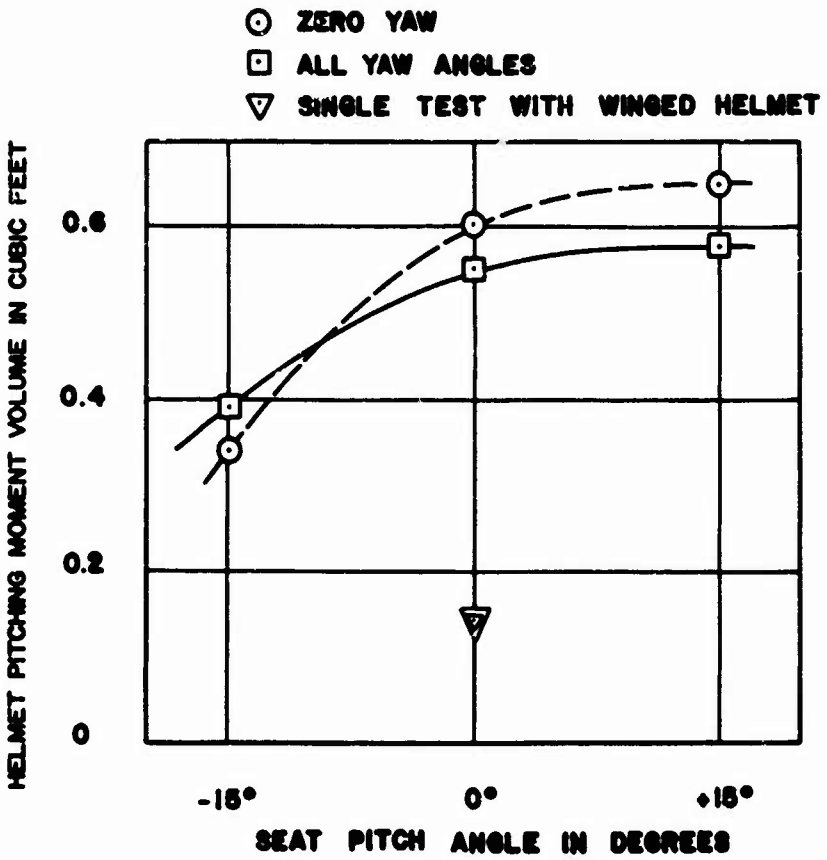

Figure I - 4. Average Helmet Pitching Moment as a Function of Seat Pitch Angle (Helmet Axes).

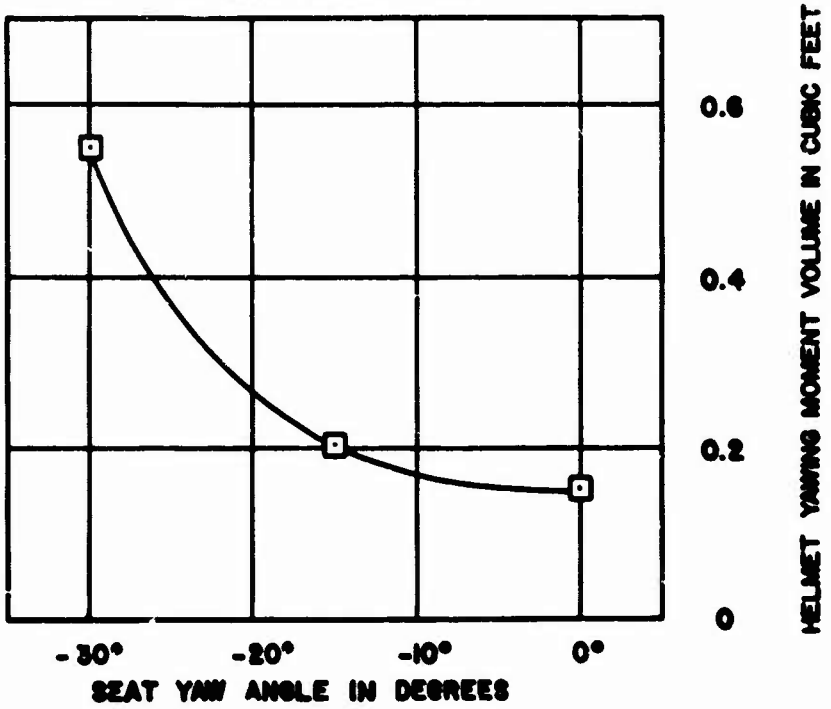

Figure I - 5. Average Helmet Yawing Moment as a Function of Seat Yaw Angle (Helmet Axes).

Figure I - 6. Inside View of Helmet, Showing Static Pressure Lines to Internal and External Static Pressure Taps.

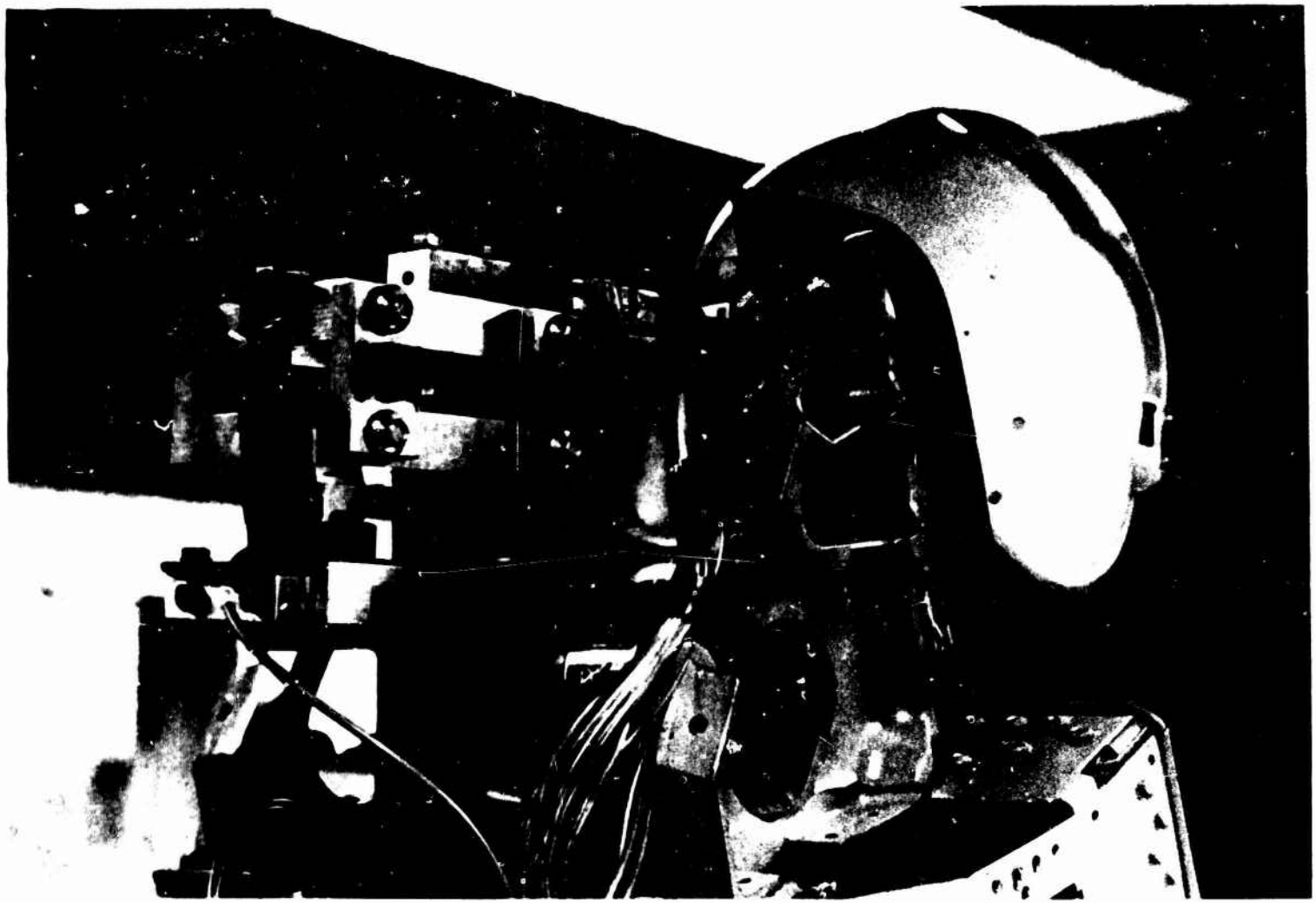

Figure I - 7. The Helmet Cantilevered on the End of Its Strain Gauged Sting.

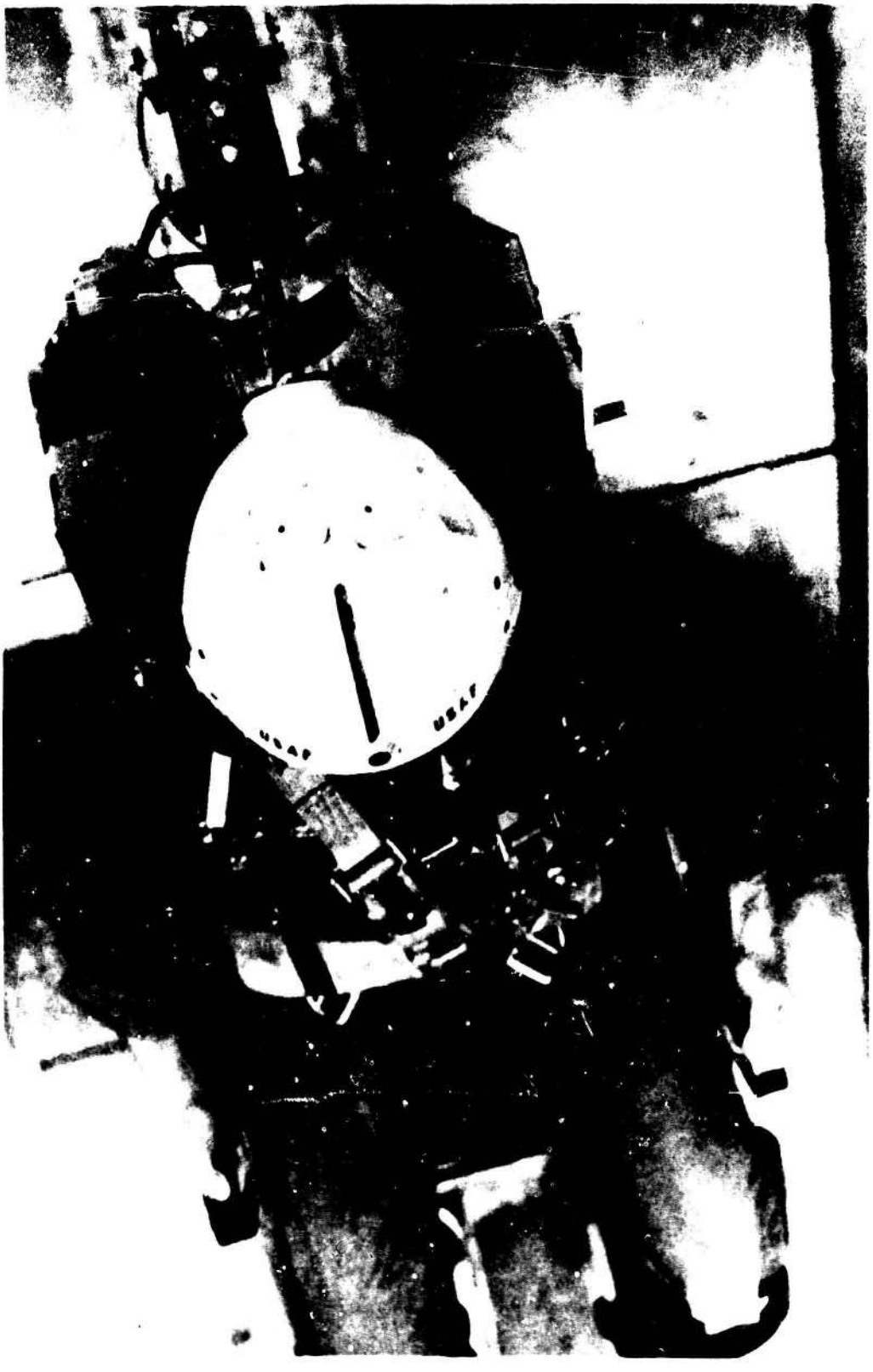

Figure I - 8. Top View of the Helmet and Sting Mounting Assembly During a Test. The Foam Headrest Has Been Pared Away so That the Sting Can Project Through It. Later in the Program, This Excessively Large Aperture Was Bridged With Tape.

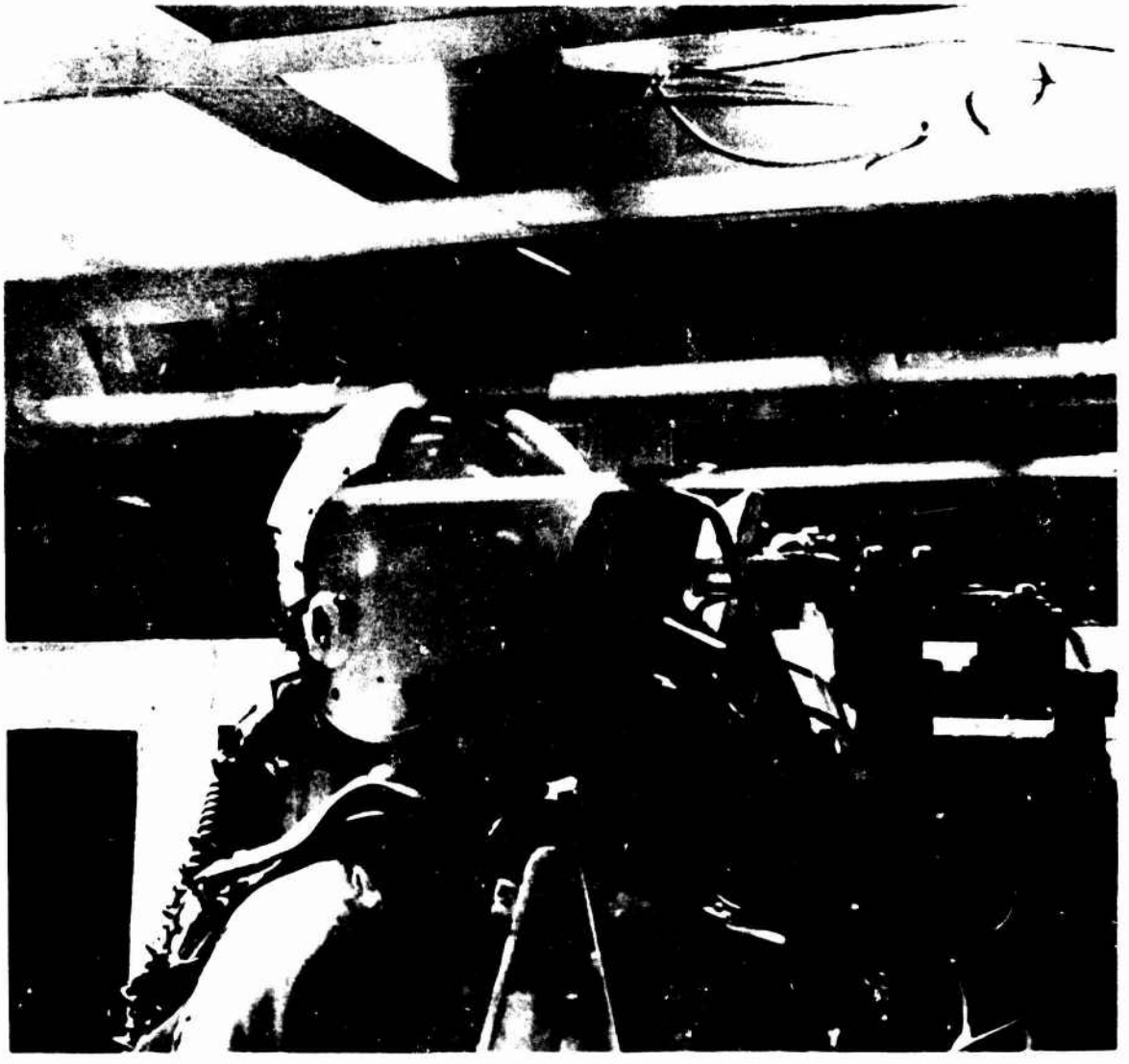

Figure I - 9. The "Crested Spoiler" Attached to the Helmet in an Effort to Reduce Helmet Lift.

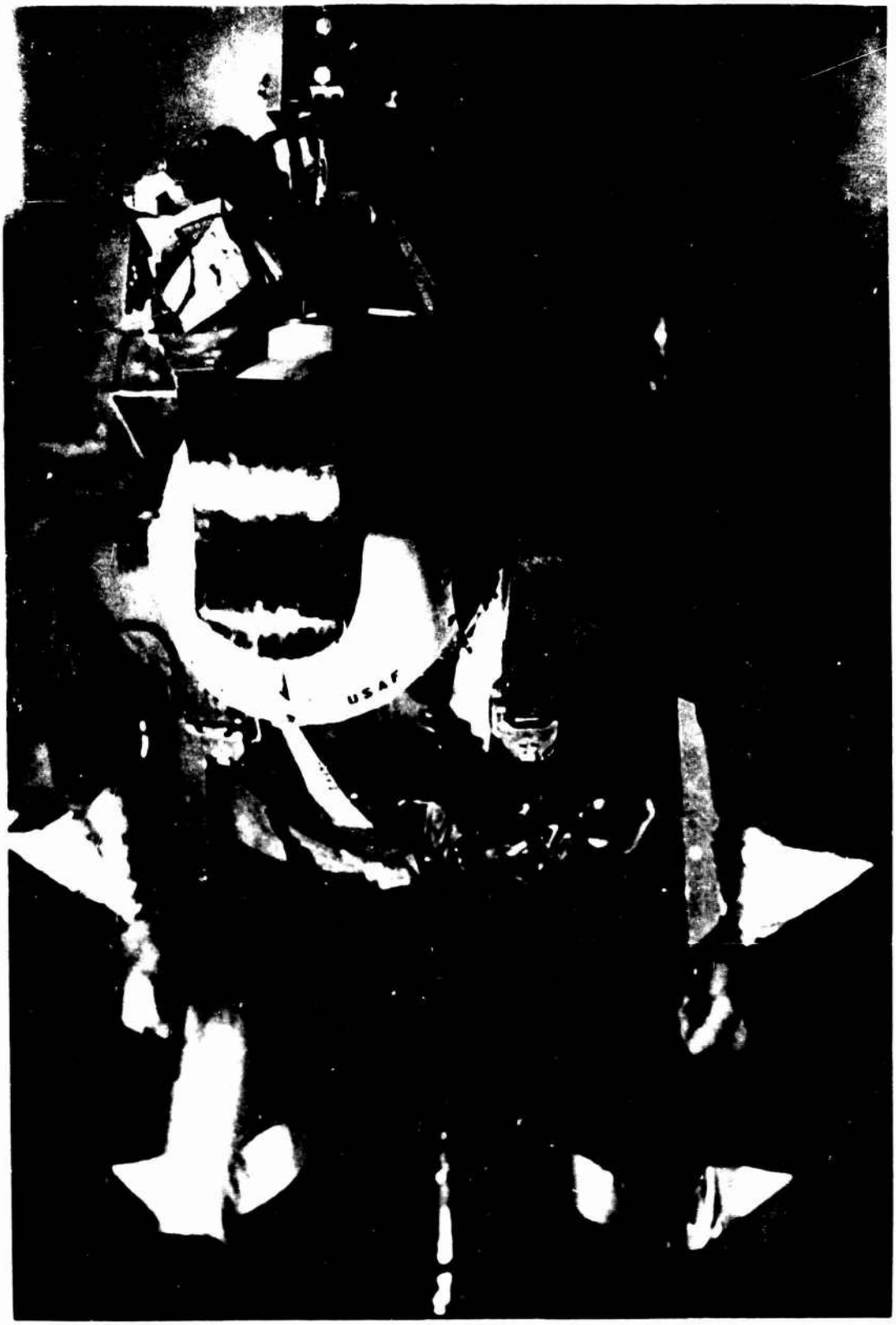

Figure I - 10. **The "Crested Spoiler" Seen From Above During a Test.** In This Case, the Subject is Also Wearing Wedge Spoilers on His Limbs.

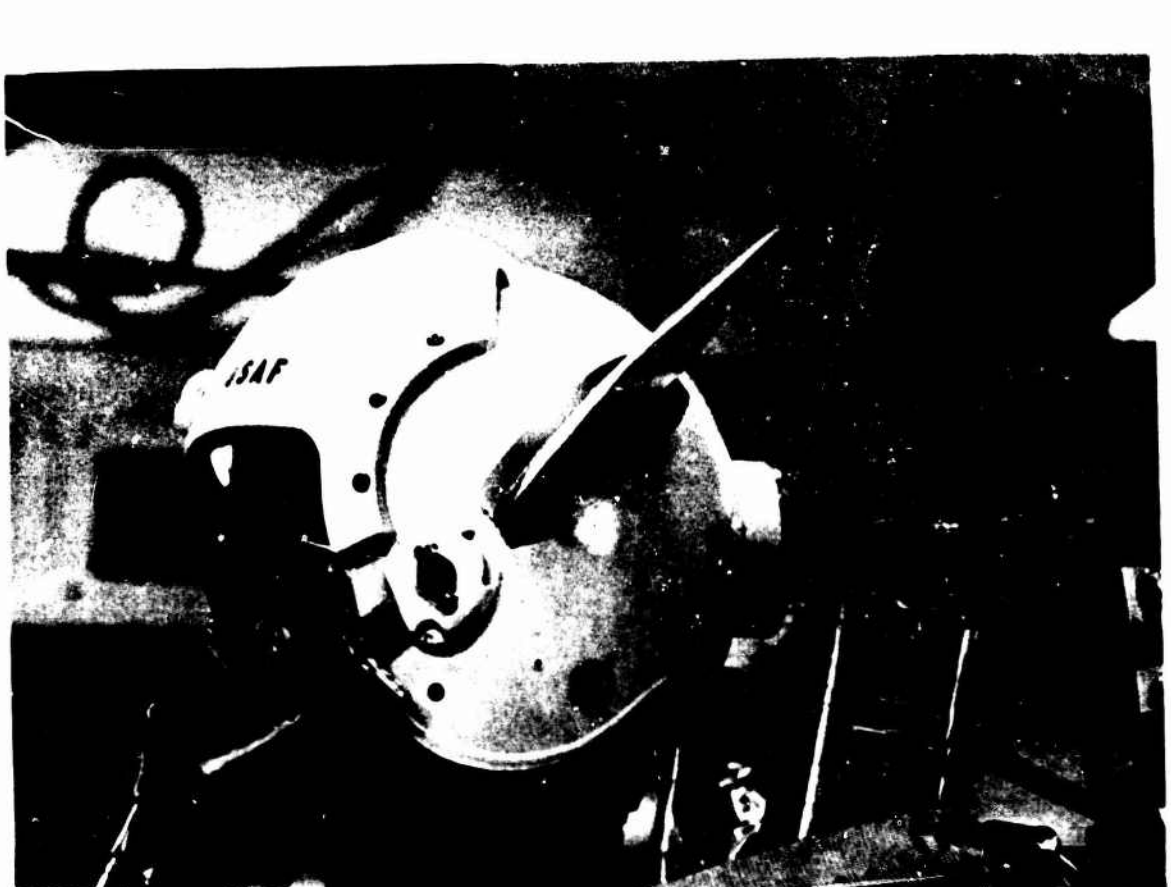

Figure I - 11. Helmet Fitted With "Viking Wings" to Reduce Lift Forces.

Figure I - 12. Tape Used to "Stiffen" the Skin of Subject JS, to Prevent Wind Generated "Waves" in the Soft Tissue of His Face.

RUN NUMBER 7

PITCH ANGLE 0°

YAW ANGLE 0°

SUBJECT BC

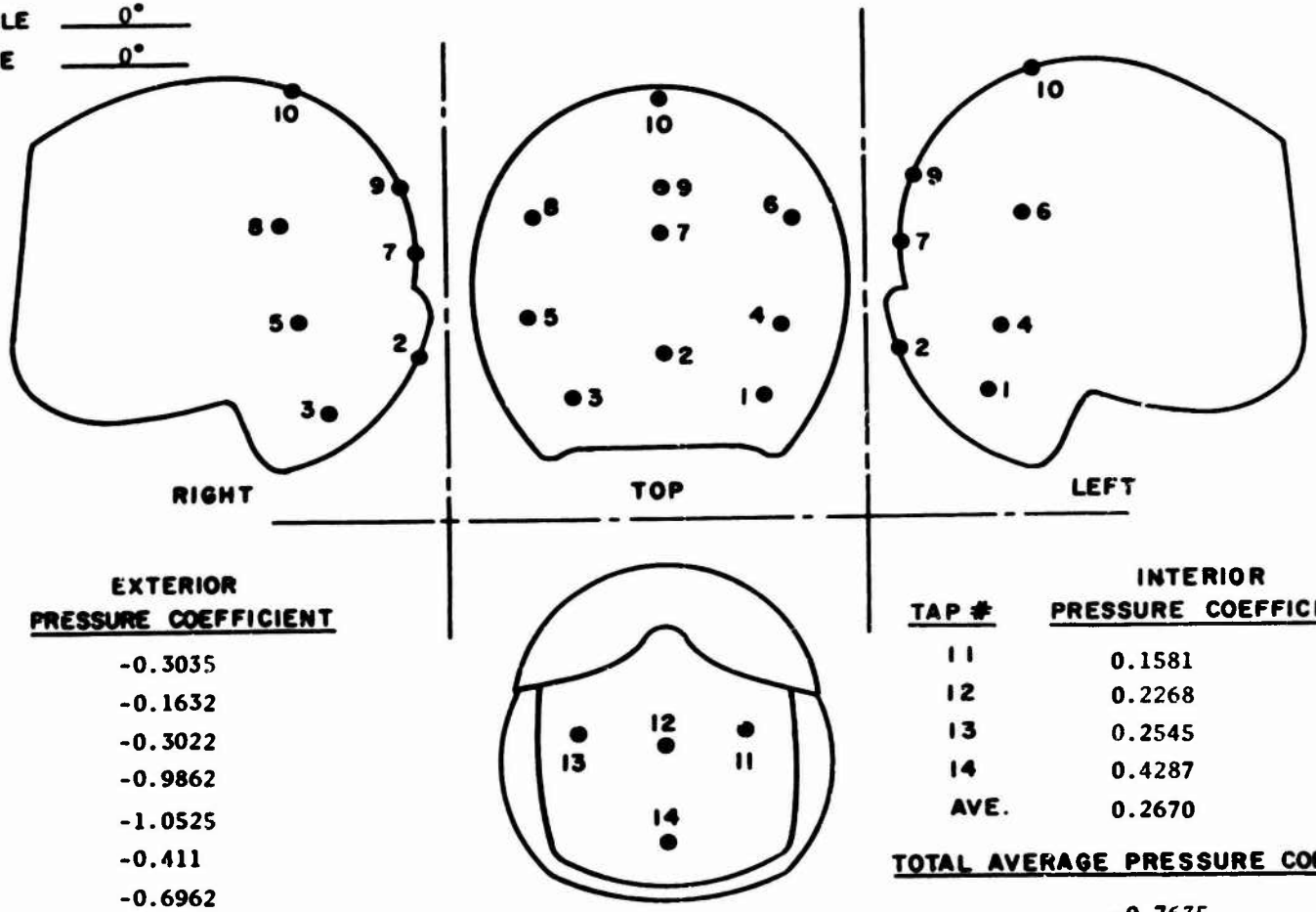

TAP #	EXTERIOR PRESSURE COEFFICIENT
1	-0.3035
2	-0.1632
3	-0.3022
4	-0.9862
5	-1.0525
6	-0.411
7	-0.6962
8	-0.3958
9	-0.3774
10	-0.2774
AVE.	-0.4965

TAP #	INTERIOR PRESSURE COEFFICIENT
11	0.1581
12	0.2268
13	0.2545
14	0.4287
AVE.	0.2670

TOTAL AVERAGE PRESSURE COEFFICIENT

-0.7635

Table I - 3. Average Pressure Coefficient of USAF Helmet with Live Subject

RUN NUMBER 8

PITCH ANGLE 0°

YAW ANGLE 0°

SUBJECT MAM

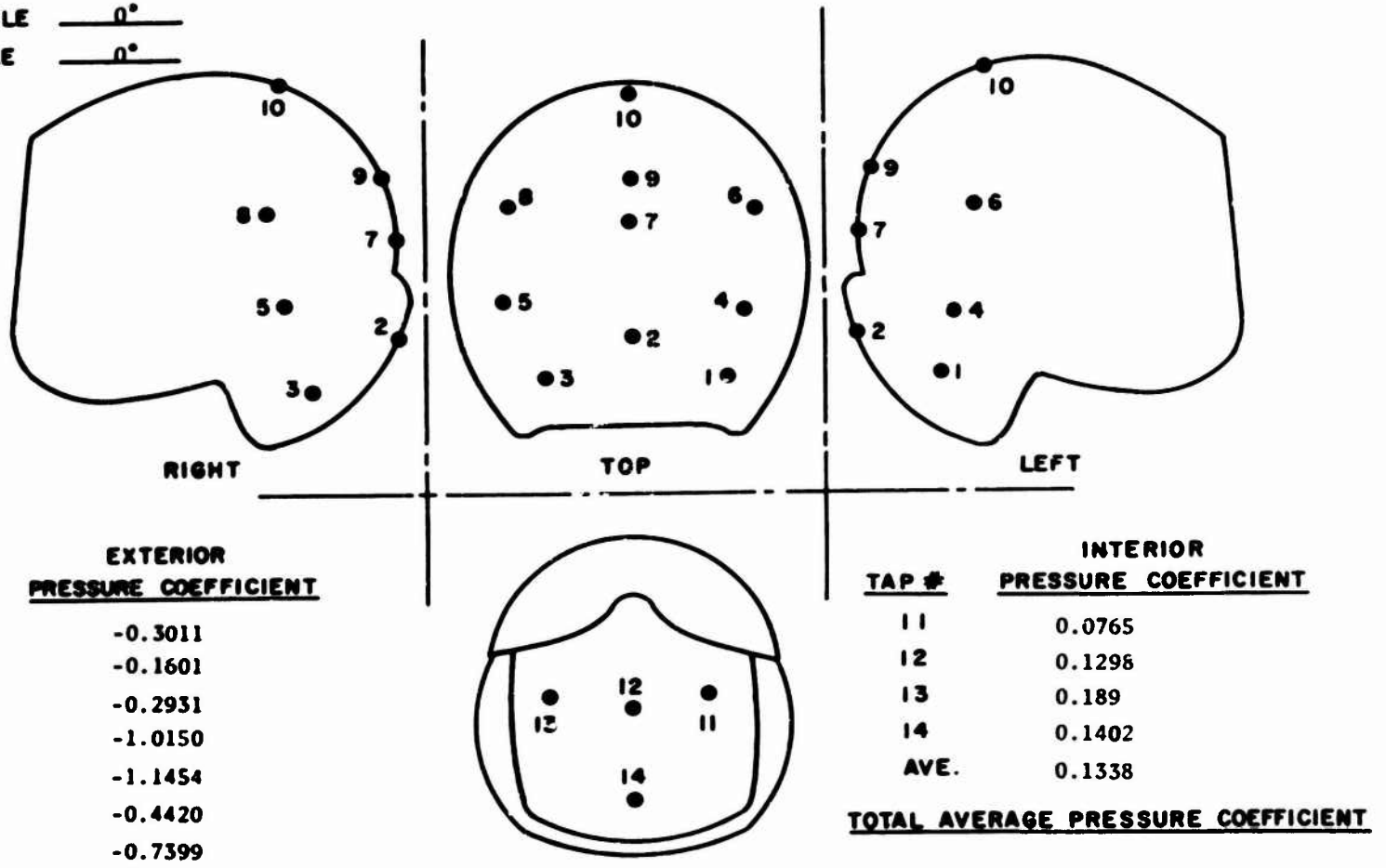

TAP #	EXTERIOR PRESSURE COEFFICIENT
1	-0.3011
2	-0.1601
3	-0.2931
4	-1.0150
5	-1.1454
6	-0.4420
7	-0.7399
8	-0.4079
9	-0.4066
10	-0.3257
AVE.	-0.5236

TAP #	INTERIOR PRESSURE COEFFICIENT
11	0.0765
12	0.1298
13	0.189
14	0.1402
AVE.	0.1338

TOTAL AVERAGE PRESSURE COEFFICIENT

-0.6574

Table I - 3. Average Pressure Coefficient of USAF Helmet with Live Subject.

RUN NUMBER 9

PITCH ANGLE 0°

YAW ANGLE -15°

SUBJECT MAM

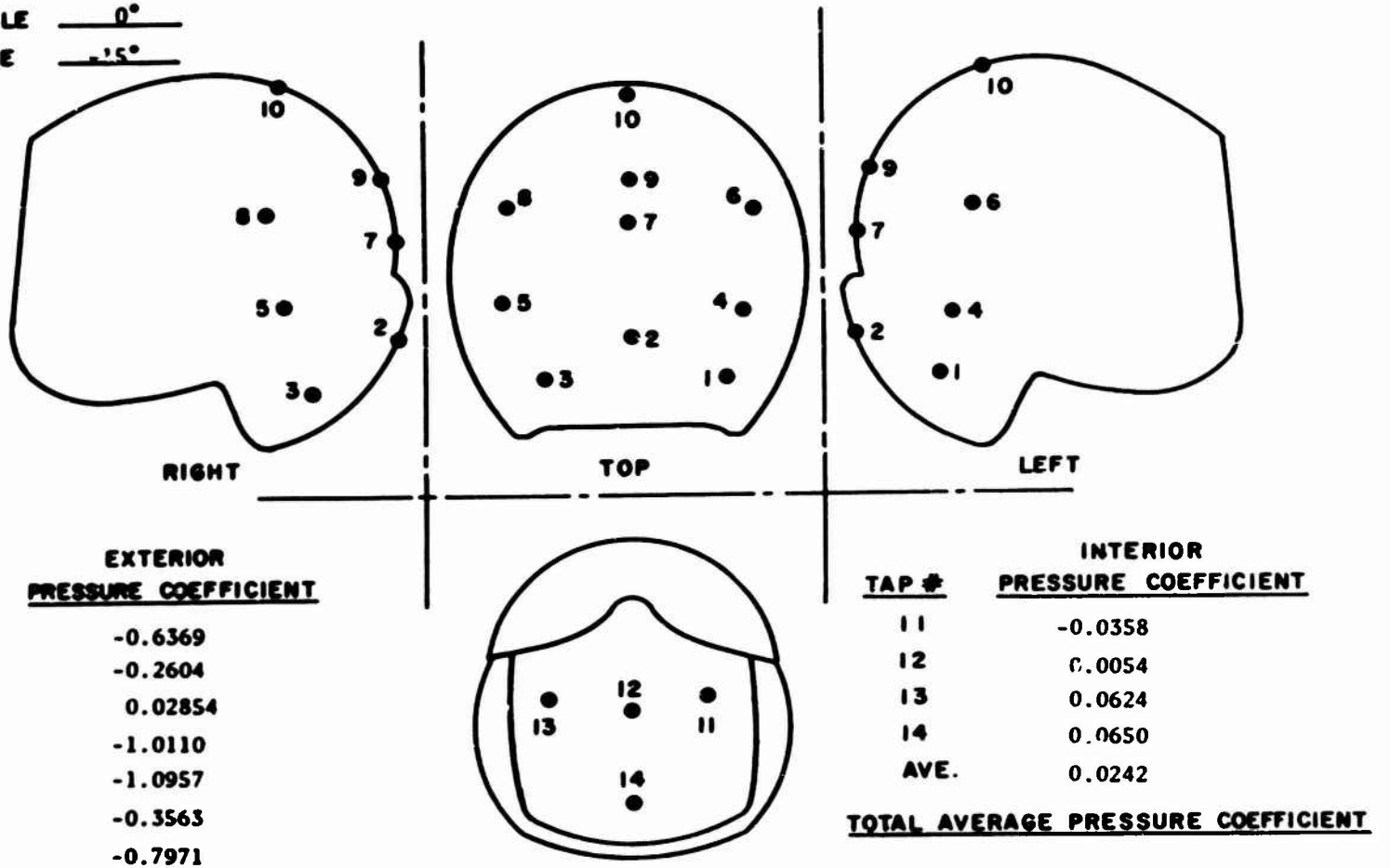

TAP #	EXTERIOR PRESSURE COEFFICIENT
1	-0.6369
2	-0.2604
3	0.02854
4	-1.0110
5	-1.0957
6	-0.3563
7	-0.7971
8	-0.5677
9	-0.4044
10	-0.3130
AVE.	-0.5414

TAP #	INTERIOR PRESSURE COEFFICIENT
11	-0.0358
12	0.0054
13	0.0624
14	0.0650
AVE.	0.0242

TOTAL AVERAGE PRESSURE COEFFICIENT

-0.5656

Table I - 3. Average Pressure Coefficient of USAF Helmet with Live Subject

RUN NUMBER 10

PITCH ANGLE 0°

YAW ANGLE -30°

SUBJECT MAM

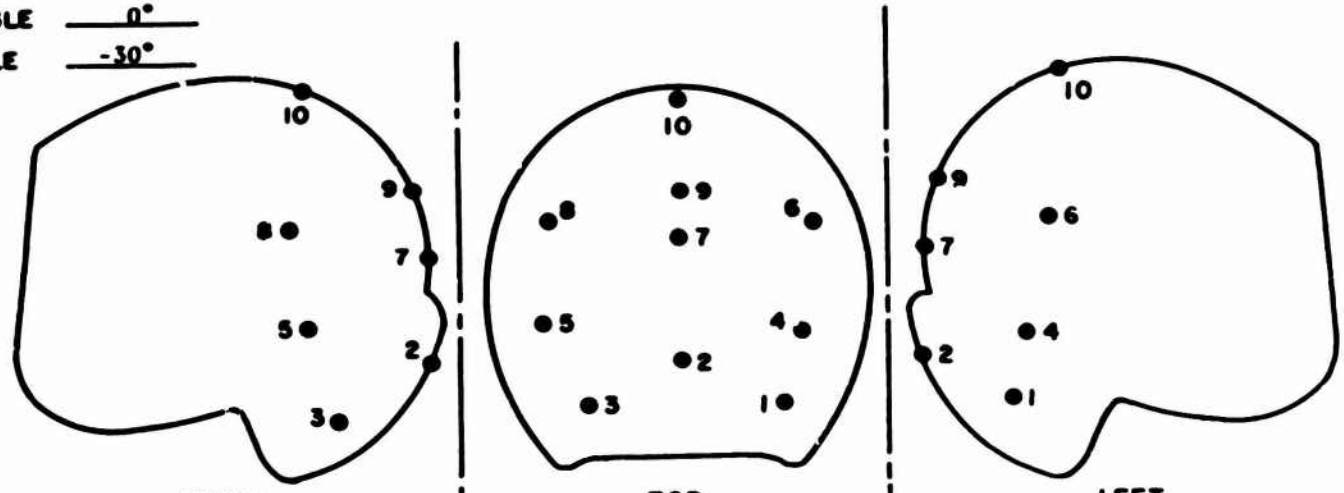

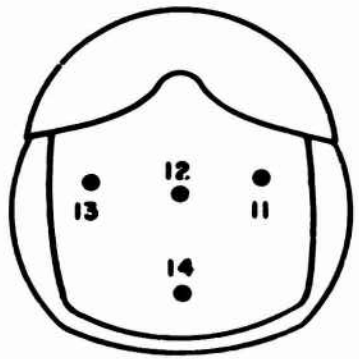

TAP #	EXTERIOR PRESSURE COEFFICIENT
1	-0.9509
2	-0.3591
3	-0.2633
4	-0.8764
5	-0.8911
6	-0.4039
7	-0.7764
8	-0.6014
9	-0.4539
10	-0.4919
AVE.	-0.5551

TAP #	INTERIOR PRESSURE COEFFICIENT
11	-0.1991
12	-0.1641
13	-0.1782
14	-0.1417
AVE.	-0.1707

TOTAL AVERAGE PRESSURE COEFFICIENT

-0.3844

Table I - 3. Average Pressure Coefficient of USAF Helmet with Live Subject

RUN NUMBER 11

PITCH ANGLE 0°

YAW ANGLE 0°

SUBJECT JP

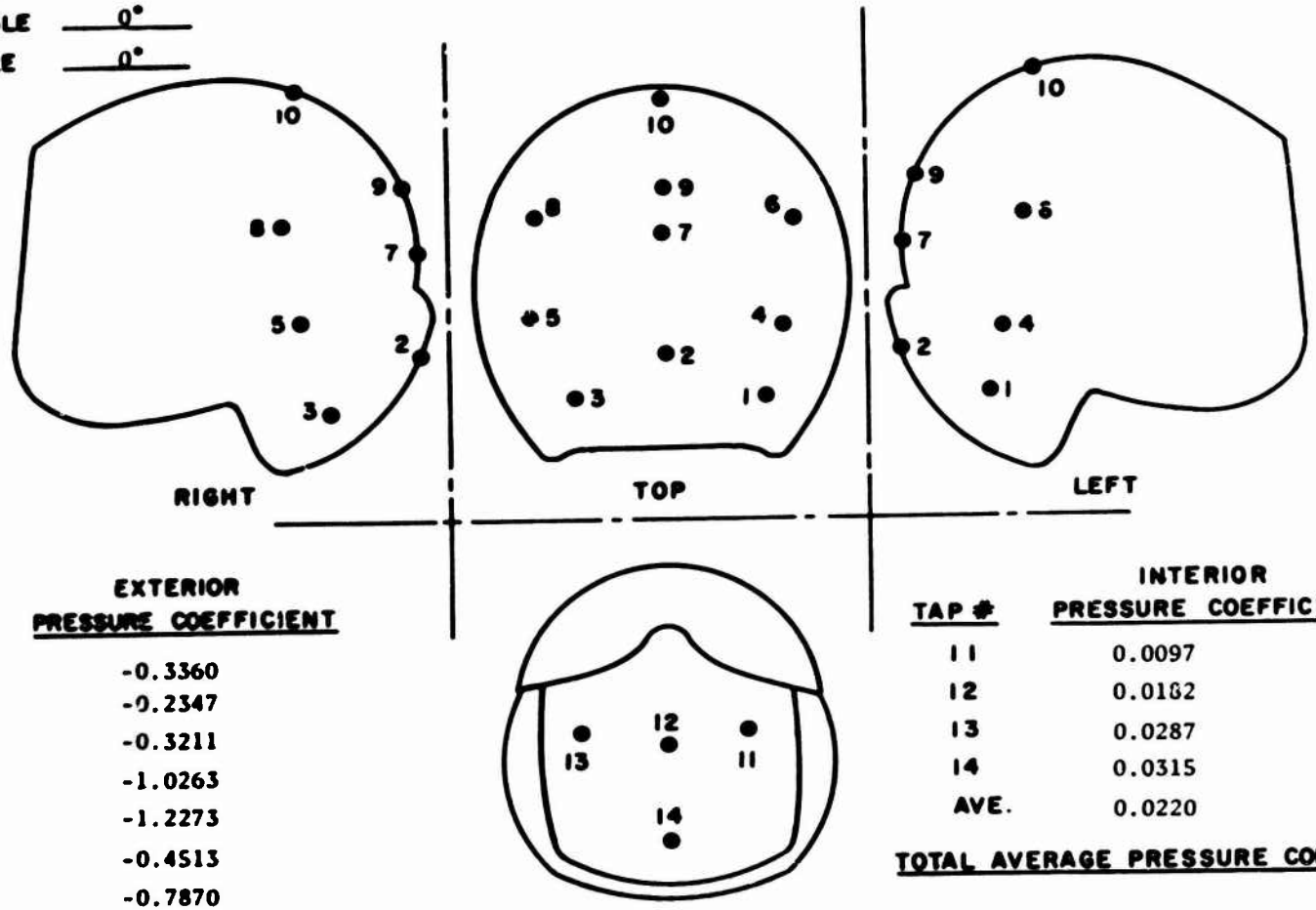

TAP #	EXTERIOR PRESSURE COEFFICIENT
1	-0.3360
2	-0.2347
3	-0.3211
4	-1.0263
5	-1.2273
6	-0.4513
7	-0.7870
8	-0.4319
9	-0.4241
10	-0.3447
AVE.	-0.5584

TAP #	INTERIOR PRESSURE COEFFICIENT
11	0.0097
12	0.0182
13	0.0287
14	0.0315
AVE.	0.0220

TOTAL AVERAGE PRESSURE COEFFICIENT

-0.5775

Table I - 3. Average Pressure Coefficient of USAF Helmet with Live Subject.

RUN NUMBER 12

PITCH ANGLE 0°

YAW ANGLE -15°

SUBJECT JP

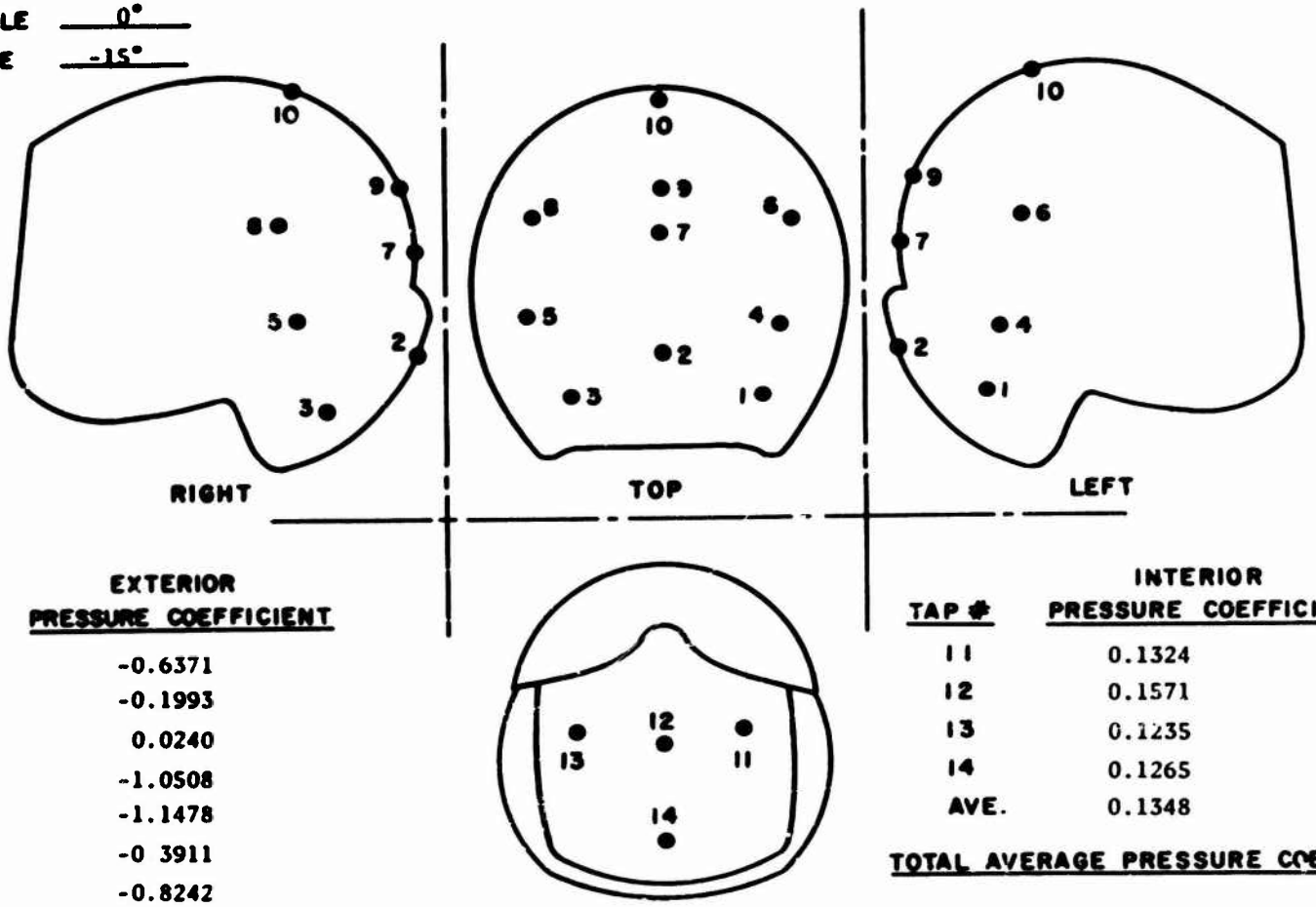

TAP #	EXTERIOR PRESSURE COEFFICIENT
1	-0.6371
2	-0.1993
3	0.0240
4	-1.0508
5	-1.1478
6	-0 3911
7	-0.8242
8	-0.6063
9	-0.4228
10	-0.3208
AVE.	-0.5576

TAP #	INTERIOR PRESSURE COEFFICIENT
11	0.1324
12	0.1571
13	0.1235
14	0.1265
AVE.	0.1348

TOTAL AVERAGE PRESSURE COEFFICIENT

-0.4228

Table I - 3. Average Pressure Coefficient of USAF Helmet with Live Subject.

RUN NUMBER 13

PITCH ANGLE 0°

YAW ANGLE -30°

SUBJECT JP

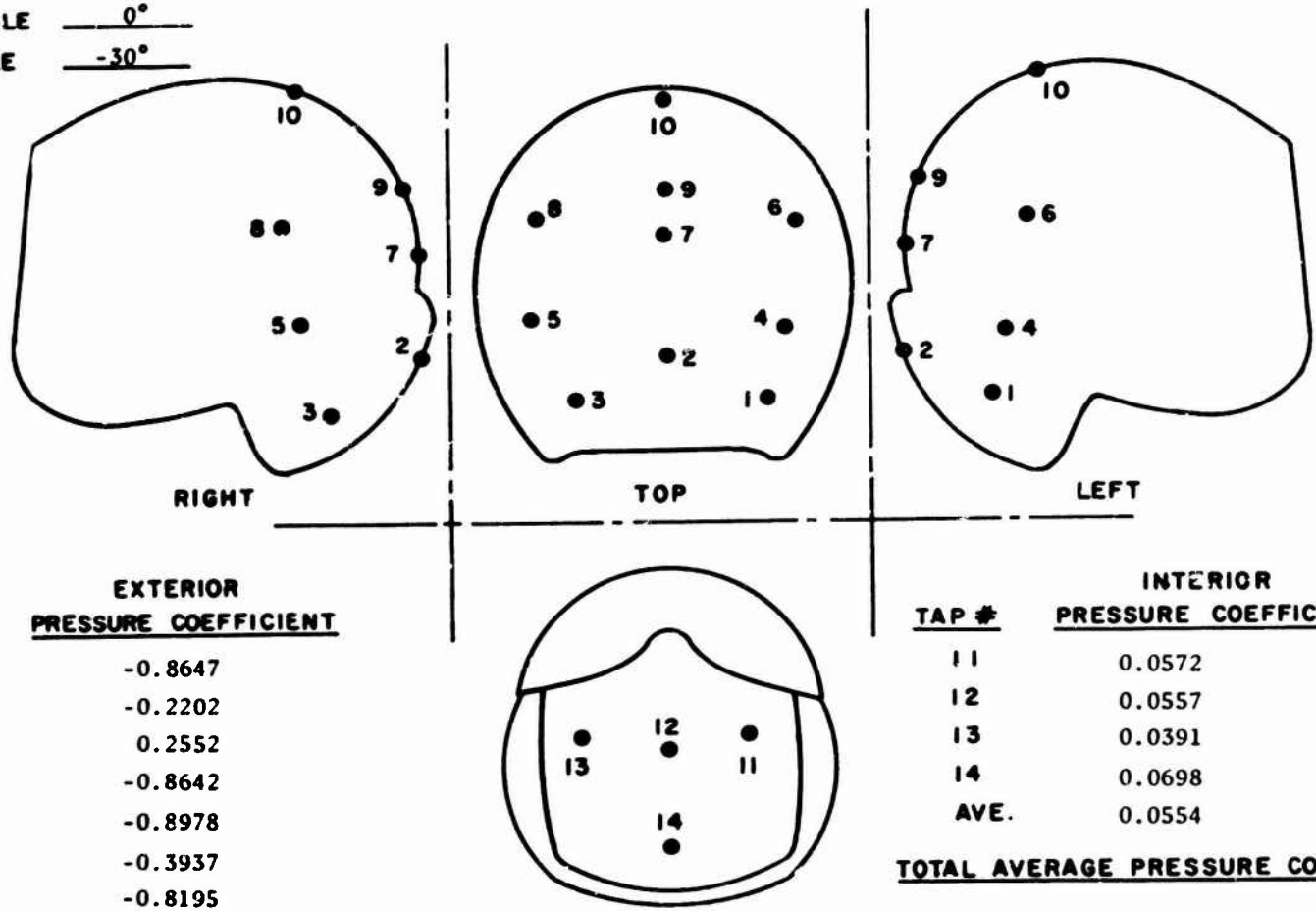

TAP #	EXTERIOR PRESSURE COEFFICIENT
1	-0.8647
2	-0.2202
3	0.2552
4	-0.8642
5	-0.8978
6	-0.3937
7	-0.8195
8	-0.6160
9	-0.4238
10	-0.4514
AVE.	-0.5296

TAP #	INTERIOR PRESSURE COEFFICIENT
11	0.0572
12	0.0557
13	0.0391
14	0.0698
AVE.	0.0554

TOTAL AVERAGE PRESSURE COEFFICIENT

-0.5850

Table I - 3. Average Pressure Coefficient of USAF Helmet with Live Subject.

RUN NUMBER 17

PITCH ANGLE 0°

YAW ANGLE 0°

SUBJECT JB

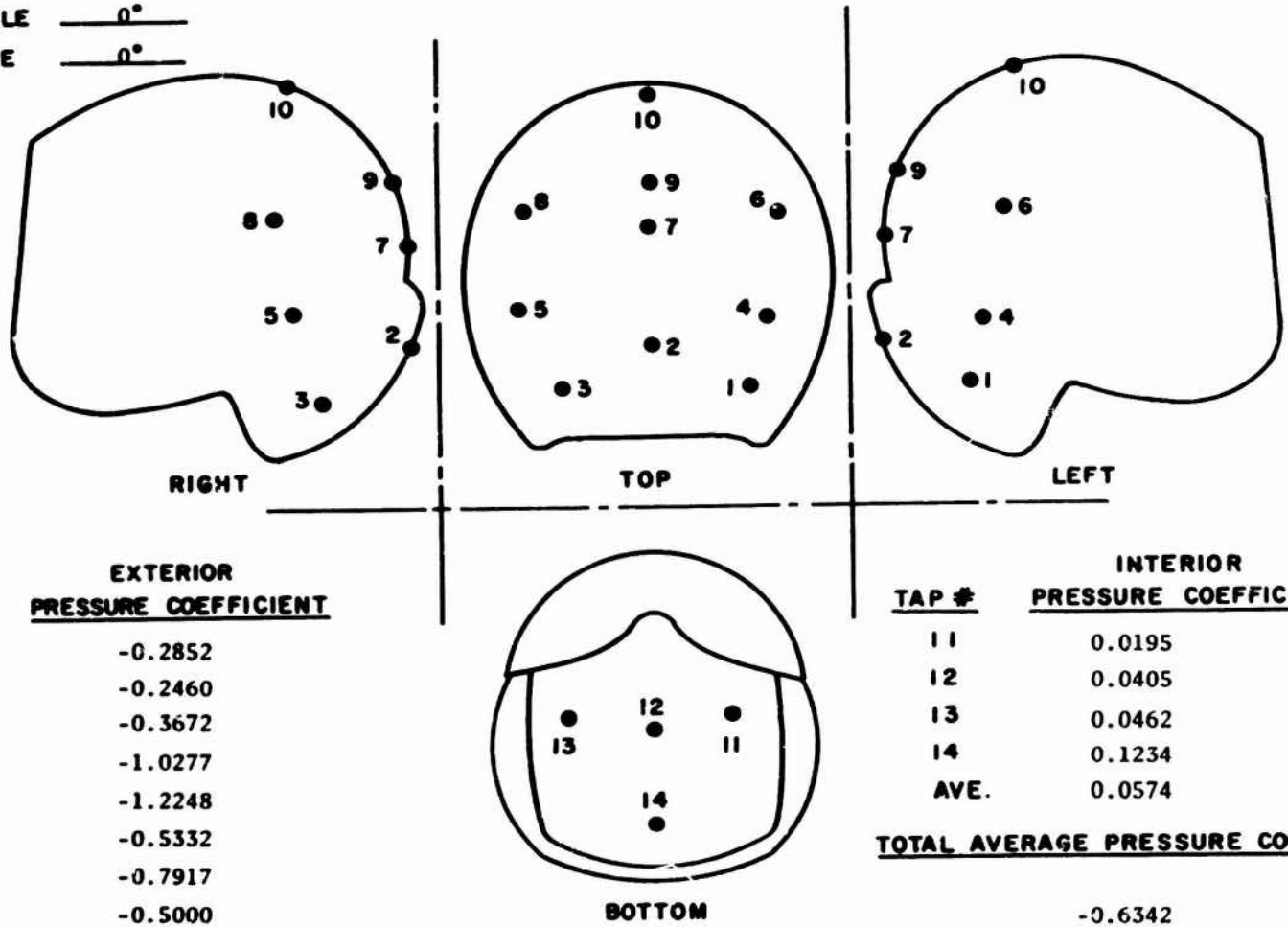

TAP #	EXTERIOR PRESSURE COEFFICIENT
1	-0.2852
2	-0.2460
3	-0.3672
4	-1.0277
5	-1.2248
6	-0.5332
7	-0.7917
8	-0.5000
9	-0.4305
10	-0.3625
AVE.	-0.5768

TAP #	INTERIOR PRESSURE COEFFICIENT
11	0.0195
12	0.0405
13	0.0462
14	0.1234
AVE.	0.0574

TOTAL AVERAGE PRESSURE COEFFICIENT

-0.6342

Table I - 3. Average Pressure Coefficient of USAF Helmet with Live Subject.

BAD DATA

RUN NUMBER 18

PITCH ANGLE 0°

YAW ANGLE -15°

SUBJECT JB

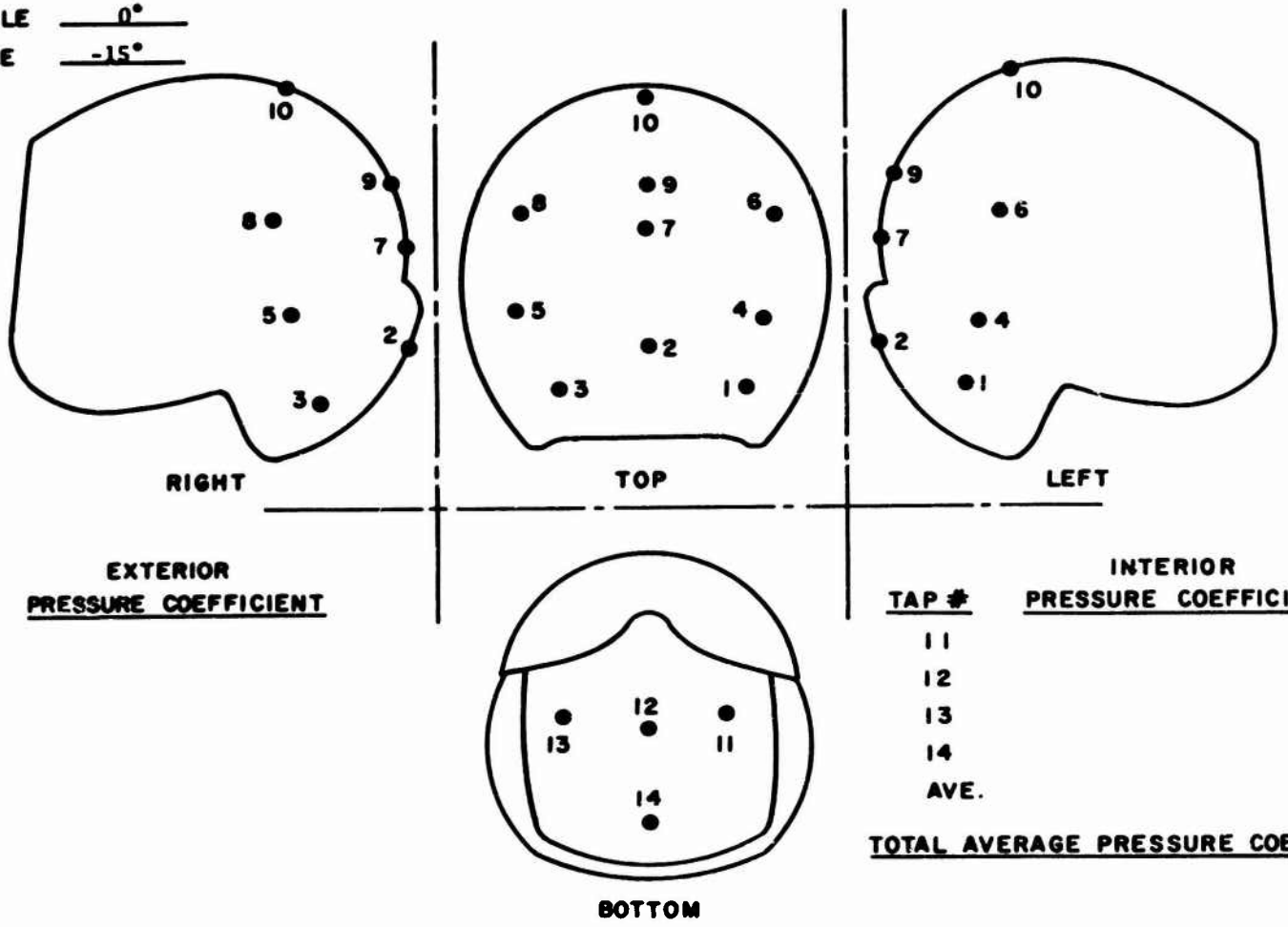

TAP #	EXTERIOR PRESSURE COEFFICIENT
1	
2	
3	
4	
5	
6	
7	
8	
9	
10	
AVE.	

TAP #	INTERIOR PRESSURE COEFFICIENT
11	
12	
13	
14	
AVE.	

TOTAL AVERAGE PRESSURE COEFFICIENT

Table I - 3. Average Pressure Coefficient of USAF Helmet with Live Subject.

RUN NUMBER 19

PITCH ANGLE 0°

YAW ANGLE -30°

SUBJECT JB

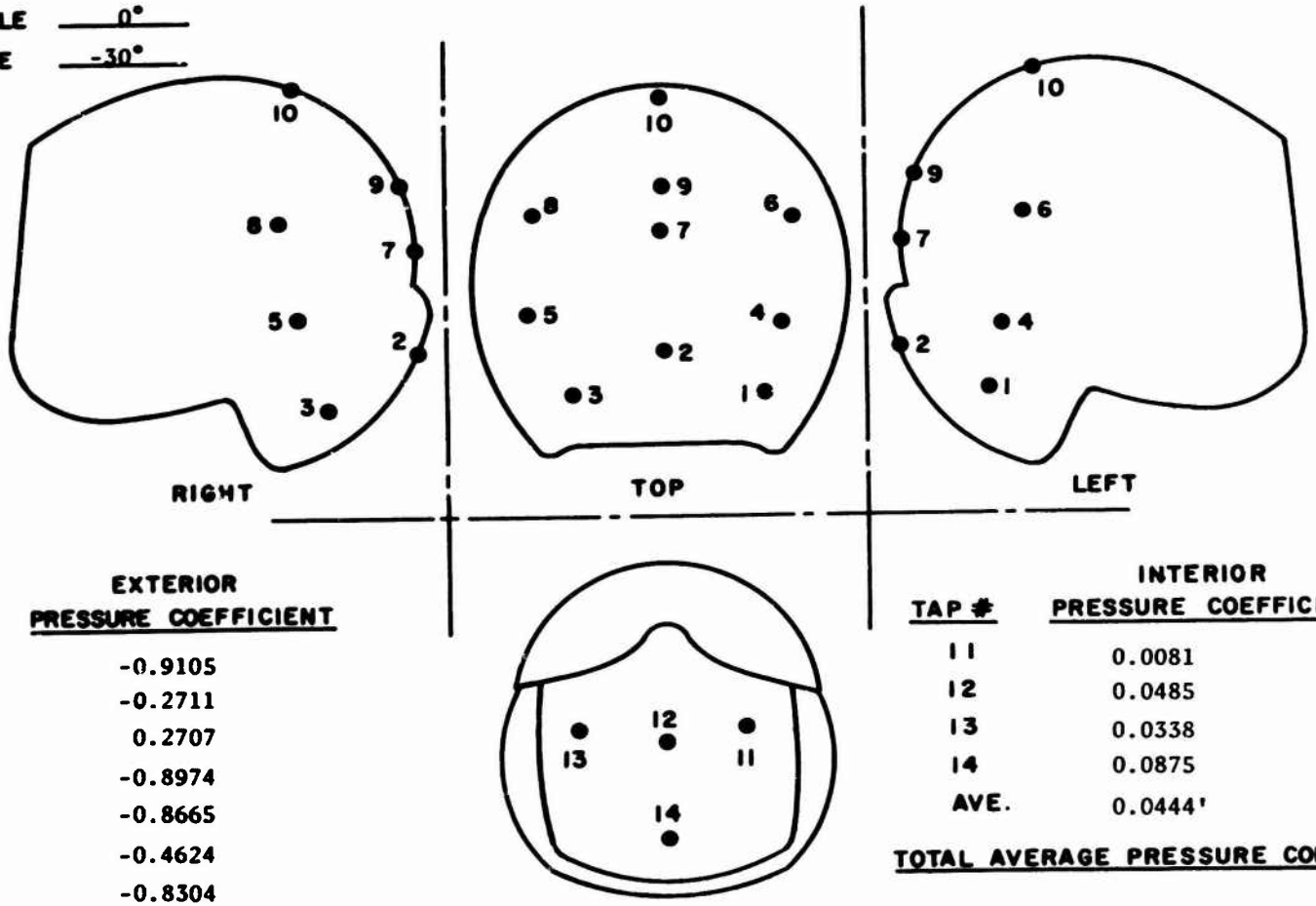

TAP #	EXTERIOR PRESSURE COEFFICIENT
1	-0.9105
2	-0.2711
3	0.2707
4	-0.8974
5	-0.8665
6	-0.4624
7	-0.8304
8	-0.6437
9	-0.4992
10	-0.4822
AVE.	-0.5592

TAP #	INTERIOR PRESSURE COEFFICIENT
11	0.0081
12	0.0485
13	0.0338
14	0.0875
AVE.	0.0444'

TOTAL AVERAGE PRESSURE COEFFICIENT

-0.6036

Table I - 3. Average Pressure Coefficient of USAF Helmet with Live Subject.

RUN NUMBER 20

PITCH ANGLE +15°

YAW ANGLE 0°

SUBJECT MAM

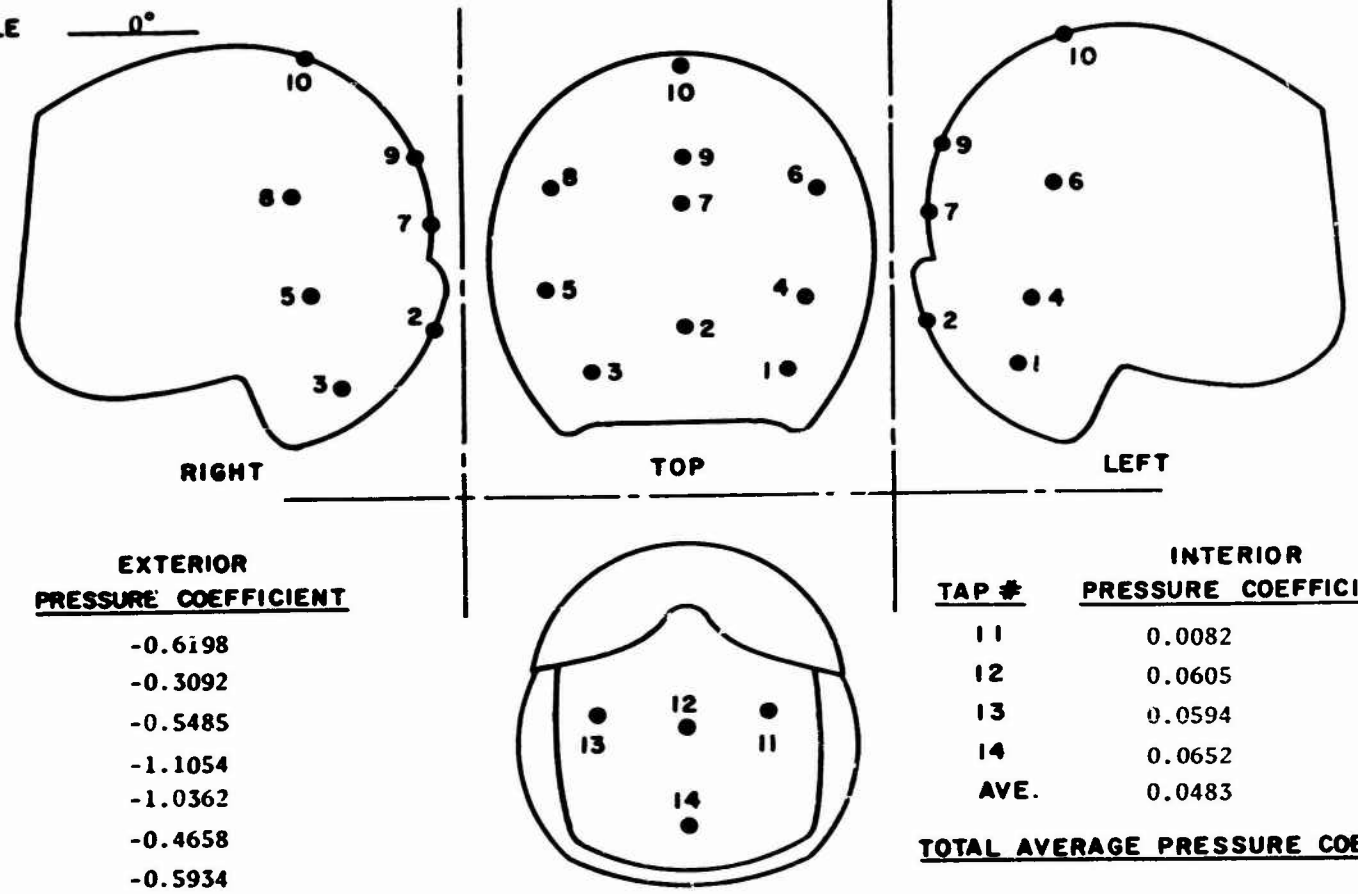

TAP #	EXTERIOR PRESSURE COEFFICIENT
1	-0.6198
2	-0.3092
3	-0.5485
4	-1.1054
5	-1.0362
6	-0.4658
7	-0.5934
8	-0.3754
9	-0.3932
10	-9.3958
AVE.	-0.5842

TAP #	INTERIOR PRESSURE COEFFICIENT
11	0.0082
12	0.0605
13	0.0594
14	0.0652
AVE.	0.0483

TOTAL AVERAGE PRESSURE COEFFICIENT

-0.6325

Table I - 3. Average Pressure Coefficient of USAF Helmet with Live Subject.

RUN NUMBER 21

PITCH ANGLE +15°

YAW ANGLE -30°

SUBJECT MAM

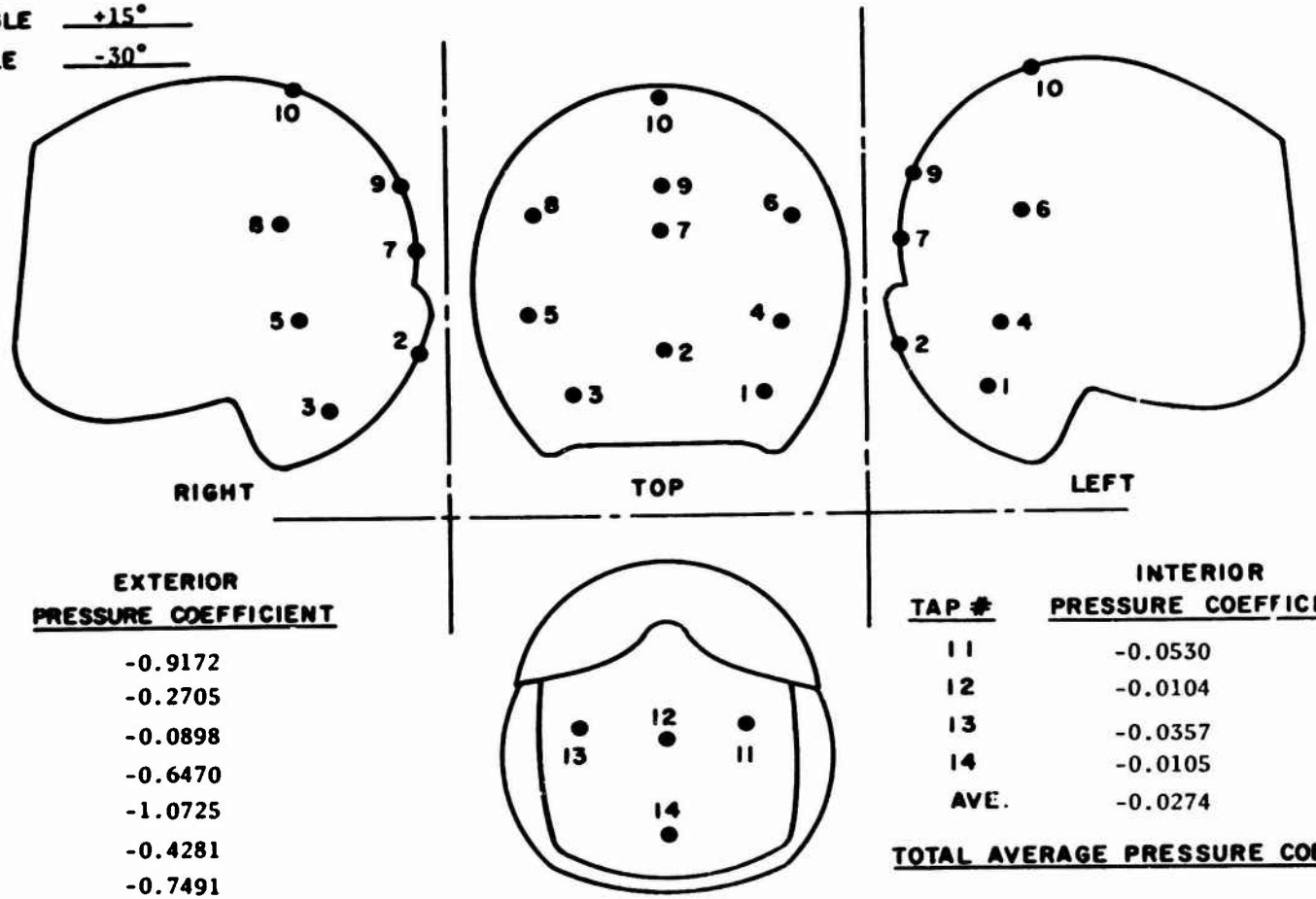

TAP #	EXTERIOR PRESSURE COEFFICIENT
1	-0.9172
2	-0.2705
3	-0.0898
4	-0.6470
5	-1.0725
6	-0.4281
7	-0.7491
8	-0.5905
9	-0.4645
10	-0.4302
AVE.	-0.5659

TAP #	INTERIOR PRESSURE COEFFICIENT
11	-0.0530
12	-0.0104
13	-0.0357
14	-0.0105
AVE.	-0.0274

TOTAL AVERAGE PRESSURE COEFFICIENT

-0.5385

Table I - 3. Average Pressure Coefficient of USAF Helmet with Live Subject.

RUN NUMBER 22

PITCH ANGLE -15°

YAW ANGLE -30°

SUBJECT MAM

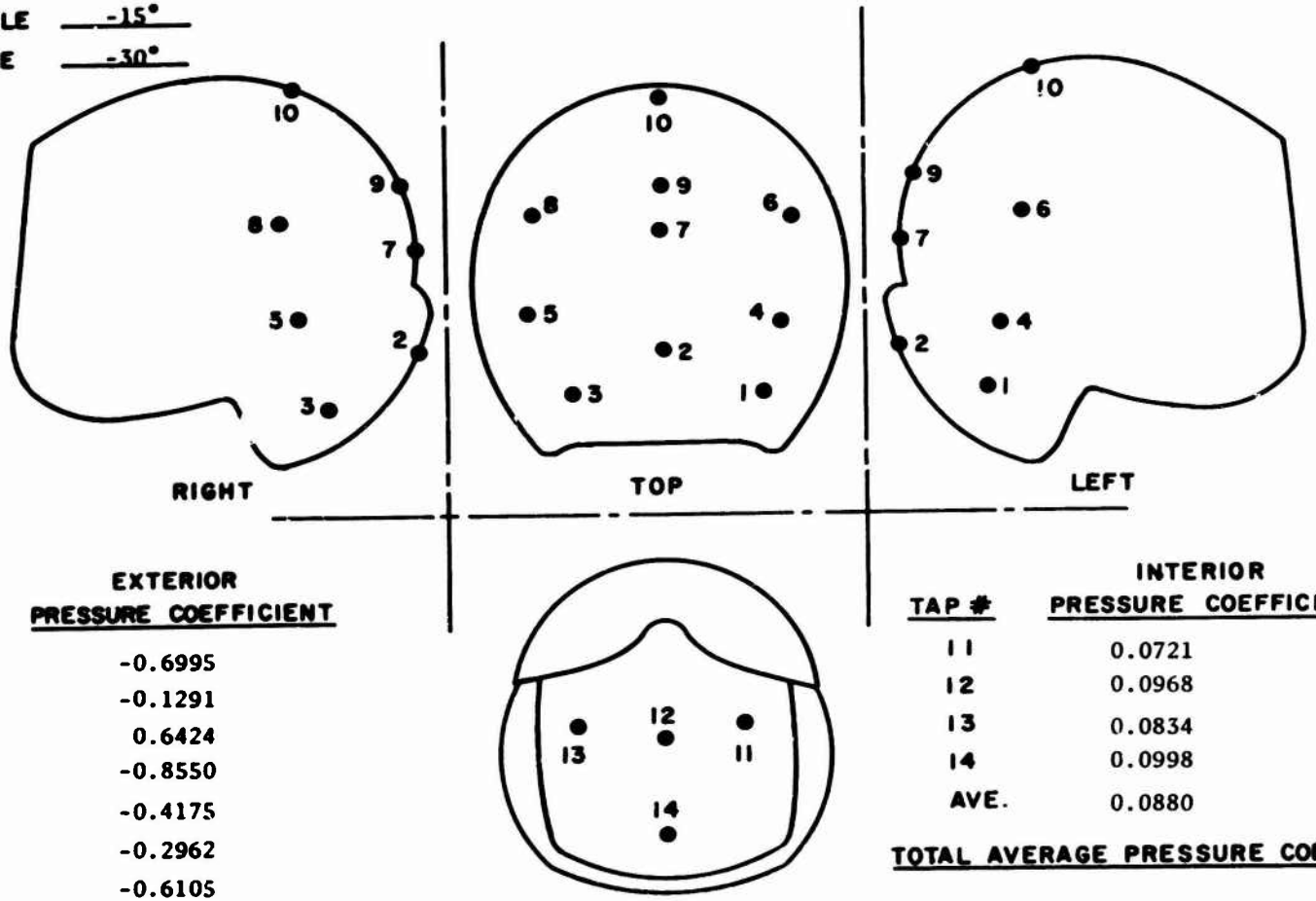

TAP #	EXTERIOR PRESSURE COEFFICIENT
1	-0.6995
2	-0.1291
3	0.6424
4	-0.8550
5	-0.4175
6	-0.2962
7	-0.6105
8	-0.5347
9	-0.3937
10	-0.2645
AVE.	-0.3558

TAP #	INTERIOR PRESSURE COEFFICIENT
11	0.0721
12	0.0968
13	0.0834
14	0.0998
AVE.	0.0880

TOTAL AVERAGE PRESSURE COEFFICIENT

-0.4438

Table I - 3. Average Pressure Coefficient of USAF Helmet with Live Subject.

SUBJECT MAM

RUN NUMBER 23

PITCH ANGLE -15°

YAW ANGLE 0°

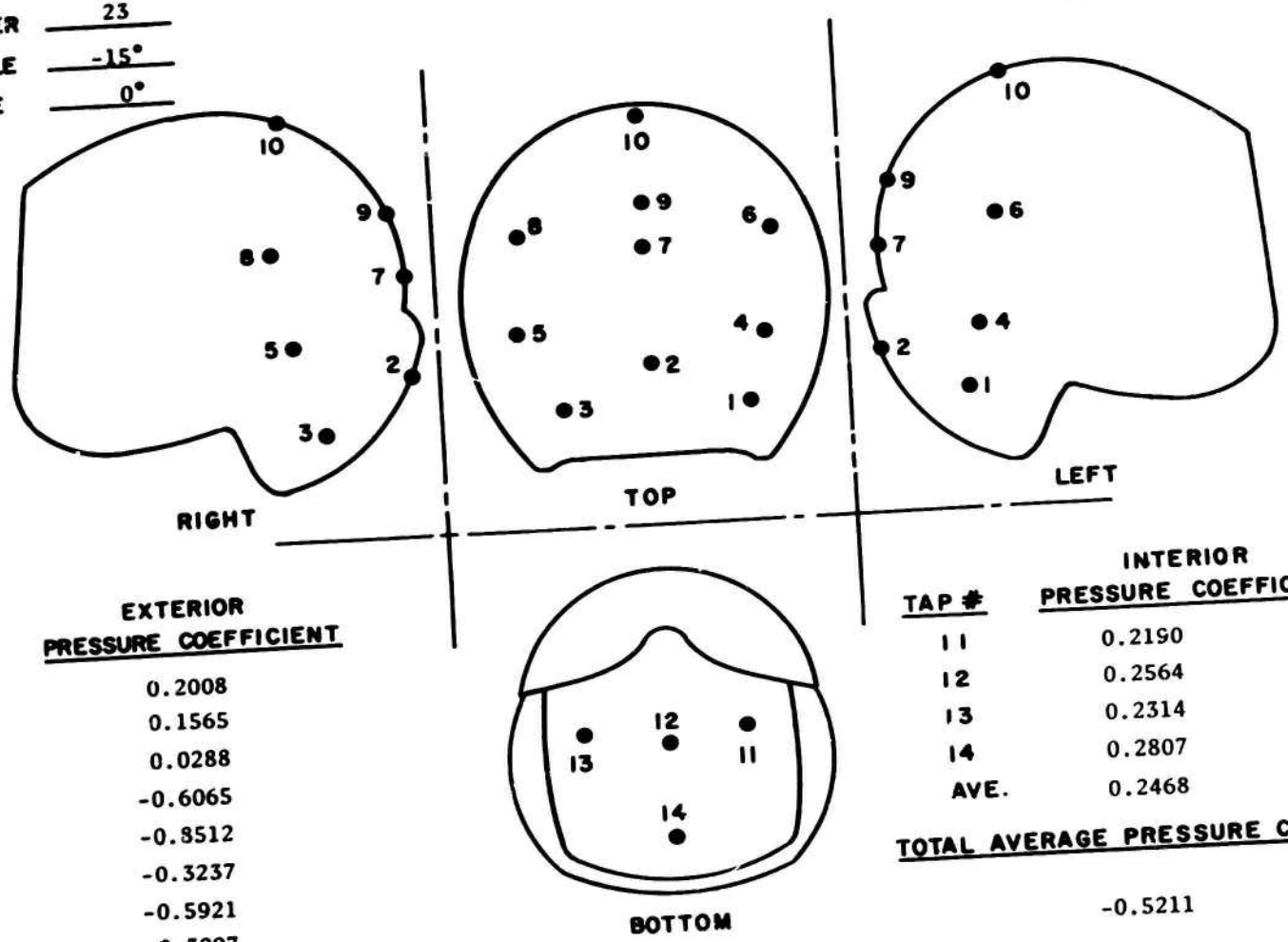

TAP #	EXTERIOR PRESSURE COEFFICIENT
1	0.2008
2	0.1565
3	0.0288
4	-0.6065
5	-0.8512
6	-0.3237
7	-0.5921
8	-0.3097
9	-0.2994
10	-0.1468
AVE.	-0.2743

TAP #	INTERIOR PRESSURE COEFFICIENT
11	0.2190
12	0.2564
13	0.2314
14	0.2807
AVE.	0.2468

TOTAL AVERAGE PRESSURE COEFFICIENT

-0.5211

Table I - 3. Average Pressure Coefficient of USAF Helmet with Live Subject.

RUN NUMBER 24

PITCH ANGLE -15°

YAW ANGLE -15°

SUBJECT MAM

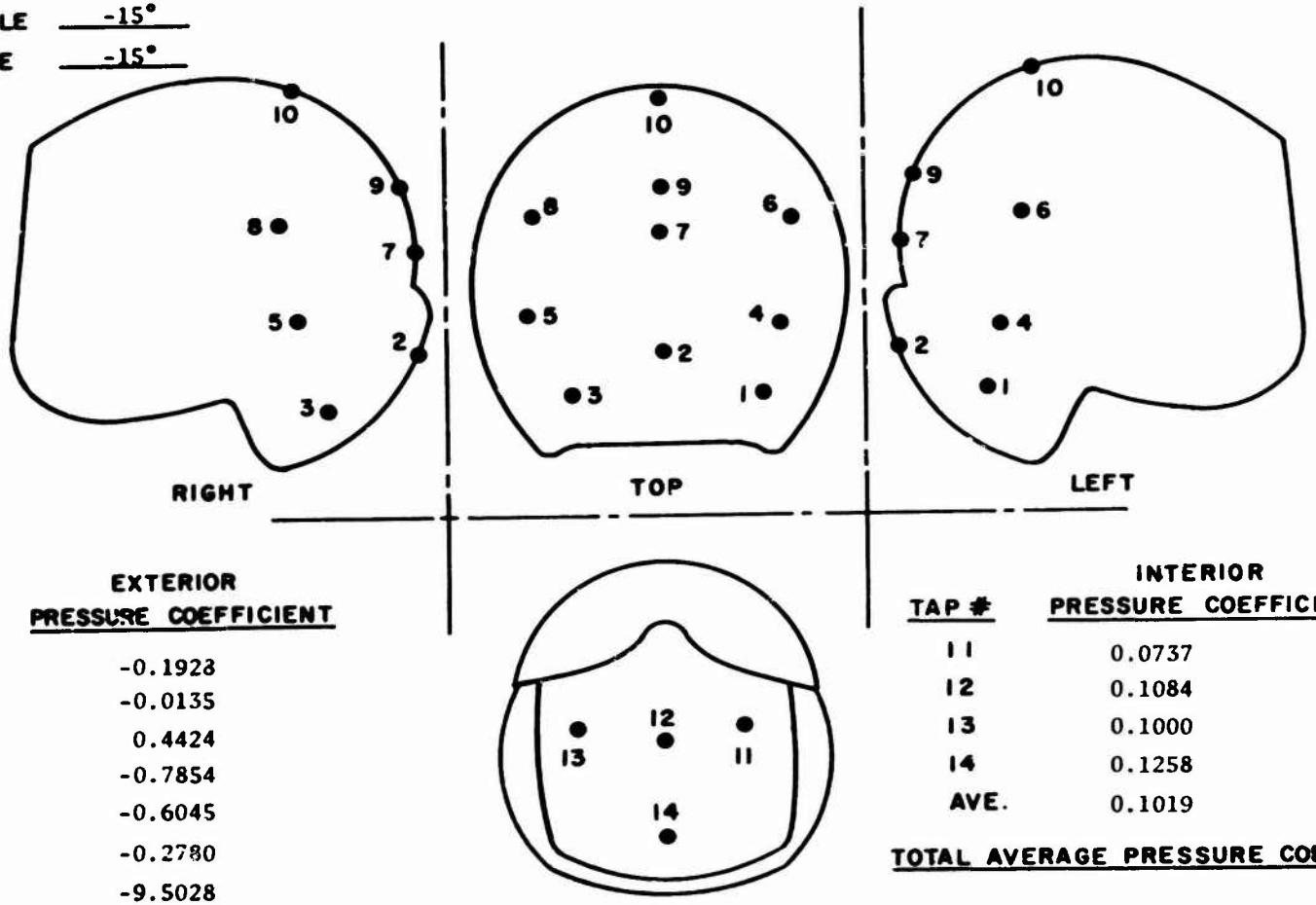

TAP #	EXTERIOR PRESSURE COEFFICIENT
1	-0.1928
2	-0.0135
3	0.4424
4	-0.7854
5	-0.6045
6	-0.2780
7	-9.5028
8	-0.4324
9	-0.3090
10	-0.2005
AVE.	-0.2876

TAP #	INTERIOR PRESSURE COEFFICIENT
11	0.0737
12	0.1084
13	0.1000
14	0.1258
AVE.	0.1019

TOTAL AVERAGE PRESSURE COEFFICIENT

-0.3895

Table I - 3. Average Pressure Coefficient of USAF Helmet with Live Subject.

APPENDIX I REFERENCES

I-1. Payne, P.R., and Hawker, F.W. — USAF Experience of Flail Injury for Noncombat Ejections in the Period 1964-1970. WPAFB, Ohio AMRL-TR-72-111 (1974)

I-2. Payne, P.R. — "The Aerodynamic Stabilization of Ejection Seats." Payne Inc. Working Paper No. 106-1 (June 1973)

APPENDIX II

ON THE STABILITY OF A BODY IN AERODYNAMICALLY DECELERATED FLIGHT

INTRODUCTION

It has sometimes been observed that a seat that appeared to be statically stable in wind tunnel tests does not fly stably after ejection during a sled test. The difference in behavior is assumed to be due to the fact that the free-flying seat is decelerating. The damping of an aircraft is reduced during deceleration and the oscillatory amplitude of a reentering space capsule will increase*, after passing through maximum dynamic pressure and the same effect is assumed to be present for a decelerating seat.

The fundamentals of this question are examined in this appendix. Although the motion of a decelerating seat appears less stable than might be predicted from wind tunnel data, the amplitude does not increase significantly until the velocity has dropped to a physiologically unimportant value. Because this conclusion is so simple, seat damping terms are neglected in the analysis; an omission which is conservative, of course.

---

* Tobak, M. and H.J. Allen, Dynamic Stability of Vehicles Traversing, Ascending or Descending Paths Through the Atmosphere. NACA Technical Note 4275 (1958).

The Effect of Deceleration on Seat Stability

Consider the pitch motion (for example) of an escape system in a horizontal trajectory. If the pitch oscillation is small the drag area may be considered constant, so that

$$m\dot{u} = -D = A_D \frac{1}{2} \rho u^2$$

or

$$\dot{u} = -\gamma u^2 \tag{1}$$

where

A_D is the seat drag area ($= C_D S = D/\frac{1}{2} \rho u^2$)

m is the seat mass

ρ is the mass density of the air

$$\gamma = \frac{\rho A_D}{2m}$$

and would typically be of the order of 10^{-3} (ft^{-1}). Performing the integration

$$\frac{u}{u_o} = \frac{1}{1 + \tau} \tag{2}$$

Where $\tau = u_o \gamma t$, a non-dimensional time. The equation of motion in pitch is then

$$I\ddot{\alpha} = V_{m\alpha} \frac{1}{2} \rho u^2 \alpha = V_{m\alpha} \frac{1}{2} \rho u_o^2 \frac{\alpha}{(1 + \tau)^2} \tag{3}$$

Where

$$V_{m\alpha} = \frac{\partial V_m}{\partial \alpha}$$

V_m = seat moment volume

= moment/$\frac{1}{2} \rho u^2$

Now

$$\frac{d\alpha}{dt} = \frac{d\alpha}{d\tau} \frac{d\tau}{dt} = u_o \gamma \frac{d\alpha}{d\tau}$$

$$\frac{d^2\alpha}{dt^2} = u_o\gamma \frac{d}{d\tau}\left(\frac{d\alpha}{d\tau}\right)\frac{d\tau}{dt} = u_o^2\gamma^2\frac{d^2\alpha}{d\tau^2}$$

also let

$$\psi = -\frac{V_{m\alpha}\frac{1}{2}\rho u_o^2}{Iu_o^2\gamma^2} = -\frac{V_{m\alpha}\rho}{2\gamma^2 I} = -\frac{2mV_{m\alpha}}{\rho A_D^2 r_G^2} \tag{4}$$

- where r_G is the radius of gyration. Equation (3) then becomes

$$\frac{d^2\alpha}{d\tau^2} + \frac{\psi\alpha}{(1+\tau)^2} = 0 \tag{5}$$

ψ is generally of order 10^2 to 10^4 for a typically stable seat, where $V_{m\alpha}$ = -0.1 to -10 ft^3/rad., τ is of the order unity per second.

If $(1+\tau)^2$ were replaced by unity, equation (5) would describe an oscillation of constant amplitude, for $\psi > 0$ ($V_{m\alpha} < 0$). The τ term causes the angular amplitude to increase with time, because the aerodynamic stiffness is decreasing with time.

The substitution

$$\eta = \log(1+\tau) \tag{6}$$

gives

$$\frac{d\eta}{d\tau} = \frac{1}{1+\tau}$$

$$\therefore \frac{d\alpha}{d\eta} = \frac{d\alpha}{d\tau}\frac{d\tau}{d\eta} = (1+\tau)\frac{d\alpha}{d\tau}$$

and

$$\frac{d^2\alpha}{d\tau^2} = \frac{d^2\alpha}{d\tau^2}\frac{d\eta}{d\tau}\frac{1}{(1+\tau)} - \frac{d\alpha}{d\eta}\frac{1}{(1+\tau)^2}$$

Substituting in the equation of motion

$$\frac{d^2\alpha}{d\eta} - \frac{d\alpha}{d\eta} + \psi\alpha = 0 \tag{7}$$

The Oscillatory Solution

The roots of the characteristic equation are

$$p = \frac{1 \pm \sqrt{1 - 4\psi}}{2} \tag{8}$$

The roots are complex if $\psi > \frac{1}{4}$; say $p_1 = (m + in)$ and $p_2 = (m - in)$. Clearly

$$m = \frac{1}{2}$$

$$n = \frac{1}{2}\sqrt{4\psi - 1} = \sqrt{\psi - \frac{1}{4}} \qquad (\psi > \frac{1}{4})$$

$$\therefore \alpha = e^{\frac{1}{2}\eta} \quad [A \cos n\eta + B \sin n\eta] \tag{9}$$

$$\therefore \frac{d\alpha}{d\eta} = e^{\frac{1}{2}\eta} \quad (\tfrac{1}{2}A + Bn) \cos n\eta + e^{\frac{1}{2}\eta} \quad (\tfrac{1}{2}B - An) \sin n\eta$$

when

$$\tau = 0,\ \eta = 0,\ \alpha = \alpha_0 \quad \frac{d\alpha}{d\tau} = \left(\frac{d\alpha}{d\tau}\right)_0$$

$$\left(\frac{d\alpha}{d\eta}\right)_0 = \left(\frac{d\alpha}{d\tau}\right)_0 \left(\frac{d\tau}{d\eta}\right)_0 = \left(\frac{d\alpha}{d\tau}\right)_0$$

$$\therefore A = \alpha_0$$

and

$$B = \frac{\left(\frac{d\alpha}{d\tau}\right)_0 - \frac{1}{2}\alpha_0}{n}$$

For

$$\left(\frac{d\alpha}{d\tau}\right)_0 = 0$$

Therefore

$$\alpha = \alpha_0 e^{\frac{1}{2}\eta} \left[\cos n\eta - \frac{1}{2n} \sin n\eta\right] \tag{10}$$

If

$$n\eta = \theta, \quad \eta = \frac{\theta}{n}$$

Then

$$\alpha = \alpha_0 e^{\frac{\theta}{2n}} \left[\cos \theta - \frac{1}{2n} \sin \theta\right] \tag{11}$$

The increase in amplitude per cycle is

$$\frac{a_{n+1}}{a_n} = \frac{e^{\frac{\theta + 2\pi}{2n}}}{e^{\frac{\theta}{2n}}} = e^{\frac{\pi}{n}} \tag{12}$$

By differentiating equation (11) with respect to θ and equating to zero we find that maxima and minima occur when

$$\sin \theta = \sin n\eta = 0$$

i.e. when $\sqrt{\psi - 1/4} \log (1 + \tau) = m\pi$ $\qquad (m = 1,2,3. \ . \ .)$

or

$$\tau_m = e^{\frac{m\pi}{\sqrt{\psi - 1/4}}} - 1 \tag{13}$$

The Divergent Solutions

When $\psi = 1/4$ the two roots of the characteristic equation (8) are the same ($p_1 = p_2 = 1/2$) and the solution is

$$\alpha = e^{\frac{1}{2}\eta}(C\eta + D)$$

$$\frac{d\alpha}{d\tau} = \frac{1}{2}e^{\frac{1}{2}\eta}(C\eta + D) + e^{\frac{1}{2}\eta}C$$

$$\therefore D = \alpha_0 \qquad \text{and} \qquad C = \left(\frac{d\alpha}{d\tau}\right)_0 - \frac{1}{2}\alpha_0$$

For

$$\left(\frac{d\alpha}{d\tau}\right)_0 = 0$$

$$\alpha = \alpha_0 e^{\frac{1}{2}\eta}(1 - \frac{1}{2}\eta) \tag{14}$$

This is obviously a divergence, after passing through $\alpha = 0$ at $\eta = 2$

i.e. $\log(1 + \tau_m) = 2$

or

$$\tau_m = e^2 - 1 = \underline{6.39} \tag{15}$$

At this point, from (2), $\frac{u}{u_o} = 0.135$, so that subsequent motion is not very material.

For $\psi < \frac{1}{4}$ the characteristic equation gives

$$p_1 = \frac{1}{2} + \sqrt{\frac{1}{4} - \psi}$$

$$p_2 = \frac{1}{2} - \sqrt{\frac{1}{4} - \psi}$$

$$\therefore \alpha = Ae^{p_1\tau} + Be^{p_2\tau} \tag{16}$$

$$\frac{d\alpha}{d\tau} = Ap_1e^{p_1\tau} + Bp_2e^{p_2\tau}$$

$$\therefore A + B = \alpha_0$$

$$Ap_1 + Bp_2 = \left(\frac{d\alpha}{d\tau}\right)_0$$

$$\therefore B = \frac{p_1\alpha_0 - \left(\frac{d\alpha}{d\tau}\right)_0}{p_1 - p_2}$$

$$A = -\frac{p_2\alpha_0 - \left(\frac{d\alpha}{d\tau}\right)_0}{p_1 - p_2}$$

For

$$\left(\frac{d\alpha}{d\tau}\right)_0 = 0$$

$$\alpha = \frac{\alpha_0}{(p_1 - p_2)} \left[-p_2e^{p_1\tau} + p_1e^{p_2\tau}\right] \tag{17}$$

This passes through $\alpha = 0$ when

$$p_2e^{p_1\tau} = p_1e^{p_2\tau}$$

i.e. at

$$\tau_m = \frac{\log p_2/p_1}{p_2 - p_1} = \frac{\log p_1/p_2}{p_1 - p_2}$$

$$= \frac{\log\left[\frac{1 + \sqrt{1 + 4\psi}}{1 - \sqrt{1 - 4\psi}}\right]}{\sqrt{1 - 4\psi}} \qquad (18)$$

Discussion

Figures II-1 through II-5 show the motion for decreasing values of ψ, the static stability parameter. When ψ is large (Figure II-1) the motion is very similar to that of an undamped linear system

viz $\quad \ddot{\alpha} + \psi\alpha = 0$

For $\psi = 100$ (Figure II-3) the amplitude has nearly doubled at the end of the second cycle; but the speed u has fallen to only 28% of the initial value u_o, corresponding to only 8% of the initial dynamic pressure. Thus the "instability" is relatively immaterial.

If we say that the relative amplitude is

$$\bar{a} = e^{\frac{1}{2}\eta} = e^{\frac{1}{2}\log(1+\tau)} = (1 + \tau)^{\frac{1}{2}}$$

Then from (2)

$$\frac{u}{u_o} = \frac{1}{(\bar{a})^2} \qquad (19)$$

- a result which is independent of speed and the stiffness parameter ψ. Thus when the amplitude doubles, the speed is one quarter, and the dynamic pressure one sixteenth. An elegantly simple conclusion.

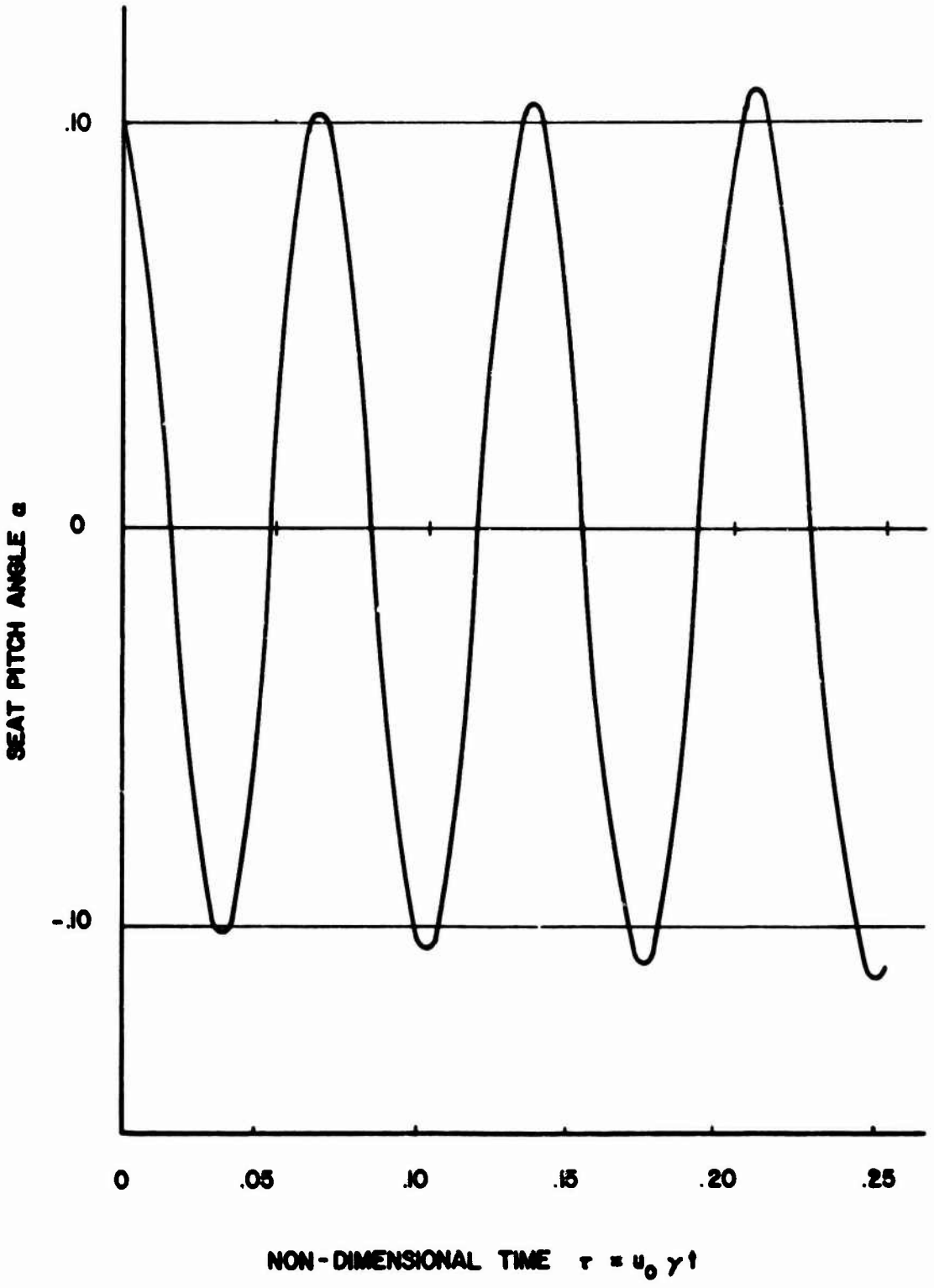

Figure II - 1. Motion for ψ = 10,000

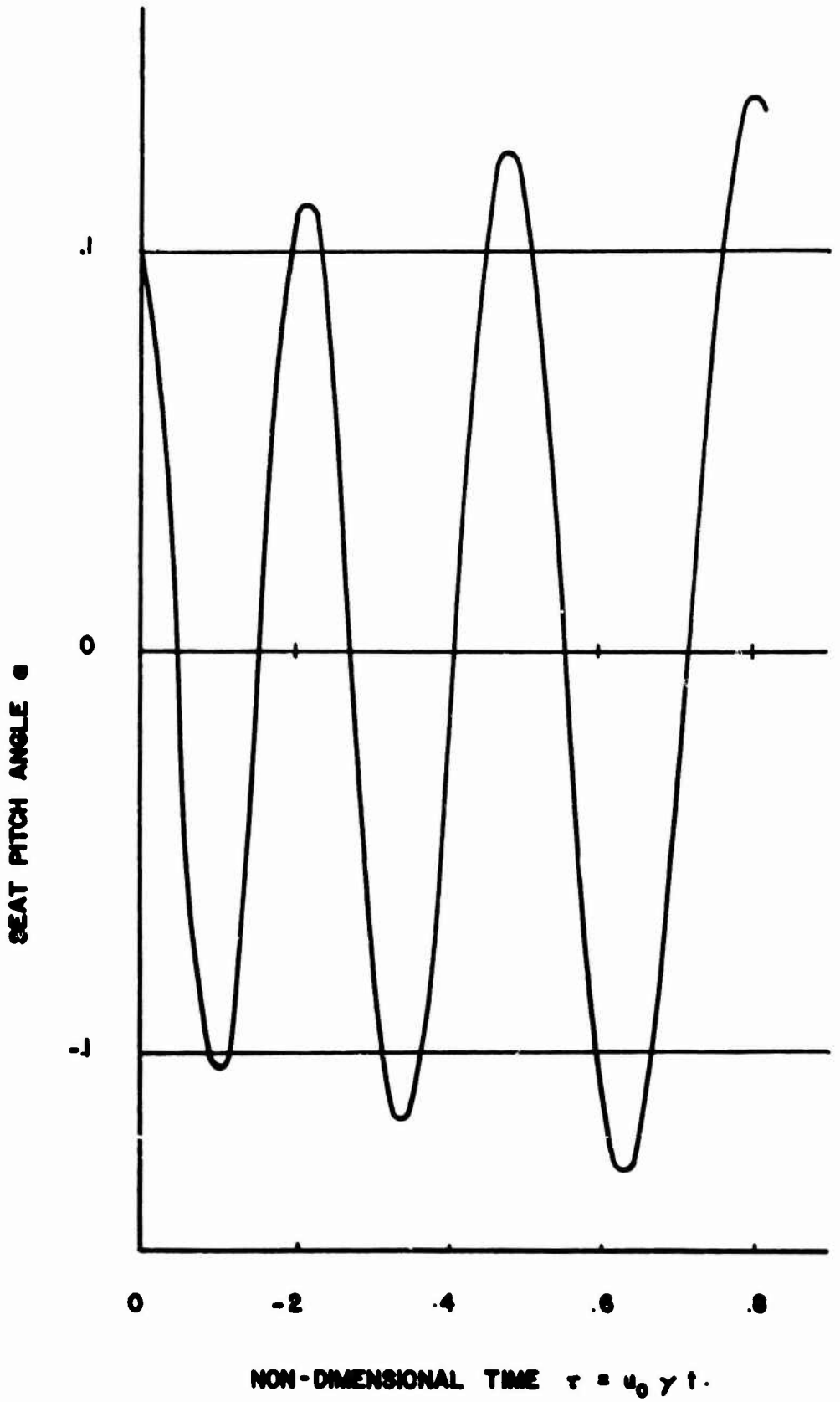

Figure II - 2. Motion for $\psi = 1000$

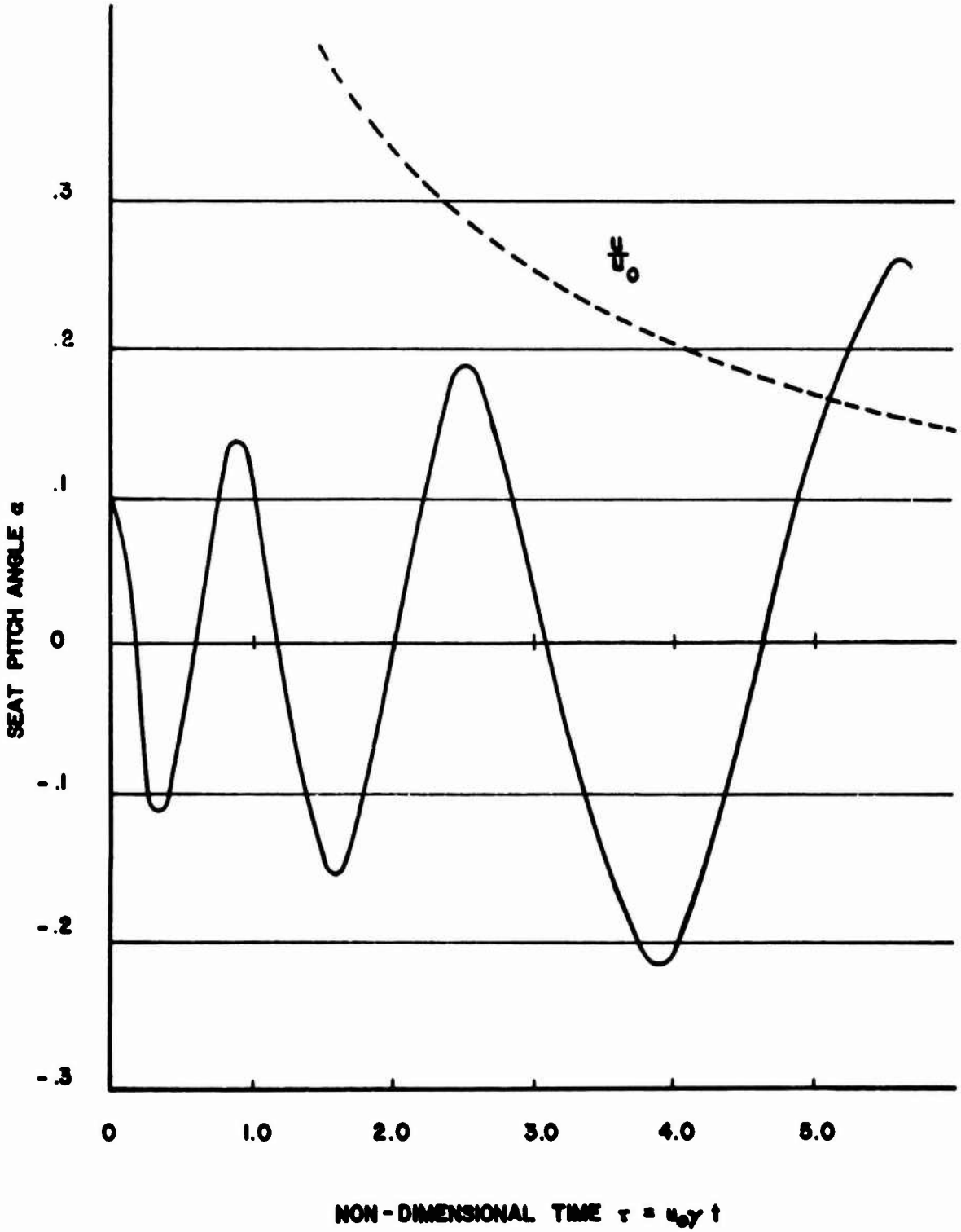

Figure II - 3. Motion for ψ = 100

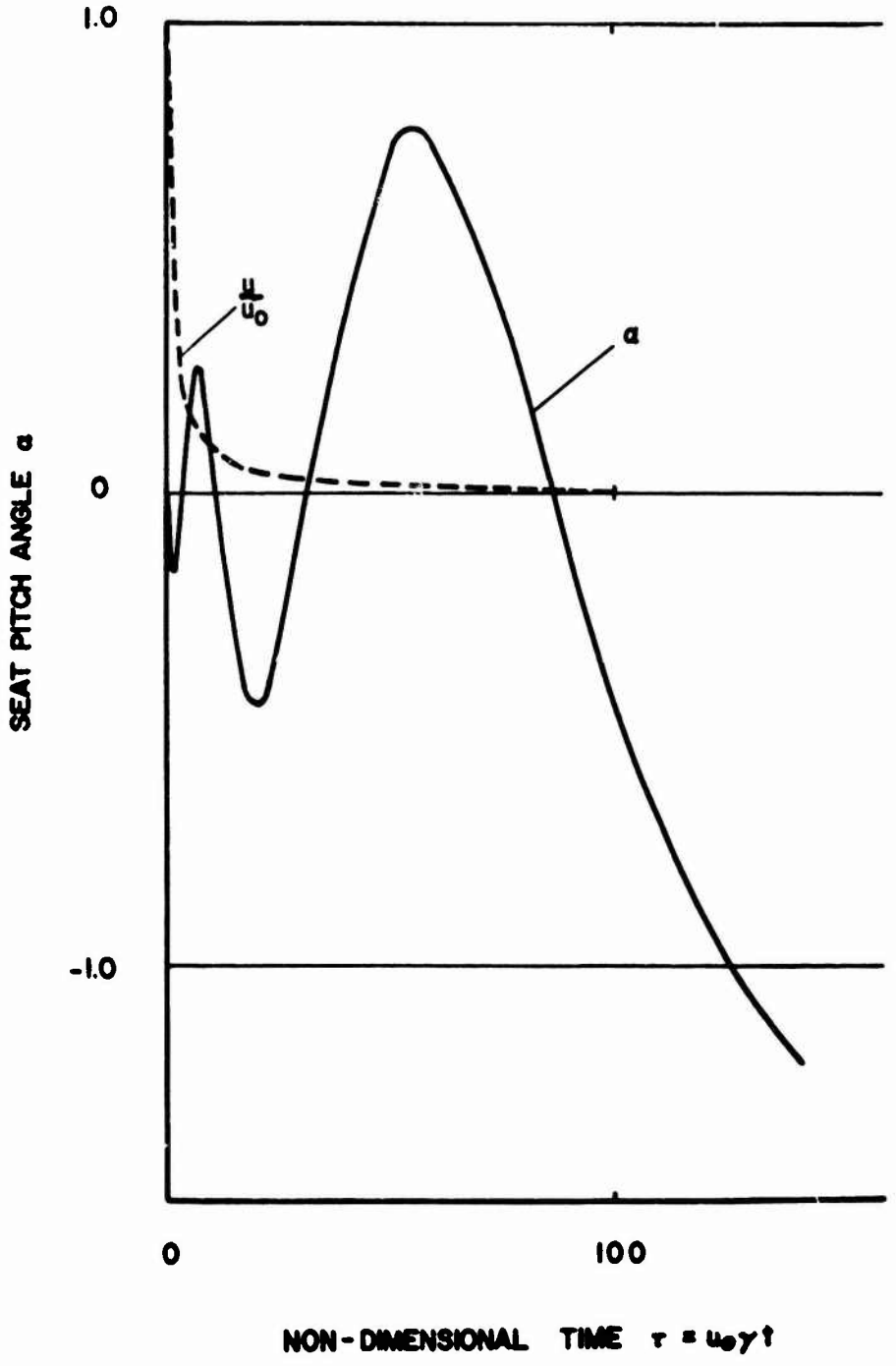

Figure II - 4. Motion for ψ = 10

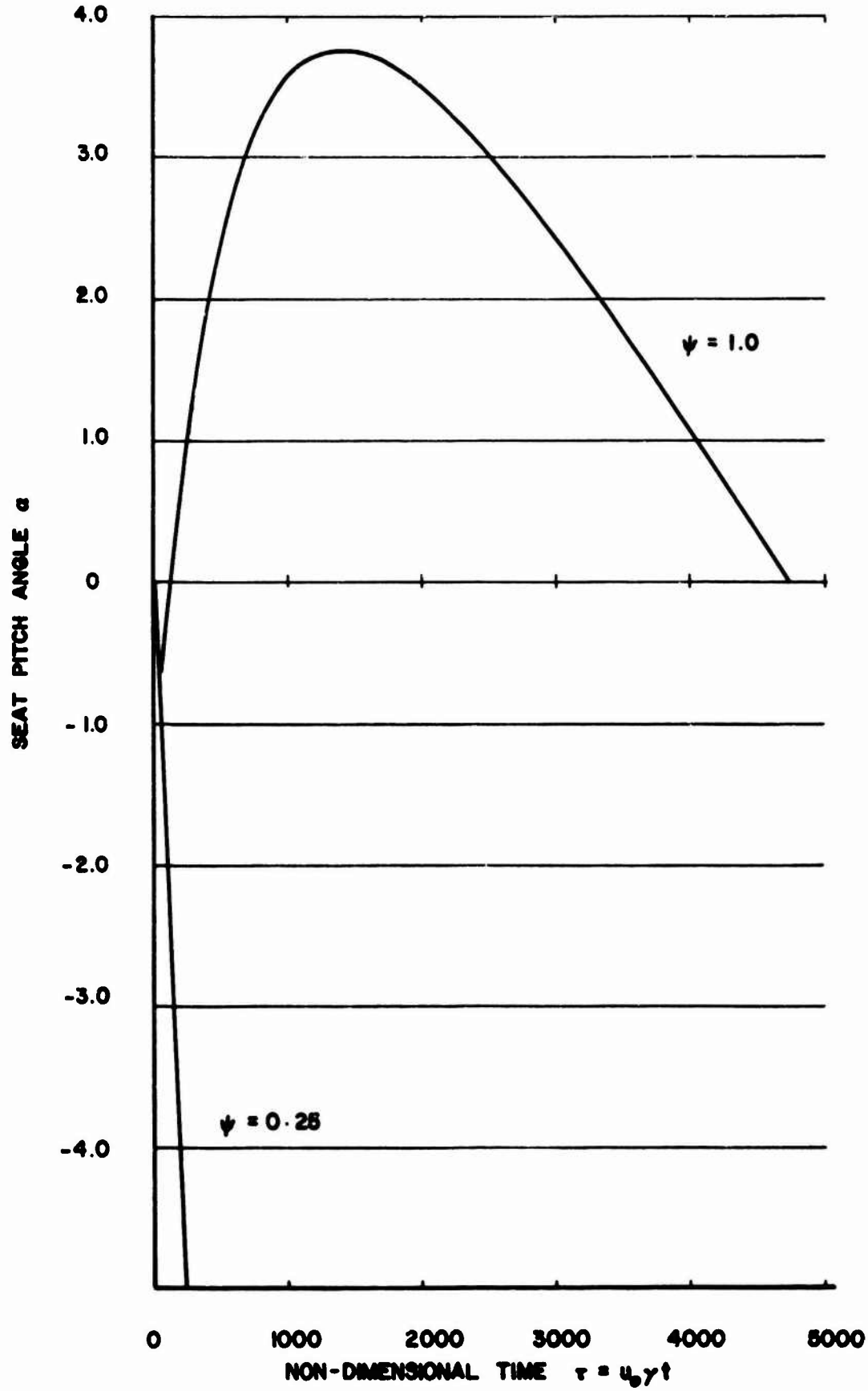

Figure II - 5. Motion for ψ = 1.0 and 0.25

REFERENCES

1. Payne, Peter R. and Hawker, Fred W. — USAF Experience of Flail Injury for Non-Combat Ejections in the Period 1964-1970., AMRL-TR-72-111, Wright-Patterson Air Force Base, Ohio 45433 AD 921780 L (May 1974)

2. Fryer, D.I. — Operational Experience with British Ejection Seats., R.A.F. Institute of Aviation Medicine; Farnborough, Hants, England (July 1961)

3. Payne, Peter R. — Some Studies Relating to "Limb Flailing" After an Emergency Escape from an Aircraft., AMRL-TR-73-24, Wright-Patterson Air Force Base, Ohio 45433 AD A005699 (December 1974)

4. Hawker, Fred W. and Euler, Anthony J. — Extended Aerodynamic Stability and Limb Dislodgement Measurements with the ACES-II Ejection Seat., AMRL-TR-75-15, Wright-Patterson Air Force Base, Ohio 45433 (July 1975)

5. Visconti, Floravante and Nuber, Robert J. — A Wind-Tunnel Investigation of the Static Stability Characteristics of a 1/8-Scale Ejectable Pilot-Seat Combination at a Mach Number of 0.8., NACA-RM-L51-08, Washington, D.C. (December 1951)

6. Reichenau, David E.A. — Aerodynamic Characteristics of an Ejection Seat Escape System with Cold Flow Rocket Plume Simulation at Mach Numbers from 0.6 Through 1.5., AEDC-TR-69-218, Arnold Air Force Station, Tennessee (October 1969)

7. Galigher, Lawrence L. — Aerodynamic Characteristics of a Full-Scale F-101 Ejection Seat with an Anthropomorphic Dummy at Mach Numbers from 0.2 to 0.8., AEDC-TR-72-38, Arnold Air Force Station, Tennessee (March 1972)

8. Euler, Anthony J. — In-Plane Stabilizer Calculations for ACES-II and F-105 Ejection Seats., Payne, Inc. Working Paper No. 119-5 (April 1974)